UNIVERSIDAD DE VALLADOLID

ESCUELA DE INGENIERIAS INDUSTRIALES

Grado en Ingeniería Química

Valorization of oil deodorizer distillates

Autor:

Rico Martínez, Daniel

Responsable de Intercambio en la UVa

Silvia Bolado

Universidad de destino

Ghent university

Valladolid, Julio 2017.

TFG REALIZADO EN PROGRAMA DE INTERCAMBIO

TÍTULO: **Valorización de destilados deodorizados de aceite**

ALUMNO: **Daniel Rico Martínez**

FECHA: 26 Junio 2017

CENTRO: **Faculty of chemical engineering**

TUTOR: **Joris Thybaut and Jeriffa de Clercq**

GHENT UNIVERSITY

ABSTRACT

In this work, simulation of supercritical extraction to concentrate minor components from oil deodorizer distillates (ODD) in the commercial software Aspen Plus ® has been investigated. The extraction process consist out of a first extraction column at 313 K and 10 MPa followed by another extraction column at the same temperature and 16 MPa. The RK-Aspen property method was selected for the supercritical extraction process. The solubility of FAME and tocopherol in CO_2 was investigated in more detail. This case study provided insights for the complex ODD mixture. Based on these results, on can assume that a supercritical process can be used to isolate tocopherols from the esterified ODD. Further, the complex ODD mixture was used to simulate the isolation of squalene. Literature data for solute/sc-CO_2 used to calculate the interaction parameters for the RK-Aspen property method. Three kinds of feedstocks were simulated: sunflower ODD, high and low tocopherol content in soybean ODDs. The highest purity of squalene is achieved using sunflower and low tocopherols content in soybean ODDs, the highest squalene amount using high tocopherols content in soybean ODDs and the highest yield using low tocopherols content in soybean ODDs.

ACKNOWLEDGEMENTS

I would like to thank Ghent University and Valladolid university for providing the opportunity to do my master thesis during the last year of my degree in Ghent (Belgium). On the one hand, it taught me the atmosphere of working in a laboratory, and on the other hand it has been a great learning about myself.

Firstly, I would like to express my sincere gratitude to my promoters Prof. Joris W. Thybaut and prof. Jeriffa de Clecq for allowing me to perform research on this interesting topic under their supervision.

Secondly, I would like to thank to my supervisor Alexandra. Being guided by her during my thesis was a very good experience. I did learn a lot about Aspen Plus® and thanks for maintaining a good working atmosphere.

I was fortunate to have an office mate as Roberto. Thanks for all the talk during the breaks.

Prof. Silvia Bolado, many thanks for all the administrative help about the exchanging.

VALORIZATION OF OIL DEODORIZER DISTILLATES

Daniel Rico

Supervisor (s): Alexandra, Bouriakova, Jeriffa de Clercq, Joris W. Thybaut

Abstract: In this work, the supercritical extraction with the aim of concentrating valuable minor components from oil deodorizer distillates (ODD) has been investigated in Aspen Plus V.9. The extraction process consist out of a first extraction column at 313 K and 10 MPa followed by another extraction column at the same temperature and 16 MPa. The RK-Aspen property method was selected for the supercritical extraction process. The solubility of FAME and tocopherol in CO_2 was investigated in more detail. This case study provided insights for the complex ODD mixture. Based on these results, on can assume that a supercritical process can be used to isolate tocopherols from the esterified ODD. Further, the complex ODD mixture was used to simulate the isolation of squalene. Literature data for solute/scCO_2 used to calculate the interaction parameters for the RK-Aspen property method. Three kinds of feedstocks were simulated: sunflower ODD, high and low tocopherol content in soybean ODDs. The highest purity of squalene is achieved using sunflower and low tocopherols content in soybean ODD, the highest squalene amount using high tocopherols content in soybean ODDs and the highest yield using low tocopherols content in soybean ODDs.

1. Introduction.

The annual production of oils and fats in 2015 was 202 million tons. Over the last decade the production rates for the major oils has varied a lot, generally with a growing trend due to increases in consumption mainly because of the additional use as biodiesel feedstock [1].

These crude oils are subjected to a refining process where these oils are made suitable for human consumption (edible oils). One of the most important by-products of this process are, the oil deodorizer distillates (ODD). ODD is a complex mixture of free fatty acids (FFA), tri- di and mono glycerides, and minor components such as tocopherols, sterols and squalene. These minor components are considered valuable compounds from cosmetic and pharmaceutical industries. The classical methods to isolate these minor components have some drawbacks, and therefore, supercritical extraction technology has been investigated. The extraction of minor components directly from ODD was not very economical due to the low solubility of FFA in scCO_2. After the esterification of the FFA, the formed free fatty ester has a higher solubility in scCO_2, which results in a better separation of the minor components.

In this study, it was simulated the extraction of squalene from several esterified ODD fractions with different vegetable oil sources.

2. Procedures

a. Thermodynamic modelling

The flexible equation-of-state method Redlich Kwong Aspen (RK-Aspen) was selected to calculate the phase equilibrium between the ODD components and the supercritical solvent.

b. Case study

The phase equilibrium of the ternary mixture FAME/CO_2/tocopherols have been studied to establish a preliminary separation strategy of the esters using scCO_2 and the behavior of the minor components during this separation. Vapor liquid equilibrium data was used from Fang [2,3].

c. Model component choice

In this study, ODD was modeled as a mixture of free fatty acids (mainly oleic acid), Tri-, di and mono glycerides (represented by tri- di- and mono- olein), fatty acid esters (methyl and ethyl oleate) and some minor components such as tocopherols (α-tocopherol), sterols (β-sitosterol) and squalene.

d. Critical properties of components

The estimation of critical properties is needed for the simulation since these pure component properties are directly included in the equation of state of the thermodynamic model. Often, the estimation of properties using group contribution method is required due to thermal decomposition of some components.

Critical pressure, temperature and acentric factor using during the simulation are summarized in Table 1.

Table 1. Pure component properties of the ODD components available in Aspen databanks.

Retrieved by Aspen				
Component	Tc (K)	Pc (MPa)	Ω (-)	Databank
FFA	781	1.39	1.17	PURE35
MG	856.9	1.20	1.10	PURE35
DG	916	0.43	1.84	PURE35
TG	935.3	0.20	2.09	PURE35
FAME	764	1.28	1.05	PURE35
TOCO	964.3	1.08	1.03	PURE35
STEROL	953	1.12	1.05	PURE35
SQUALENE	832	0.71	0.63	NIST-TRC
FAEE	772.1	1.10	0.94	PURE35

As a comparison, the estimation of these properties using the Aspen Plus estimation properties tool using group contribution method and values of these properties founded in literature have been included in this work.

In order to get a reliable model, binary interaction parameters should be included in the model. Binary interaction parameters can be determined applying a regression of equilibrium data. In this study, phase equilibrium data used for the system ODD components/supercritical CO_2 are presented in Table 2.

Table 2. Literature phase equilibrium data for system of EEODD components/sc CO_2.

EEODD compound/ CO2	Ref.	Temp. (K)	Pressure (MPa)
FAEE	[4]	313,323, 333	1.14-18.62
FFA	[5]	313,333, 353	10-30
TG	[5]	313, 333	15-31
FAME	[6]	313, 333	2.91-13.69
tocopherol	[7]	292-333	9-26
Ethanol +Water	[8]	283-305	4.5-8.8
FAME+ Squalene	[9]	313-343	11-21
Sterol+TG	[10]	323- 383	20-35

For the calculation of binary interaction parameters for RK-Aspen, the Deming algorithm was applied to perform a maximum likelihood estimation. The results are shown in Table 3.

Table 3. RK-Aspen model parameters.

	CO2		
	$k_{a, ij}$	$k_{b, ij}$	η
FAEE	-1.0051	-4.7929	2
FFA	0.0637	0.1814	-0.918
TG	-0.0015	-0.0946	-2
FAME	0.1047	0.0757	2
TOCOS	0.2151	-0.0326	2
ETHANOL	-0.6979	-1.6887	2
WATER	-0.3819	-0.088	-0.2168
SQUALENE	0.0783	-0.0321	-2
STEROLS	1.06	1.0257	2

e. Supercritical extraction process simulation

The supercritical extraction process simulated in Aspen Plus consist in a first extraction column (E-1) working with a S/F mass ratio of 10 at 313 K and 10 MPa followed by a second extraction column (E-2)working with a S/F mass ratio of 7.9 at 313 K and 16 MPa. After every extractor, the solvent is recovered by decreasing the pressure and recycled. The process is shown in Figure 1.The extraction column was simulated using EXTRACTOR block unit.

3. Results

a. Case study

Analysing the binary systems has been shown that distribution coefficient of FAME is one or two order the magnitude higher than tocopherol so separation of these components is possible. Analyzing the effect of pressure and temperature has been concluded that 313 K and 10 MPa are the best conditions to our target in E-1.

b. Supercritical process

Using EEODD from sunflower (see composition in Section 5.2.1.) as a raw material the optimization of the simulated extraction columns was done.

Optimization E-1

Influence of pressure on first extraction column in the range 9.25 to 10 MPa was analysed. At higher pressure, the FFA content in the refined phase is minimum and squalene content in the refined phase is not too low.

The influence of temperature on the refined phase after the extraction in the range of 308 to 318 K is also studied. 313 K is the optimum temperature for the extraction due to above this temperature, FFA and FAME content in the refined phase increase a lot.

Table 4. Composition of EEODD.

	Sunflower	HT soybean	LT soybean
Component		%wt	
Ethanol	9.99	6.9137	13.4874
FFA	2.16	0.3926	2.3911
TG	15.91	1.9483	0.8024
Tocopherols	3.34	24.1818	0.4518
FAEE	49.5	19.9323	74.5836
Water	1.29	0.6435	1.8720
MG	2.27	3.856	0.2336
DG	2.17	6.526	0.2806
FAME	1.31	1.8669	4.7599
Sterols	9.55	30.7675	0.4908
Squalene	2.49	2.972	0.6466
Total minor components	15.38	57.9213	1.5892

Optimization E-2

Influence of pressure on the second extraction column is studied. To minimize the squalene content in the refined phase higher pressures are needed. Squalene content in refined phase start to be independent on pressure after 16 MPa so that pressure was selected.

Running the simulation with sunflower, high tocopherol soybean and low tocopherol soybean ODD as a raw materials for the extraction process at the same conditions, the different quality, global yield and production of squalene was compared in Table 5. According these results, sunflower ODD feedstock is the most viable.

Table 5. Simulation results of the squalene stream at same conditions using several feedstocks in Aspen Plus.

	Sunflower	HY soybean	LT soybean
Production (kg/h)	0.017	0.019	0.0046
Quality (wt%)	98.43	92.66	98.81
Global recovery (wt%)	68.27	64.17	70.46

4. Conclusions

An extraction process for the production of squalene based on supercritical extraction technique was successfully simulated using Aspen Plus® steady state process simulator.

A two-step extraction process using supercritical CO_2 as a solvent was found to isolate squalene from EEODD. In the first extraction column, FAMES and FFA are removed from EEODD using $scCO_2$. The refined phase, consisting mainly FAEE and minor components is sent to a second extraction column where the squalene is collected in the extract phase. Sunflower ODD seems to be the best alternative as raw material due to it has the highest production with a quality above the company criteria (95 %wt) and a global squalene recovery of 68.27%.

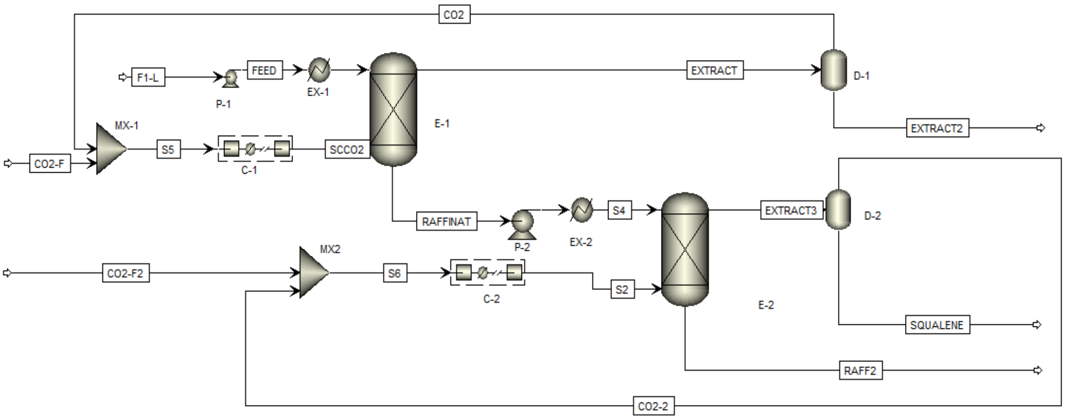

Figure 1. Supercritical extraction process.

5. References

1. REA Holding, World production of oils & fats.

2. Fang, T., et al., Phase equilibria for binary systems of methyl oleate–supercritical CO 2 and α-tocopherol–supercritical CO 2. The Journal of supercritical fluids, **2004**. 30(1): p. 1-16.

3. Fang, T., et al., Phase equilibria for the ternary system methyl oleate+ tocopherol+ supercritical CO2. Journal of Chemical & Engineering Data, **2005**. 50(2): p. 390-397.

4. Ragunath Bharath, H.I.a.K.A., Vapor-Liquid Equilibria for binary mixtures of Carbon Dioxide and Fatty Acid Ethyl Esters. Fluid Phase Equilibria, **1989**. 50: p. 315-327.

5. Ragunath Bharath, H.I., Tadafumi Adschiri and Kunio Arai, Phase equilibrium study for the separation and fractionation of fatty oil components using supercritical carbon dioxide. Fluid Phase Equilibria, **1992**. 81: p. 307-320.

6. Yu, Z.-R., S.S. Rizvi, and J.A. Zollweg, Phase equilibria of oleic acid, methyl oleate, and anhydrous milk fat in supercritical carbon dioxide. The Journal of Supercritical Fluids, **1992.** 5(2): p. 114-122.

7. Paulo J. Pereira, M.G., Baudilio Coto, Edmundo Gomes de Azevedo, Manuel Nunes da Ponte, Phase equilibria of CO2 + Dl-alpha-Tocopherol at Temperatures from 292 K to 333K and Pressures up to 26 MPa. Fluid Phase Equilibria, **1993**. 91: p. 133-143.

8. H. Inomata, K.A., S. Saito, S. Ohba and K. Takeuchi, Measurement and prediction of phase equilibria for the CO2-Ethanol-Water system. Fluid Phase Equilibria, **1989**. 53: p. 23-30.

9. Rui ruivo, A.P., Pedro Simoes, Phase equilibria of the ternary system methyl oleate/squalene/carbon dioxide at high pressure conditions. The Journal of supercritical fluids, **2004**. 29: p. 77-85.

10. J. Stoldt, G.B., Phase equilibrium measurements in complex systems of fats, fat compounds and supercritical carbon dioxide. Fluid Phase Equilibria, **1998**. 146: p. 269-295.

CONTENTS

LIST OF TABLES

LIST OF FIGURES

List of Abbreviations and Acronyms

DG	Diglycerides
FAEE	Fatty Acid Ethyl Esters
FAME	Fatty Acid Methyl Esters
FFA	Free Fatty Acids
MG	Monoglycerides
ODD	Oil Deodorizer Distillates
SDD	Sunflower Deodorizer Distillate
TG	Triglycerides
EOS	Equation-of-state
RKA	Redlich-Kwong-Aspen
EE ODD	Ethyl Esters of Oil Deodorizer Distillates
$scCO_2$	Super Critical Carbon Dioxide
RKA	Redlich Kwong Aspen
Property Constant Estimation System	PCES
Vapor Liquid Equilibrium	VLE
Liquid Liquid Equilibrium	LLE
Average Absolute Deviation	AAD

LIST OF APPENDICES

1 INTRODUCTION

1.1 Justification

Annual production of oils and fats in 2015 was 202 million tons of which palm oil and soybean oil production represents respectively 61 million tons and 47 million tons, so together accounting for 50 % of the total production [1]. Over the last decade the production rates for the major oils has varied a lot, generally with a growing trend due to increases in consumption mainly because of the additional use as biodiesel feedstock [1]. Most of the current oil and fat production is used for food consumption, e.g. frying oil, salad oils, cooking fat, etc. Around 14% of current oil and fat production is used as raw material for the oleo chemical industry and only 6% is used as animal feedstock.

Vegetable oils are mostly obtained from beans or seeds and consist out of two different products: an oil and a protein rich meal. Extracting the vegetable oil from the seed can be achieved by pressure or by adding a solvent. The resulting oil has very varied compositions. Average oil production yield in the world are: coconut (62.4 %), palm kernel (44.6 %), sesame (42.4 %), sunflower (40.9%), groundnut (40.3 %), rapeseed(38.6 %), linseed (33.5 %,; soybean (18.3 %) and cottonseed (15.1%) [2].

Crude vegetable oils are very complex. The major component is triglyceride and the various minor components are diglycerides, monoglycerides, free fatty acids (FFA), phospholipids, tocopherols, sterols, squalene, color pigments, waxes, aldehydes, ketones, triterpene alcohols and metals that may affect the quality of the final product [2]. Some minor components such as squalene, tocopherols and sterols have a lot of interest for cosmetic, pharmaceutical and food companies.

These crude oils are subjected to a refining process where these oils are made suitable for human consumption (edible oils). Through the refining process, the desired organoleptic characteristics are obtained as well as the stability to oxidation and the suitability for frying or cooking. There are two refining processes, i.e. the alkaline refining (chemical) and the physical refining. Through those processes, minor components are partially or totally eliminated.

The classical alkaline refining method usually consists out of several steps. First, water is added (the so-called degumming) to remove the easily hydratable phospholipids and metals. This is followed by an addition of a small amount acid (phosphoric or citric acid) to convert the remaining non-hydratable phospholipids, such as Ca or Mg salts, into hydratable phospholipids. Then, the free fatty acids are neutralized with a slight excess of sodium hydroxide solution. Next, there is a washing step where coloring components are adsorbed. Finally, a deodorizing process, which is essentially a steam distillation, is carried out at low pressures (200-600 Pa) and elevated temperatures (450-495 K) to remove volatile components, mainly aldehydes and ketones. Deodorization is the last major processing step in the refining of edible oils. The main purpose of this process is removing the undesirable ingredients, occurring in natural fats and oils and those which may be imparted by prior unit processes, such as caustic refining, bleaching, hydrogenation, or even storage conditions. After this processing step, the oil establishes finally characteristics of "flavor and odor" which are those most readily recognized by the consumer [3].

In physical refining, the FFA's are removed by a steam distillation (stripping) process similar to deodorization. That process requires higher temperatures than those required for deodorization because of the low volatility of the FFA's [4].

Oil deodorizer distillate (ODD) is the name that receives the resulting product from the deodorization process, which is the last major step in vegetable oil refining process. It is a complex mixture of free fatty acids, mono-, di- and triglycerides, sterols and their esters, tocopherols, hydrocarbons, pesticides, and breakdown products of fatty acids, aldehydes, ketones and acylglycerol species [5]. Deodorizer distillate is an excellent source of valuable compounds such as phytosterols, tocopherols and squalene, which can be isolated and used as food additives, in pharmaceutical and cosmetics industries. Their commercial value however, is mainly dependent on their tocopherol content [6]. The growth of the phytosterols market has led to an increase in the study of isolation methods [6]. Several methods have been described to isolate bioactive compounds from oil deodorizer distillate to make the oil refining process more profitable due to the use of one of its waste streams. All these procedures can be grouped in three categories: crystallization and precipitation, chemical and enzymatic modification, and finally extraction and fractionation. Currently, conventional vacuum and molecular distillation methods have been applied for the commercial production of tocopherols from sunflower oil deodorizer distillates but this methods have some drawbacks such as residual solvents, they need high temperature, large amounts of energy consumption, high production costs and the unreliable quality of the products that require further developments. Moreover thermal degradation of tocopherols is commonly caused by processing at high temperatures [7], so new alternative isolation methods are needed. Supercritical carbon dioxide ($scCO_2$) extraction is a promising alternative because of the carbon dioxide characteristics. ScCO2 is inert, non-toxic, has a low cost and a high volatility. Due to the last characteristic, the separation of the solvent after the extraction process is usually very easily achieved by depressurization. This way, reluctant process does not contain solvent residue and hence natural quality extracts can be obtained. Moreover, CO_2 has a near-ambient critical temperature so is suitable for thermolabile products and the process is carried out at low temperatures. However, the use of high pressure conditions to concentrate minor components makes the system need large amounts of energy.

Sunflower oil deodorizer distillate as such will not be feasible to work with $scCO_2$ for the isolation of minor components, due to its poor $scCO_2$ solubility. So, a pretreatment of the ODD is needed by means of a esterification reaction with an alcohol, e.g. ethanol [8]. In this process, triglycerides and FFA's are transformed to their ethyl esters (FAEE). In this work, ethanol is used in the esterification process in place of methanol, because of ethanol can be renewable when it is produced agriculturally and it is environmentally friendly.

The most important reaction involved in the esterification process is:

$$\mathrm{FFA} + \mathrm{EtOH} \leftrightarrow \mathrm{FAEE} + \mathrm{H_2O} \qquad (1)$$

The target of esterification process is to transform FFA into FAEE. Moreover these other reactions are carried out:

$$\mathrm{TG} + \mathrm{EtOH} \leftrightarrow \mathrm{FAEE} + \mathrm{H_2O} \qquad (2)$$

$$\mathrm{DG} + \mathrm{EtOH} \leftrightarrow \mathrm{FAEE} + \mathrm{H_2O} \qquad (3)$$

$$MG + EtOH \leftrightarrow glycerol + H_2O \qquad (4)$$

So glycerides are transformed in FAEE, glycerol and water using 3 molecules of ethanol.

1.2 SUCCeSS project

This master thesis will be performed in the framework of the 'SUCCeSS' project (SUperCritiCal Solutions for Side-Stream valorization) of FISCH (Flanders Innovation Hub for Sustainable CHemistry). A close collaboration will be established in this project between Ghent university and Eco Treasures, Cargill and VITO.

The initial focus of the 'SUCCeSS'-project is located on the production of isolates and concentrates of so-called' minor 'components from vegetable oil distillates by means of integrated, supercritical technologies (esterification, followed by extraction) and their use in the food and cosmetic industry. An ester fraction is produced as a by-product that will be evaluated for main grade technical applications such as biodegradable lubricants, bio-solvent and bio-surfactants.

This project aims to provide added value by

- Improving the utilization of specific organic (side) flows, which are currently being burned, by improved exploitation of valuable components (Cargill).
- The development of sustainable technologies and production processes for the isolation of these components (Eco Treasures and Indinox).
- The B2B marketing of these commodities in advanced technical applications and the cosmetics industry and possibly to the pharmaceutical industry (Gova, Tecter, Cargill). The targeted products, squalene and esters, have potential as new extracts and are marketed for the cosmetics industry ('minor' components) or as high-quality niche products for technical applications (ester-based products). The potential of including the concentrates 'minor' mixtures, ester-based products will be evaluated using the market knowledge of Cargill, Gova and Tectero.

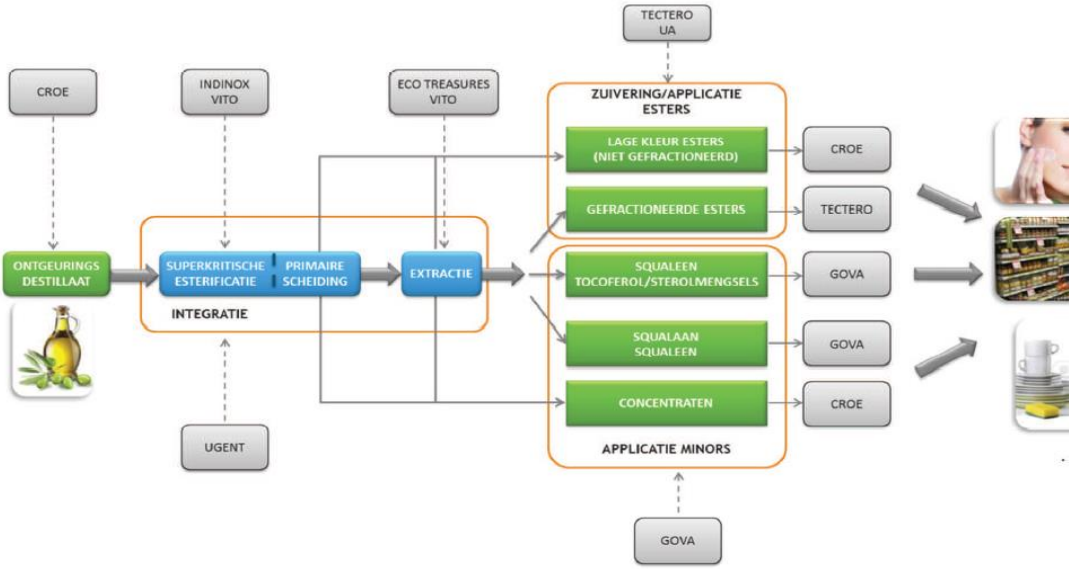

Figure 1-1. Structure of the project success: raw materials, process steps and the intended products. In various aspects, the partners are displayed.

1.3 Scope of this thesis

In this thesis, the implementation of an extraction process in the simulation software Aspen Plus® is studied. The aim of the thesis is isolation of minor compounds, especially squalene widely used as a protective agent in the cosmetics industry, from a side stream originating from the refining of several vegetable oils. To this end, an integrated (two-step) supercritical process (supercritical methanol esterification of the triglycerides/FFAs, followed by supercritical CO_2-extraction of squalene) will be used.

Chapter 2 of this thesis provides a survey about the different compositions of vegetable oils and of the oil deodorizer distillates obtained after the refining process. An insight into the structure and chemistry of minor components and the ester fraction, as well as their different applications and current production processes is acquired. Finally, a vision of how these minor components are currently isolated is provided.

One of the most important aspects of this thesis is the selection of a suitable thermodynamic model which represents suitable the behavior of the real mixture. In Chapter 3, the selection of model components for the real mixture as well as selection of the thermodynamic model are discussed. Further, the implementation of supercritical fluids in Aspen Plus® is described, together with the estimation of critical pure parameters. Finally, data regression for VLE and LLE systems is presented in this chapter.

Case study of ternary mixture is conducted for understanding the performance of the extractor column and are presented in Chapter 4 (Fatty acid methyl esters/Carbon dioxide/tocopherols). In the case study, influence of several factors on the phase equilibrium is studied, and a initial proposal for the tocopherol isolation process is given. In the same way, a real mixture is used for the simulation and those results are described in detail in Chapter 5.

In Chapter 6 a summary of the findings of this thesis is given, together with some concluding remarks.

2 LITERATURE SURVEY

2.1 Production of oil deodorizer distillates

As previous mentioned, there are two refining processes for the production of edible oils: physical refining and chemical refining. The main difference between chemical and physical refining lies in how acids and gum are removed. In physical refining gums are removal by special methods and FFA's by distillation. However, chemical refining remove FFA's chemically and gum and soap elimination is carried out by centrifugation as you can see in Figure 2-1 and Figure 2-2.

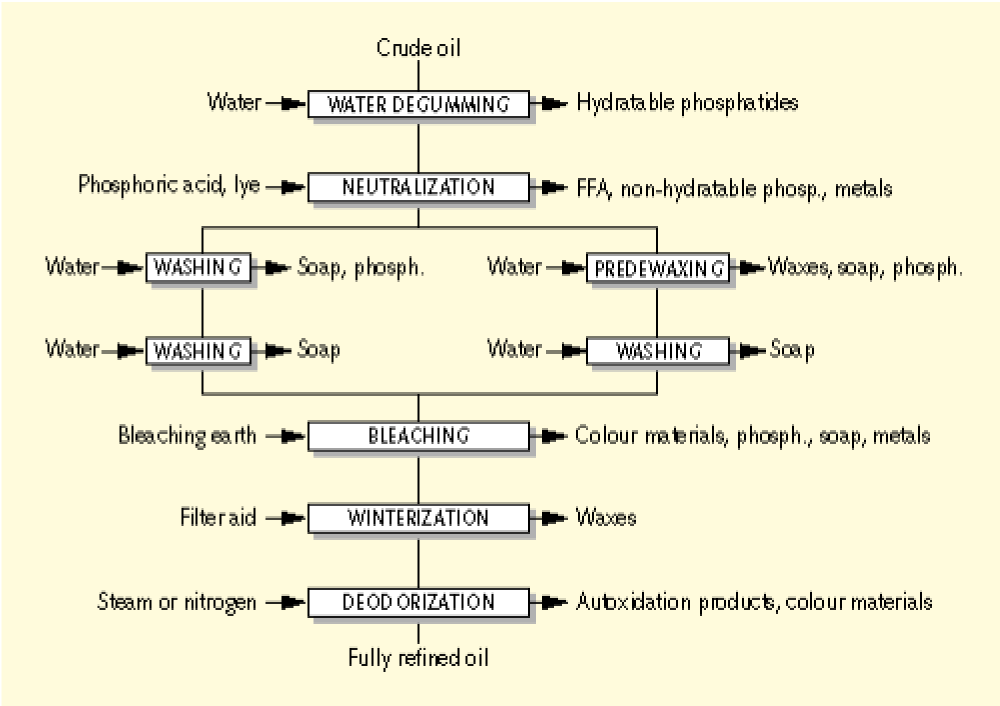

Figure 2-1. Chemical refining oil process [9].

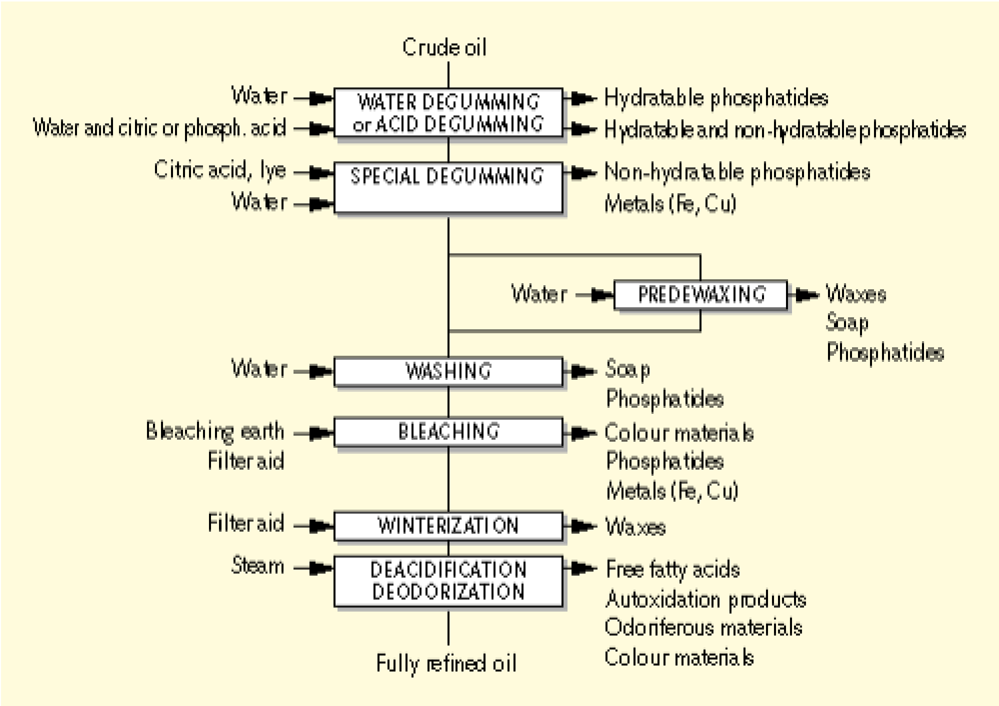

Figure 2-2. Physical refining oil procedure [9].

Classical chemical refining and physical refining produce different byproducts. The most important difference is the composition of the oil deodorizer distillate. The ODD from chemical refining is employed as a raw material by tocopherol and sterol plants.

Deodorizer distillates originating from physical refining are not attractive as a tocopherol and sterol source, because it is diluted with free fatty acids. The tocopherol content of sunflower deodorizer distillates from a physical refining process is lower (1-2 %) compared to chemical one (5-7 %) [9].

Nevertheless, physical refining of vegetable oils has several advantages compared to chemical one: higher yield, lower investment costs, less environmental impact due to no soap stock treatment and less waste water production. The most important drawback is that the process is more sensitive to the feedstock oil quality. Currently there is a tendency to change the chemical refining process, since the demand for more plant origin tocopherols and sterols is high [9].

In the next paragraphs, the different steps in a refining process are discussed in more detail.

2.1.1 The degumming process

During this process phospholipids contained in vegetable oils have to be removed. Phospholipids, also called phosphatides, are di-esters of glycerol and phosphoric acid. The phosphoric acid can be esterified by an alcohol, such as choline- or ethanolamine, or a polyol, such asinositol). Phosphoric acid in phosphatidic acid is not linked to any alcohol or polyol. Phosphatidic choline and phosphatidic inositol are completely hydratable, while the phosphatidic etanolamine is partially hydratable and phosphatidic acid is non hydratable when they form salt with cations such as Ca^{+2}, Mg^{+2} or when they are in non-dissociated forms. Degumming process ought convert the non-hydratable phosphatides to hydratable and then remove the phospholipids by hydrating and separation processes.

2.1.2 The pre-dewaxing process

Waxes are long chain fatty acid ester with long chain alcohol (C_{44}-C_{60}) and are present in crude vegetable oil. At room temperature, these waxes crystallize and cause “turbidity” in the oil, so it is necessary to remove them. The classical method is to cool down the oil allowing the wax crystallization and filter the produced crystals. The filtration proceeds in the presence of filter aid to prevent the clogging effect of the waxes. This operation has a huge influence on the operating cost because 1 kg of filter aid is required per ton of oil for each 100 ppm of waxes. Also, this decreases the refining yield: per kg of filter aid used, one kg of fat is lost.. Therefore, in physical refining, degumming step can be combined with pre-dewaxing.

2.1.3 The bleaching process

In the case of physical refining, bleaching process aims at the removal of coloring materials and also phosphatides and metals. This to reduce the bleaching earth and decreasing the solid waste production (environmental impact, disposal). There are a wide range of new highly activated bleaching earths and synthetic silica products available on the market. Synthetic silica products do not have effect on the plant colorings, but they have 4-6 times higher adsorption capacity for phosphatides, metals, soap than the bleaching earths [10]. There are some new and promising techniques like countercurrent bleaching and electrofiltration (ÖHMI) still under investigation [11]. Sunflower seeds or crude sunflower oil from some countries can contain PAHs (polyaromatic hydrocarbons). These originate from environmental pollution or from direct fuel gas drying of the seeds. These components, like benzo-a-pyrene, have to be removed during refining because of they are carcinogenic. Activated carbon is the only solution to remove heavy PAHs.

2.1.4 The deacidification process

The core process in physical refining is high temperature steam (or nitrogen) distillation under vacuum (100-200 Pa). Through this process the free fatty acids, the volatile flavor and smell compounds, oxidative byproducts, pesticides and light PAHs are removed by distillation. The final product has a neutral taste and smell, a light color and a long shelf life. During the last decade, the risk of trans isomer fatty acid formation during the refining process has become more worrying. Trans monoene isomer fatty acids have been reported as “bad”, since saturated fatty acids increase the risk of cardiovascular diseases by nutritional studies [9]. “Trans-free” margarine products, in which total trans fatty acid content is below 1% has been offering by margarine producers. In the same way, liquid oil producers should obtained refined oil with less than 1% and 1.5 % total trans for sunflower and rape respectively [9]. Another requirement for the fatty acid composition of the oil is the degree of isomerization should be max. 5-10 % of the total C18:3 and max. 0.7-1 % of the total C18:2 [3].

2.1.5 The nitrogen saturation-bottling

This process is necessary because vegetable oil is sensitive to oxidation. A solution is the saturation of the oil with an inert gas, such as nitrogen, just after cooling the oil and before leaving the deodorizer. The dissolved nitrogen will make oxygen diffusion difficult.

By-products, like tocopherols, sterols and squalene, produced during deodorization and deacidification are distilled together with free fatty acids, and volatile and flavor components. Keeping these natural components in the oil as much as possible (mild conditions) is a priority. If the process is carried out below 473 K at least 85 % of the original tocopherol content is preserved [9].

2.2 Vegetable oils

Vegetable oils are normally obtained from beans or seeds. Oil extraction generally generates two valuable commodities an oil and a protein-rich meal. Seed extraction is achieved by pressing and/or solvent extraction. Fats from plants seeds remain in a fluid state at room temperature because they are polyunsaturated. Most of oils need a refining process but some oils, such as virgin olive oil, are used without any treatment.

There are different kinds of commercially refined vegetable oils including rapeseed oil, soybean oil, canola oil, corn oil, sunflower oil, safflower oil, olive oil, palm and peanut oil. Table 2-1 shows that soybean oil, palm oil, rapeseed oil and sunflower oil have become market dominants.

Table 2-1. Annual average production in million tonnes of oils from 1976 with forecast up to 2020 [2].

	1976-1980	1986-1990	1996-2000	2006-2010	2016-2020
World total	52.65	75.66	105.06	165.65	184.77
Soybean oil	11.23	15.28	23.14	33.6	41.12
Cottonseed oil	2.83	3.64	4	5.35	6.51
Groundnut oil	3.01	3.7	4.55	5.72	6.38
Sunflower oil	4.21	7.25	9.11	12.43	16.97
Rapeseed oil	3.01	7.51	12.64	17.72	22.69
Sesameseed oil	0.51	0.64	0.7	0.86	0.96
Corn oil	0.83	1.35	1.91	2.49	3.16
Olive oil	1.68	1.8	2.47	2.75	2.98
Palm oil	3.69	9.22	18.72	31.43	43.36
Palmkernel oil	0.46	1.21	2.34	3.84	5.28
Coconut oil	2.85	3.07	3.01	3.7	4.55
Fish oil	1.13	1.53	1.25	1.18	11.59
Linseed oil	0.79	0.73	0.7	0.81	0.97
Castorseed oil	0.32	0.4	0.46	0.71	0.78

Soybean oil is the most produced worldwide and one of the most traded oil. This is due to its high-quality protein, its value as edible oil and its agronomic characteristics. Currently, palm oil takes second place in the list of oils produced and will probably take the first place in 10-15 years. It is already the oil traded in largest amount, it represents 44 % of all oil and fat exports.

In the past two decades, rapeseed oil has become in one of the sources most used for vegetable oils production. Rapeseed oil has a high level of erucic acid. Canola oil, is the result after a modification of the original high-erucic acid content in rapeseed oil. This oil is considered one of the best nutritional edible oil available [2].

In this thesis we will be focused on sunflower oil because of it is the source of our studied process.

2.2.1 Sunflower oil

Traditional sunflower oil is characterized by a high linoleic acid content. Linoleic composition varies, but sunflower oils presents an average of 65-70 % linoleic acid from most common varieties. Another categories are high-oleic oil (>80% oleic acid and only 5–9% linoleic acid) and mid-oleic varieties (55–75% oleic acid and 15–35% linoleic acid) [2].

The typical fatty acid composition of these three varieties of sunflower oils is represented in Table 2-2.

Table 2-2. Typical fatty acid composition of three varieties of sunflower oil (%) [2].

Fatty acid	Traditional	High-oleic	Mid-oleic
Total saturates	11-13	9-10	<10
Oleic acid	20-30	80-90	55-75
Linoleic acid	60-70	5-9	15-35
Linolenic acid	<1	<1	<1

Minor components compositions in sunflower oil is shown in Table 2-3 .

Table 2-3. Minor components in crude sunflower oil [2].

Cultivar	Tocopherols (ppm)	Sterols (%)	Phospholipids (%)	Carotenoids (ppm)
Armavriski 3497	684	0.3	0.86	1.1
Peredovik	672	0.28	0.75	1.3
Salyut	517	0.26	0.72	1.5
VNIMK 8931	698	0.3	0.82	1.6

Sunflower oil is resistant to photo-oxidation because of its high content in α-tocopherol. γ-tocopherol provides oxidative stability against autoxidation but these levels in sunflower oil are low. For comparison, values for tocopherols and sterols from soybean and sunflower oil are shown in Table 2-4 and Table 2-5. Soybean oil have much higher levels of γ, δ on the other hand, α –tocopherol levels are higher in sunflower oil.

Table 2-4. Tocopherols composition (ppm) in crude sunflower and soybean oil [12].

Oil	α	β	γ	δ
Sunflower	608	17	11	-
Soybean	116	34	737	275

Sterol distribution do not show many differences between both oils. Sterol esters composition are higher in sunflower oil.

Table 2-5. Typical distribution (%) sterols and sterol esters in crude sunflower and soybean oil [13].

Oil	Sterols	Sterol esters
Sunflower	72	28
Soybean	97	3

2.3 Sunflower deodorizer distillate

The stream collected from the steam distillation of sunflower oil is called sunflower deodorizer distillate . It is a mixture of free fatty acids, tocopherols, phytosterols and their esters, squalene and secondary lipid oxidation products. Quality and composition of SDD varies because of feedstock oil composition and on processing conditions. Table 2-6 shows the composition of an example of an SDD, obtained by the refining sunflower oil from the company Cargill.

Table 2-6. Example of a composition of a sunflower-deodorization distillate produced by Cargill [14].

Component	**Wt %**
FFA	43.03
Total tocopherol content	3.05
α-tocopherol	2.85
β-tocopherol	0.12
δ-tocopherol	0.05
γ-tocopherol	0.03
Total sterol content	8.27
Brassicasterol	0.04
β-sitosterol	4.19
Campesterol	0.65
Cholesterol	0.07
Minor sterol	1.71
Stigmasterol	0.93
Steryl esters	1.12
Triglycerides	14.51
Diglycerides	1.98
Monoglycerides	2.07
FAME	1.16
Squalene	2.27

As can be seen, the major component of ODD are FFA's and TG. Minor compounds compositions in this ODD represents 13.5 % of the total feed. The FFA's present are badly soluble in supercritical carbon dioxide so the first step of the process is to transform FFA's and TG into corresponding esters.

2.3.1 Minor components

'Minor' components such as squalene, sterols and tocopherols presents in ODD are valuable for many companies. Nowadays tocopherols and sterols are especially synthetically produced by means of a series of complex chemical reactions [15]. However, there is a growing interest in the extraction of these components it natural sources. This can be attributed, among other things to the growing market of functional food, in which both tocopherols and sterols, can be used as active ingredients [16, 17].

2.3.1.1 Tocopherols

Tocopherols are organic chemical molecules with the structure of several methylated phenols, many of them have vitamin E activity. Vitamin E has eight different forms, four tocotrienols and four tocopherols. All have in their structure a chromane ring, with an hydrophilic side chain formed by an hydroxyl group that can donate a hydrogen atom to reduce free radicals and a long hydrocarbons chain (hydrophobic) that allows for penetration into biological membranes.

Both tocopherols and tocotrienols have α (alpha), β (beta), γ (gamma) and δ (delta) positions of methyl groups on the chromanol ring. Tocopherol structure is shown in Figure 2-3 till Figure 2-6.

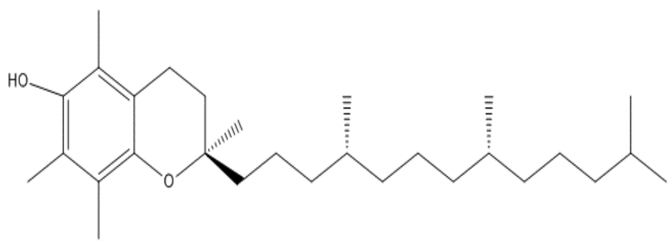

Figure 2-3. α-tocopherol structure.

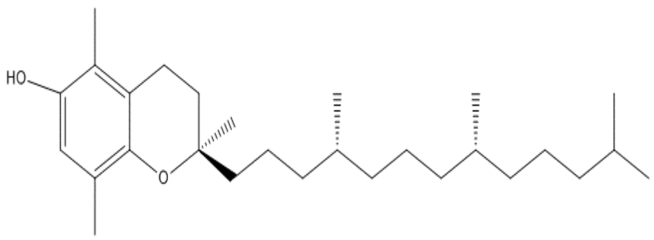

Figure 2-4. β-tocopherol structure.

Figure 2-5. γ-tocopherol structure.

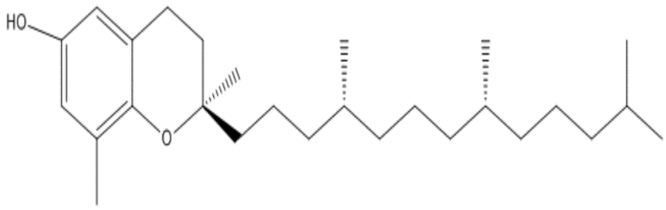

Figure 2-6. δ-tocopherol structure.

Tocopherols receive the following E-numbers when they are used as a food additive: E-306 (α-tocopherol), E-307(β-tocopherol), E-308(γ-tocopherol)and E-309 (δ-tocopherol). Using these compounds as an additive is approved in the EU, USA, Australia and New Zealand. In Europe, α-tocopherol is mainly common which main origin is olive and sunflower oils [18]. In America the most consumed form is γ-tocopherol because of a higher intake of soybean and corn oil [18, 19].

Commercial production of tocopherols from ODD [20-23] is based in molecular distillation also called short-path distillation. This process is characterized by high vacuum inside the column, short contact during the distillation because of high temperatures and the evaporator and the condenser are close (20 to 70 mm) [21] . Some problems are present in the commercial production of tocopherols using molecular distillation. First of all, molecular distillation process is usually performed with multistage columns (3 to 5) at high vacuum (0.1 to 10 Pa) and high temperature (433 to 503 K). An important economic factor is the equipment, a high quality vacuum pump is needed for ensuring enough vacuum condition for each distillatory so equipment investment and operation cost are very large. As a result of this, the operation temperature has to be increased to compensate when vacuum pressure decrease for stabilizing the concentration of the fractions. Consequently such fluctuations lead to a varied quality of the tocopherol final product. Furthermore, molecular distillation definition is not very accurate because rectification effect due to fraction condensation and reflux is not exist. As we know, this rectification effect is the main difference between distillation and vaporization. In addition entrainment phenomenon probably occurs in molecular distillation and influences on the selectivity separation. Third, the general idea that short contact of the components at high temperatures during distillation process does not cause any degradation and does not affect the quality of the product. Despite all, Mau [23] investigations on concentrating tocopherols by molecular distillation have reported the existence of tocopherol dimmers and other degradation products at 433 to 493 K, even though working with very low pressure (less than 0.133 Pa) total recovery of tocopherols in every stream was only about 75.16 % of the initial amount of tocopherols in feed. Finally, in the commercial operation process the residence time of tocopherols in the second or third distillation column is no less than 1 hour, a long time for a separation operation [24]. For these reasons, development of new and promising isolation techniques is required.

2.3.1.2 Sterols

Sterols, also called steroid alcohols, are an important class of organic molecules belonging to the group of the steroids. They are present in plants, animals and fungi, the most famous type of animal sterol is cholesterol. Cholesterol is part of animal cell membrane structure and is a precursor to fat-soluble vitamins and steroid hormones.

Sterols of vegetable origin are called phytosterols and sterols of animal origin are called zoosterols. Remarkable phytosterols include campesterol, sitosterol and stigmasterol are mostly supplied by vegetable oils. The most abundant components are vegetable oils is β-sitosterol (Figure 2-7) and stigmasterol (Figure 2-8) [25].

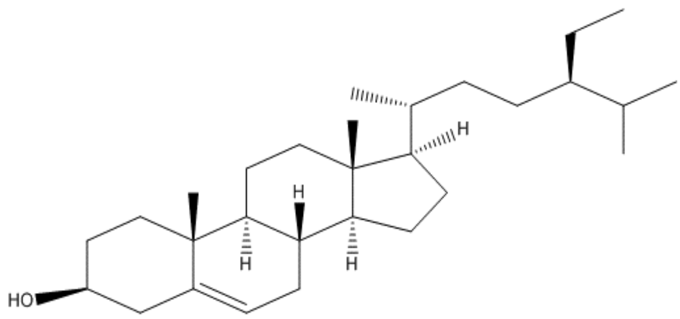

Figure 2-7. β-sitosterol structure.

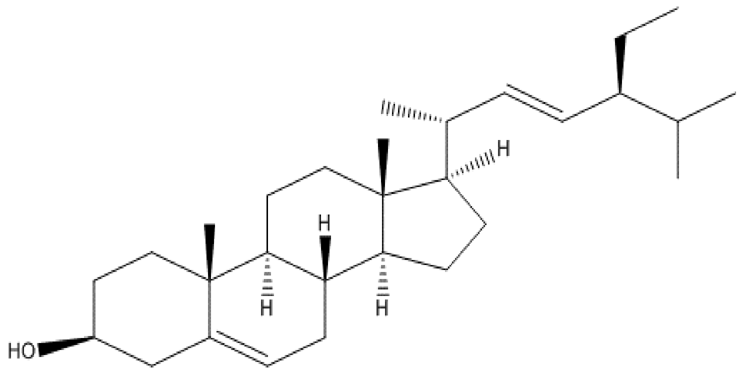

Figure 2-8. Stigmasterol structure.

Phytosterols have several applications, it has been demonstrated in clinical trials to block cholesterol absorption sites in the human intestine, so helping to decrease cholesterol absorption in humans [26]. Nowadays, they are approved for use as a food additive by the U.S. Food and Drug. Moreover, preliminary investigations has shown that phytosterols may have anticancer effects.

As a natural source of sterols nuts and oils come into consideration. They contain a higher concentration of sterols (> 1%) as compared to fruit and vegetables (<0.05%). Two important raw materials for the isolation of sterols are vegetable oils and tall oil [6].

All these 'minor' components, however, content is too small in their natural matrix to be isolated in an economical manner. one might also hereby enter into competition in an unauthorized manner with the food chain.

2.3.1.3 Squalene

Squalene (2,6,10,15,19,23-hexamethyl 2,6,10,14,18,20- tetracosahexaene the structure is shown in Figure 2-9) is a terpenoid hydrocarbon present in fish liver oils . Its natural or hydrogenated form, squalene is used in cosmetic preparations as a emollient or moisturizing agent. Squalene is a metabolite and precursor of the cholesterol synthesis, it can be converted into useful HDL-cholesterol in our body increasing the level of good cholesterol and reducing the level bad LDL-cholesterol.

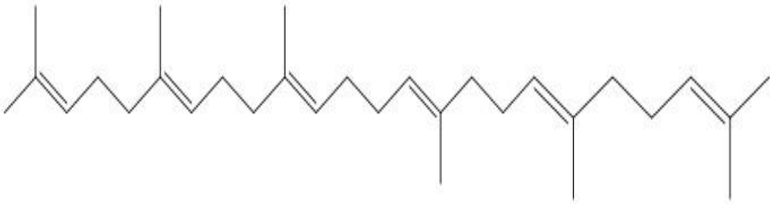

Figure 2-9. Squalene structure.

The traditional source of squalene is the livers of deep sea sharks which is composed of 40-80% for this compound. However, the extraction of squalene from the liver oil of deep-sea sharks will continue to lie under fire because this particular species of sharks are threatened with extinction. As the cosmetics market this is very sensitive, leading cosmetic companies like L'Oreal and Unilever, decided to stop the use of squalene from deep-sea sharks, also in response to the increasing pressure from international organizations that fight for the preservation of the oceans and protecting marine ecosystems. This means that one is looking for alternative sources of squalene can be isolated in an efficient and inexpensive way. Vegetable oils which squalene is present in a residual fraction of the oil, were all identified as possible sources, including through the same quality character to the squalene of animal origin.

Several sources have already been tested as a source of squalene and other 'minor' components as an alternative to liver oil of deep-sea sharks. The literature study can be found on the extraction of these 'minor' components from seeds, grains, nuts, pulp of olives, vegetable oils and ODD [4, 16, 17, 27-31]. Often the natural resources rather than waste concerns being worked.

It is known that the unsaponifiable fraction of olive oil contains squalene (60-75%) but, for economic reasons, its recovery directly from the oil is not feasible. On the other hand, olive oil deodorization distillate is inexpensive and readily available and contains squalene in high concentration, so that its purification and isolation by different was have been proposed [14].

2.3.2 Esters

Fatty acid ethyl esters (FAEE) are esterification products of fatty acids and ethanol. Ethyl oleate is a fatty acid ester formed by the condensation of oleic acid and ethanol. It is a colourless to light yellow liquid.

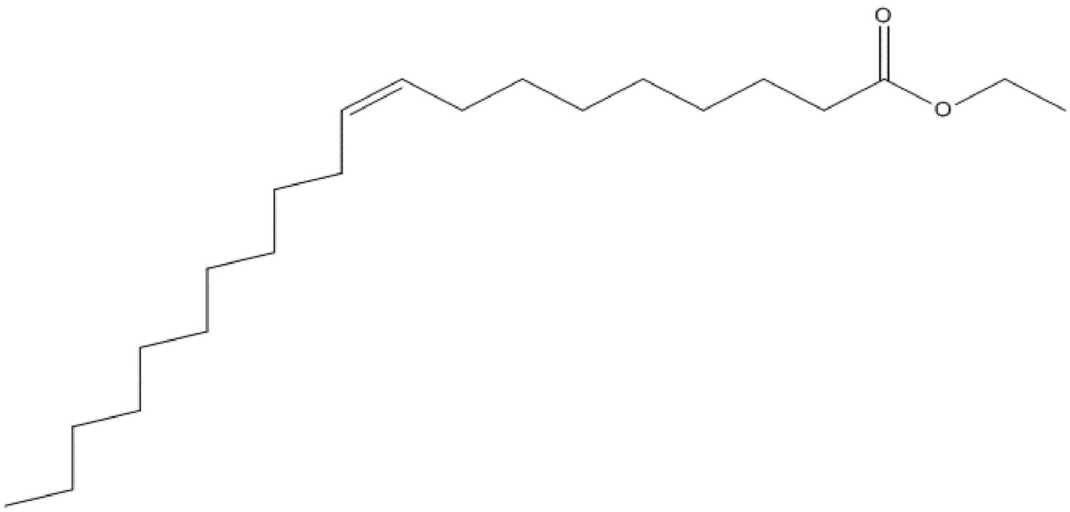

Figure 2-10. Ethyl oleate structure.

Esters can be used for several applications such as agro chemicals, coatings, inks, solvents, food, lubricants, personal care and pharmaceutics. Moreover they are interesting raw materials to produce products with industrial value being a renewable and biodegradable building block. Many esters are responsible of favor and taste, they are present in several flowers and fruits such as strawberries, pears and apples therefore esters are widely used as a fragrance components in cosmetic products and as a flavorings components in food industry [14]. The use as a biofuel is also an option and is already applied on a large scale [32]. The use of biofuel, however, serves more as 'low value' and 'bulk' to be considered in comparison with the other applications mentioned above.

The conclusion is that the ester fraction obtained from the integrated process not only as the side stream of the purification of the 'minor'- fraction should be considered, but also has the potential to be a full product flow for various applications. Tectero company is interested in evaluate the esters produced.

2.4 Process to isolate the minor components

In the past, recovering tocopherols, squalene and sterols from deodorizer distillates and related mixtures has been difficult and expensive. One of the most important difficulty is obtaining fractions enriched in tocopherols and/or sterols, since sterols and tocopherols have similar molecular weights and volatilities [33]. Streams with high concentrations of phytosterols and tocopherols with good yield are difficult to obtain [34]. Moreover, in order to separate the squalene from ODD, the main challenge is the separation between itself and the other components, especially in the case of the couple of components: tocopherol-squalene, tocopherol–fatty acids, tocopherol–sterol and sterol– squalene[4].

Another difficulty in the isolation process is that exposing the deodorizer distillate to high temperatures at which sterols and tocopherols vaporize for extended periods thermal degradation of ODD takes place. These temperatures may cause conversion of fatty acids to undesirable trans isomeric forms and tocopherols degradation [35].

Classical methods for isolating tocopherols, squalene and sterols include solvent extraction, chemical treatment, crystallization, complexation, and molecular distillation [36]. In general, most processes have two main parts. In the initial step, they are designed to remove either fatty acids or sterols, followed by tocopherol and squalene concentration by other methods.

2.4.1 Crystallization

Based on experimental results crystallization appears to be a simple and efficient process for isolating sterols and tocopherols from ODD of soybean oil. These conventional method, however, make use of organic solvents [4], which is undesirable for the intended applications [14]. This process has the advantage of not using high pressure neither high temperature, so it does not cause tocopherol oxidation. Nevertheless, crystallization has several disadvantages. Currently solvents available are not enough selective to obtain a suitable separation between the unsaponifiables (e.g. tocopherols, squalene, sterols) and FFA's. To solve this problem, it is often necessary to use more than one solvent increasing the cost of recovery and recycling of these solvents. In addition, solvents are used in very large proportions compared to the quantity of material feeding the extraction process and is necessary additional processes for recovery the valuable products. These factors make solvent based-processes, expensive and less environmentally friendly proving to be unattractive.

2.4.2 Saponification

Saponification is a common way for isolation of minor compounds from ODD. It produces an alkali metal soap which, because of its insolubility in the solvent used in the process, permit the separation of the dissolved tocopherols. The process is costly and tocopherols yield is very low. Sterols are isolated from the resulting concentrate mixture by crystallization [37].

2.4.3 Enzymatic modification

In order to modify chemical or physical properties of some compounds selective biotransformation by enzymatic reactions can be used. Thereby, utilization of enzymes makes easier tocopherols separation by transformation sterols to steryl esters, aglycerols to free fatty acids and free fatty acids to fatty acid esters (FAMEs or FAEEs). After that transformation, is easier to separate the new product mixture by distillation or supercritical fluid extraction. Enzymatic processes present difficulties such as numerous parameters are involved: moisture content, enzyme concentration, time, temperature.. etc [5, 38].

Due to similar boiling points between tocopherols and FFAs the conversion of FFAs to FAMEs or FAEEs is necessary to achieved tocopherol purification [39]. In addition, if methanol is used for the esterification, sterol transformation is inhibited. To avoid this problem, a lipase can be used to carry out hydrolysis of aglycerols and then esterification of sterols with free fatty acids. The main drawback of this method is the high costs due to the use of enzymes at industrial level.

2.4.4 Molecular distillation

Molecular distillation is also have been already used in the commercial production of tocopherols from oil deodorizer distillates of soybean oil [14]. These conventional methods are, however, characterized by a high production cost, and result in an unstable product [40, 41]. For that separation FFAs are converted to fatty acid methyl esters, which are more easily separated by vacuum distillation because of their higher vapor pressure. Nevertheless, this transformation made the whole process more complicated and labor-intensive than the saponification process. Another drawback is the high levels in energy consumption to achieve high vacuum during the operation obtaining an expensive final product.

Most of the substances presents in deodorizer distillate are molecules of high molecular weight and thermally sensitive. These mixture properties hinder the separation or purification of these compounds through traditional methods, because they are decomposed when they are exposed to high temperatures. Due to this problem, an alternative procedure is the use of molecular or short-path distillation. This method consist of transferring molecules from the surface of an evaporating liquid to the cooled surface of a condenser through a short path (2-5 cm). In this way thermal decomposition of heat-sensitive materials is almost neglected [42] because the mixture are submitted to relatively low temperatures and short residence times [42]. Moreover, this process does not use toxic or flammable solvents as the separation agent avoiding toxicity and environmental problems.

2.4.5 Supercritical fluid extraction.

Commercial production of minor compounds from ODD have been applied using conventional methods (vacuum and molecular distillation). However, there are some drawbacks such as employing residual solvents, high temperature, high levels of energy consumption (large production costs) and the unreliable quality of the products that require more developments. New alternative isolation methods are desired since thermal degradation of tocopherols is caused by processing at high temperatures [7].

A promising technique is supercritical fluid extraction using carbon dioxide. The process consist in flows carbon dioxide through a mixture of interest at CO_2 supercritical conditions until it reaches an extractor. Supercritical carbon dioxide has very interesting mass transfer properties: a low viscosity, a high diffusivity and a low surface tension providing selective extraction, fractionation and purification. Carbon dioxide is the most suitable supercritical fluid solvent for the isolation of natural products in foods and medicines because of its inertness, nontoxicity, low cost and high volatility. Furthermore, the easy post-reaction separation of the solvent by depressurization permit obtain natural quality extracts. In addition, carbon dioxide has a near-ambient critical temperature (304 K), so CO_2 is very useful for thermolabile natural products.

High pressure conditions are necessary to concentrate tocopherols so the process is energetically expensive, but the industrial process can be economically viable using conditions of $9\ 10^6$ Pa and 313 K [15]. At these conditions, only fatty acids/tocopherol separation is achieved [16]. An increase in pressure and temperature increases the oil extraction and tocopherol recovery, although different pressure-temperature conditions need to be used to separate the different components (sterols, tocopherols and squalene). Compression cost of this process represents more than 59 % of de total production cost [15], therefore recycling the solvent improve a lot the viability of the process. Ass discussed above, ODD solubility with SC-CO_2 is low. Therefore pretreatment of the raw materials is needed through esterification of free fatty acids in to methyl esters.

2.7. Criteria project

Finally, it is also important to note that there were a number of criteria by the SUCCeSS project for both the supercritical CO_2 extraction and esterification. When performing simulations and calculations takes into account the limitations on the parameters used [14].

- Supercritical alcohol esterification:

- Glycerides and free fatty acids conversion >95 %.
- Residence time inside reactor <30 min.
- Reaction temperature <553 K and pressure $<1.5\ 10^7$ Pa.\
- Ratio alcohol/ODD <1 g/g.

- Supercritical CO_2 extraction
  - Minimum squalene yield mass recovery of 95 %. At least purity of squalene 95 wt%.
  - Minimum esters yield mass recovery of 90 %. Esters fraction purity > 90 wt%.
  - Total feedstock flow treated > 10 l/h.
  - Maximum CO_2 feed extraction ratio of 10 v/v%.
  - Pressure should be optimize as low as possible. Maximum pressure allowed 2.80 10^7 Pa.
  - Maximum temperature allowed 353 K due to thermolabile compounds are presents.
  - Residence time in the column must be lower than 5 min.

Based on the criteria, the following process flow diagram for isolating minor compounds is proposed.

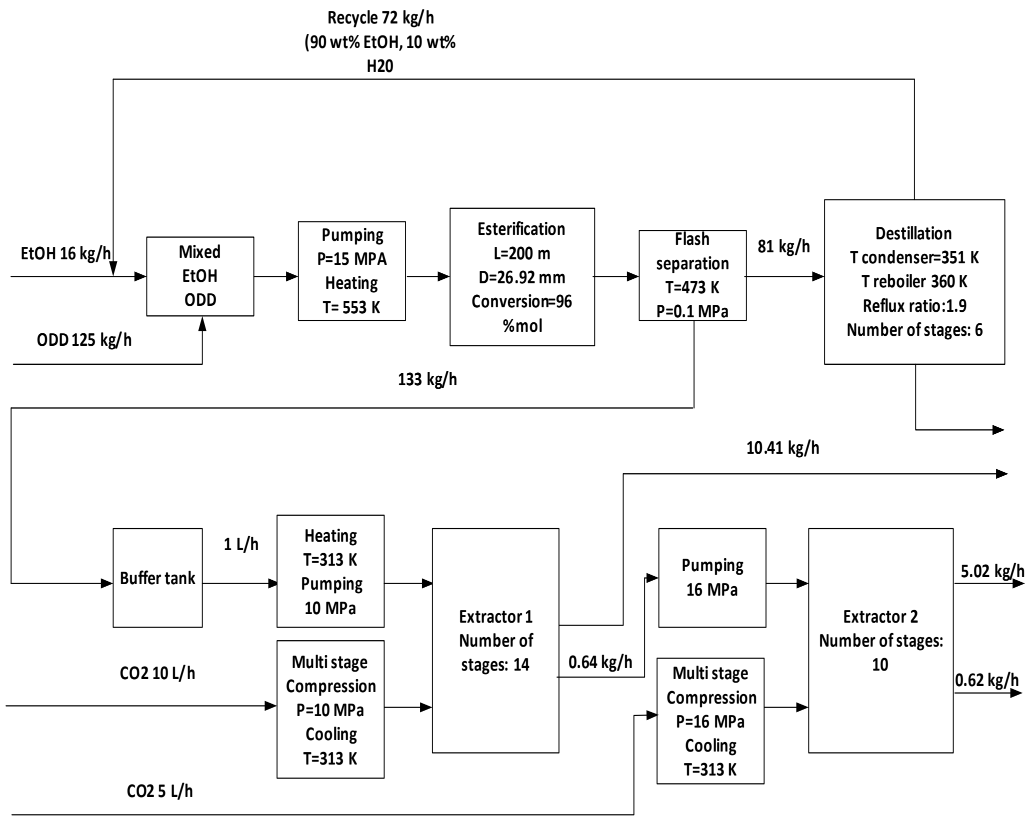

Figure 2-11. Block diagram for the supercritical esterification followed by supercritical extraction process.

The feedstock ODD is a side stream for the refining of edible oil process. It is mixed with ethanol and is pumped up and heated to 15 MPa and 553 K respectively to achieve supercritical ethanol conditions. Then esterification takes place in a tubular reactor already existing in the plant with a length of 200 m and a diameter of 26.92 mm achieving a conversion of 96 % mol from FFA into FAEE. Next, one want to obtain a stream without ethanol and enriched in minor compounds. This process take place in a flash separator at 473 K and 0.1 MPa followed by a distillation column. The obtained ethanol is recycled to ethanol feedstock. The fraction enriched in esters and minor compounds is stored in a buffer tank and goes to the extraction section where is heated to 313 K and pumped up to 10 MPa this stream is introduced by the top of the extraction column. Carbon dioxide stream is compressed in a multistage compressor to 10 MPa with refrigeration after every compression stage and is cooled in the last stage to 313 K. This stream is introduced by bottom in the extraction column. The extract phase obtained is a side-stream of the process, on the other hand, the refined phase is pumped up to 16 MPa and introduced by top to a second extraction column. A second carbon dioxide stream flows from bottom to the top into the extraction column. The extract phase content a high amount of carbon dioxide (which should be recover by depressurization) and almost all the squalene from ODD. The refined phase is a stream enriched in sterols and tocopherols

3 PROCEDURES FOR SIMULATION

3.1 Selection of the thermodynamic model

Property calculations are requested to generate results by unit operations models and they have a high impact on the calculation results. Phase equilibrium is the key thermodynamic property calculation [43].

One system at equilibrium follow the next equation:

$$f_i^v = f_i^l \tag{5}$$

Where:

$$f_i^v = Fugacity\ of\ component\ i\ in\ the\ vapor\ phase \tag{6}$$

$$f_i^l = Fugacity\ of\ component\ i\ in\ the\ liquid\ phase \tag{7}$$

There are two methods to represent the fugacities from the phase equilibrium in terms of measurable state variables by applied thermodynamics: the equation-of-state and the activity coefficient method.

In the equation of state method:

$$f_i^v = \varphi_i^v y_i p \tag{8}$$

$$f_i^l = \varphi_i^l x_i p \tag{9}$$

The fugacity coefficient φ_i^α is obtained from the equation of state:

$$ln\,\varphi_i^\alpha = \frac{-1}{RT}\int_\infty^{V\alpha}\left[\left(\frac{\partial p}{\partial n_i}\right)_{T,V,n_{kj}} - \frac{RT}{V}\right]dV - ln\,Z_m^\alpha \tag{10}$$

Where:

α = v (vapor phase) or l (liquid phase)

V = Total volume

n_i = Mole number of component i

In the activity coefficient method:

$$f_i^v = \varphi_i^v y_i p \quad (11)$$

$$f_i^l = x_i \gamma_i f_i^{*l} \varphi_i^v \quad (12)$$

The fugacity coefficient is calculated according to equation of before.

γ_i = Liquid activity coefficient of component i

f_i^l= Liquid fugacity of pure component I at mixture temperature.

Aspen property methods are based on either the equation-of-state method or the activity coefficient method for phase equilibrium calculations. Through phase equilibrium methods, other thermodynamic properties, such as enthalpies and molar volumes calculations are determined.

Using an equation-of-state method, all properties can be obtained from the equation of state for both phases. Using an activity coefficient method, an equation of state is used to calculate the vapor phase properties, the same that using an equation-of-state method. On the other hand, liquid properties calculations are done from summation of the pure component properties adding a mixing term or an excess term .

3.1.1 Equation of state method

The partial pressure of a component i in a gas mixture is:

$$p_i = y_i p \quad (13)$$

In an ideal gas mixture, fugacity of component i is equal to its partial pressure however in a real mixture is the effective partial pressure:

$$f_i^v = \varphi_i^v y_i p \quad (14)$$

φ_i^v is a correcting factor called fugacity coefficient. For a vapor at low pressure, φ_i^v is close to unity. The same equation can be applied to a liquid:

$$f_i^l = \varphi_i^l x_i p \tag{15}$$

A liquid differs much more from an ideal gas than a real gas, so the liquid has fugacity coefficient that is very different from unity. For instance, the fugacity coefficient of liquid water at mild conditions is about 0.03 [44].

Pressure, volume and temperature (P, V, T) of pure components and mixtures are described by an equation of state. Most of them have terms to represent interaction forces between molecules. Every thermodynamic property can be calculated using the equation-of-state from ideal gas properties of the same mixture at the same conditions.

3.1.1.1 Vapor-liquid equilibrium

The vapor-liquid equilibrium is calculated by substituting Eq. (14) and (15) in (5) resulting in:

$$\varphi_i^v y_i = \varphi_i^l x_i \tag{16}$$

Fugacity coefficients calculations are done through the equation-of-state Eq (**10**). Vapor-liquid equilibrium calculation is the same for supercritical and subcritical components.

Phase equilibrium depends on temperature and on pressure. There is a pressure range where liquid and vapor phase co-exist. However, at the critical point just one phase exist and there are not any difference between vapor and liquid. Eq. (**16**) represent that behaviour because $\varphi_i^v$and $\varphi_i^l$are evaluated by the same equation of state. Equations-of-state can represent the pressure dependency in vapor-liquid equilibria very well, but they cannot represent critical phenomena correctly.

3.1.1.2 Liquid-liquid and liquid-liquid-vapor equilibria

Vapor-Liquid equilibria are more affected by pressure changes than liquid-liquid equilibria. The activity coefficient method can represent phase equilibria at low pressure as a temperature function but with pressure changes the equation-of-state method is needed.

Applying the equation of state to liquid-liquid equilibria we obtain:

$$\varphi_i^{l1} x_1^{l1} = \varphi_i^{l2} x_i^{l2} \tag{17}$$

And applying to liquid-liquid-vapor equilibria:

$$\mathrm{\varphi_i^v y_i = \varphi_i^{l1} x_i^{l1} = \varphi_i^{l2} x_2^{l}} \tag{18}$$

All the fugacity coefficients are evaluated using the same equation-of-state and they are function of the composition, the temperature and the pressure. Therefore the pressure dependency of liquid-liquid equilibria can be described.

3.1.1.3 Properties calculation using an Equation-of-State method

Using fundamental thermodynamic equations properties are calculated.

- Fugacity coefficient:

$$f_i^v = \varphi_i^v y_i p \tag{19}$$

- Enthalpy departure:

$$\begin{aligned}\left(\mathrm{H_m - H_m^{ig}}\right) = -\int_\infty^{\mathrm{V}} \left(\mathrm{p} - \frac{\mathrm{RT}}{\mathrm{V}}\right) \mathrm{dV} \\ - \mathrm{RT}\ \ln\left(\frac{\mathrm{V}}{\mathrm{V^{ig}}}\right) + \mathrm{T}\left(\mathrm{S_m - S_m^{ig}}\right) + \mathrm{RT}(\mathrm{Z_m} - 1)\end{aligned} \tag{20}$$

- Entropy departure:

$$\left(S_m - S_m^{ig}\right) = -\int_\infty^V \left[\left(\frac{\partial p}{\partial T}\right)_v - \frac{R}{V}\right] dV + R\, ln\left(\frac{V}{V^{ig}}\right) \tag{21}$$

- Gibbs energy departure:

$$\left(G_m - G_m^{ig}\right) = -\int_\infty^V \left(p - \frac{RT}{V}\right) dV - RT\ \ ln\left(\frac{V}{V^{ig}}\right) + RT(Z_m - 1) \tag{22}$$

- Molar volume:

Solve p(T,V_m) for V_m.

Fugacities calculation from a given equation-of-state are done through Eq. (19). The other thermodynamic properties of a mixture can be estimated using the departure functions:

- Vapor enthalpy

$$H_m^v = H_m^{ig} + (H_m^v - H_m^{ig}) \tag{23}$$

- Liquid enthalpy:

$$H_m^l = H_m^{ig} + (H_m^l - H_m^{ig}) \tag{24}$$

The molar ideal gas enthalpy, H_m^{ig} is estimated by:

$$H_m^{ig} = \sum_i y_i \left[\Delta_f H_i^{ig} + \int_{Tref}^{T} C_{p,i}^{ig}(T)dT \right] \tag{25}$$

Where:

$C_{p,i}^{ig}$ = Ideal gas heat capacity

$\Delta_f H_i^{ig}$ = Standard enthalpy of formation for ideal gas at 298.15 K and 1 atm

T_{ref} = Reference temperature = 298.15 K

Entropy and Gibbs energy can be computed in a similar manner:

$$G_m^v = G_m^{ig} + \left(G_m^v - G_m^{ig}\right) \tag{26}$$

$$G_m^l = G_m^{ig} + \left(G_m^l - G_m^{ig}\right) \tag{27}$$

$$S_m^v = S_m^{ig} + \left(S_m^v - S_m^{ig}\right) \tag{28}$$

$$S_m^l = S_m^{ig} + \left(S_m^l - S_m^{ig}\right) \tag{29}$$

Volume of vapor and liquid phase is computed by solving p(T,Vm) for Vm or through an empirical correlation.

3.1.1.4 Advantages of the Equation-of-State method

Equation-of-state methods can be used over wide ranges of temperature and pressure, even in supercritical regions. Vapor and liquid phases can be estimated with a small amount of component data for ideal or slightly non-ideal systems. They are recommended for modelling hydrocarbon system with light gases such as CO_2.

Non-ideal systems need obtain binary interaction parameters from regression of experimental vapor-liquid equilibrium data . Some pairs of binary interaction parameters are available in the Aspen Physical Property System.

Highly non ideal systems, such as alcohol-water can be represented by equation-of-state methods at low pressures and using the flexible and predictive equation of state at high pressures [43].

3.1.2 Activity coefficient method

For ideal liquid solution, liquid fugacity is directly proportion to the mole fraction:

$$f_i^l = x_1 f_i^{*,l} \tag{30}$$

An ideal solution assumes all molecules in the liquid solution have the same size and shape and are randomly distributed. Energy asymmetry occurs for example in the mixture alcohol and water.

Including the activity coefficient γ_i, the deviation of the mixture from ideality is represented:

$$f_i^l = x_i \gamma_i f_i^{*l} \tag{31}$$

Fugacity can be understood as the tendency to vaporize. If compounds are in the vapor phase, their average distance increases so the activity coefficients will be greater than unity which means a repulsion between unlike molecules.

If the activity coefficient is smaller than unity strong attraction between unlike molecules occurred. That behavior is less common.

3.1.2.1 Vapor-liquid equilibria

Vapor liquid relationship is modelling by:

$$\varphi_i^v y_i p = x_i \gamma_i f_i^{*l} \tag{32}$$

The fugacity coefficient of the vapor phase is estimated from an equation of state and the liquid activity coefficient from liquid phase by an activity coefficient model.

There are three ways to compute the liquid phase reference fugacity f_i^{*l}:

1. For solvents.

   At the same temperature and pressure as the system, a reference state is defined for the solvent . The solvent is treated as pure components in the liquid state.

The liquid phase reference fugacity f_i^{*l} is calculate through:

$$f_i^{*l} = \varphi_i^{*,v}\left(T, p_i^{*,l}\right) p_i^{*,l} \theta_i^{*,l} \tag{33}$$

Where:

   $\varphi_i^{*,v}$= Fugacity coefficient of pure component i at the system temperature and vapor pressures, calculated from the vapor phase equation of state.

   $p_i^{*,l}$= Liquid vapor pressures of component i at the system temperature

   $\theta_i^{*,l}$= Poynting correction for pressure: $e^{\left(\frac{1}{RT}\int_{p_i^{*,l}}^{p} V_i^{*,l} dp\right)}$

   At low pressures, the Poynting correction is close to one, and can be neglected.

2. For dissolved gases.

   Light gases are often supercritical at the temperature and the pressure of system. Therefore they cannot serve for the reference fugacity (vapor pressure is meaningless). The reference state is at infinite dilution at the temperature and pressure of the mixtures.

   The Henry's constant for component i in the mixture H_i is the liquid phase reference fugacity $f_i^{*,l}$.

   The activity coefficient is transformed into the infinite dilution through the equation:

$$\gamma_i^* = \left(\frac{\gamma_i}{\gamma_i^\infty}\right) \tag{34}$$

   Where:

   γ_i^∞ = infinite dilution activity coefficient of component i in the mixture.

3. Empirical correlation.

   Reference state fugacity is estimated through an empirical correlation such as Chao-Seader or the Grayson-Streed model.

Vapor-liquid equilibria are calculated using binary interaction parameters. As was said before, this parameters are fitted by regression of binary phase equilibrium data. The prediction of multicomponent phase equilibrium from binary information is normally good.

3.1.2.2 Liquid-liquid and liquid-liquid-vapor equilibria

The equilibrium relationship is:

$$x_i^{l1}\gamma_i^{l1}f_i^{*,l} = x_i^{l2}\gamma_i^{l2}f_i^{*,l} = \varphi_i^v y_i p \tag{35}$$

Liquid-liquid equilibria relationship is:

$$\mathrm{x_i^{l1}\gamma_i^{l1} = x_i^{l2}\gamma_i^{l2}} \tag{36}$$

Liquid-liquid equilibria depend on temperature since the activity coefficient is dependent of the temperature. Eq. (36) is independent of pressure. At low to moderate pressures, the activity coefficient method represent well liquid-liquid equilibria because of the mutual solubility is not affected by the pressure. For high-pressure, the mutual solubility is affected and then an equation-of-state method is needed.

Fitted binary interaction parameters from multi-component liquid-liquid equilibria are not enough to achieve good predictions. In general, regression of binary components from multicomponent data equilibrium is needed.

Activity coefficients models model experimental liquid-liquid equilibria giving different results. The Wilson model cannot describe liquid-liquid separation at all. UNIQUAC, UNIFAC and NRTL are able to describe.

3.1.2.3 Calculation of other properties using activity coefficients

- Vapor phase

Vapor enthalpy, entropy, Gibbs energy and density are calculated using an equation of state as its shown in 3.1.1.3.

- Liquid phase

Liquid mixture enthalpy is calculated as follows:

$$H_m^l = \sum_i x_i \left[H_i^{*v} - \Delta_{vap} H_i^* \right] + H_m^{E,l} \tag{37}$$

Where:

H_i^{*v} = Pure component vapor enthalpy at T and vapor pressure

$\Delta_{vap} H_i^*$ = Component vaporization enthalpy

$H_m^{E,l}$ = Excess liquid enthalpy

Excess liquid enthalpy $H_m^{E,l}$, is related to the activity coefficient :

$$H_m^{E,l} = -RT^2 \sum_i x_i \frac{\partial \ln \gamma_i}{\partial T} \tag{38}$$

Liquid mixture Gibbs free energy and entropy are estimated as:

$$S_m^l = \frac{1}{T} (H_m^l - G_m^l) \tag{39}$$

$$G_m^l = G_m^v - RT \sum_i \ln \varphi_i^{*,l} + G_m^{E,l} \tag{40}$$

Where:

$$\mathrm{G_m^{E,l}} = \mathrm{RT} \sum_\mathrm{i} \mathrm{x_i} \ln \gamma_\mathrm{i} \tag{41}$$

3.1.2.4 Advantages and disadvantages of activity coefficient method

They are suitable to represent highly non-ideal liquid mixtures at low pressures, less than 10 atm. Binary parameters should be estimated or obtained from regression. For the Wilson, NRTL and UNIQUAC models, parameters for some components pairs are available in Aspen Physical Property System. They can be used in the pressure and temperature ranges of the data. When there are no parameters available, predictive models such as UNIFAC can be used [43].

3.2 Equation of state models

The ideal gas law is the simplest equation of state:

$$P = \frac{RT}{V_m} \tag{42}$$

It assumes molecules without size and without intermolecular interaction.

There are two types of engineering equation of state: cubic equation of state and the virial equation of state.

3.2.1 Cubic equation of state

As is said before, molecules in an ideal gas have no size and therefore no repulsion. To correct deviations due to repulsion, the total volume must be corrected for the volume of the molecule (co-volume parameter b). An ideal gas must have higher pressure compared to a real component, so a negative term is needed. Energy parameter a, is divided by and expression with dimension m^3. Attractive forces are proportional to $\frac{1}{r^6}$, where r is the distance between molecules.

Soave-Redlich-Kwong is an example of this class of equations of state [45]:

$$p = \frac{RT}{(V_m - b)} - \frac{a\ (T)}{V_m(V_m + b)} \tag{43}$$

That equation can represent non-ideality because it includes compressibility effects.

Another example is the Peng-Robinson equation of state [46]:

$$p = \frac{RT}{(V_m - b)} - \frac{a}{V_m(V_m + b) + \mathrm{b}(V_m - b)} \tag{44}$$

In the Aspen Physical Property System, cubic equations of state are based on the Redlich-Kwong-Soave and Peng-Robinson equation of state [43]. These cubic equations of state are listed in Table 3-1.

Table 3-1. Cubic equation of state based on Redlich-Kwong Soave and Peng Robinson available in Aspen.

Redlich-Kwong(Soave) based	Peng Robinson based
Redlich-Kwong	Standard Peng-Robinson
Standard Redlich-Kwong-Soave	Peng-Robinson
Redlich-Kwong-Soave	Peng-Robinson-MHV2
Redlich-Kwong-ASPEN	Peng-Robinson-WS
Schwartzentruber-Renon	
Redlich-Kwong-Soave-MHV2	
Predictive SRK	
Redlich-Kwong-SOAVE-WS	

The main disadvantages of cubic equation of states is that they do not represent liquid molar volume accurately. Using volume translation we can correct that problem for example the Schwartzenruber-Renon equation of state model [43].

3.2.1.1 Pure components parameters

The pure component parameters are calculated from correlations based on critical properties (P_c, T_c) and acentric factor. For polar compounds or long chain hydrocarbons these correlations are not accurate. The quality of vapor pressure representation improves introducing the alpha function, a more flexible temperature dependency on the attraction parameter.

3.2.1.2 Mixtures parameters

Properties calculation using a cubic equation of state consider just one (imaginary) component. When the fluid is a mixture, parameters a and b must be calculated using mixing rules from pure component parameters of the real mixture components. The classical mixing rules using just one binary interaction parameter for the attraction parameter have problems to describe mixtures with strong shape and size asymmetry.

$$a = \sum_i \sum_j x_i\, x_j \sqrt{a_i a_j}(1 - k_{a,ij}) \tag{45}$$

$$b = \sum_i x_i b_i = \sum_i \sum_j x_i x_j \left(\frac{b_i + b_j}{2}\right) \tag{46}$$

Another interaction coefficient is included for the b parameter in the Redlich-Kwong-Aspen [47] and Schwartzentruber-Renon [48] equations of state:

$$b = \sum_i \sum_j x_i x_j \left(\frac{b_i + b_j}{2}\right)(1 - k_{b,ij}) \tag{47}$$

This is suitable to represent vapor-liquid equilibrium behaviour for system with strong size and shape asymmetry but the drawback is that $k_{b,ij}$ is strongly correlated with $k_{a,ij}$ and that $k_{b,ij}$ affects the excess molar volume [49].

In mixtures with polar and non-polar compounds with strong energy asymmetry, the interaction parameters should depend on composition, for good VLE predictions. Huron-Vidal mixing rules use activity coefficients models as mole fraction function [50]. These mixing rules achieve good results because they has the advantages of flexibility with a minimum of drawbacks [49]. However, it is not possible to use activity coefficient parameters obtained at low pressures to predict high pressure equation of state interactions. To achieve that, several modifications of Huron-Vidal mixing rules are done.

3.2.2 Virial equation of state

In the Aspen Physical property System these virial equations of state can be selected:

- Hayden- O'Connell
- BWR-Lee-Starling
- Lee-Kesler-Plocker

These equation of state are based on a selection of powers of expansion:

$$p = RT\left(\frac{1}{V_m} + \frac{B}{V_m^2} + \frac{C}{V_m^3} + \cdots\right) \tag{48}$$

This equation is truncated after the second term and second virial coefficient B can describe the behavior of gases in a long pressure range. The Hayden-O'Connell equation of state uses a complex computation of B to account for the association and chemical bonding in the vapor phase.

Higher order terms are required to describe vapor and liquid properties. The order is usually higher than cubic for example the Benedict-Webb-Rubin equation of state, It has many parameters in terms of critical properties and acentric factor by Lee and Starling [51]. Another example is The Lee-Kesler- Plocker equation of state.

These equations are more accurate than cubic equations of state. They are not recommended for polar compounds.

3.3 Activity coefficients models

There are three categories of activity coefficient models:

- Molecular models
- Group contribution models
- Electrolyte activity coefficient models

3.3.1 Molecular models

These models assume ordering of liquid solution, according to the interaction energies between different molecules. Some examples are Wilson, NRTL and UNIQUAC. Molecular models are used for non-electrolyte solutions. These models use correlations.

The Wilson model cannot represent liquid-liquid separation but give good results for types of non-ideality. The NRTL and UNIQUAC can describe VLE, LLE and enthalpic behavior of highly non-ideal systems. The WILSON, NRTL and UNIQUAC are used on modelling applications at low pressures of highly non-ideal systems.

3.3.2 Group contribution models

Group contribution models are used for non-electrolyte systems. These models are predictive. Through a limited number of functional groups, many different molecules can be represented. Group-group interactions are good enough to predict activity coefficients between almost any pair of components.

UNIFAC is an extension of the UNIQUAC model because it uses the same functional groups fundamentation of functional groups that UNIQUAC applies for molecules.

3.4 Justification of the thermodynamic models selection

In this section, the selection of Aspen thermodynamic models will be discussed.

3.4.1 Extraction column

In this thesis RK-Aspen model (RKA) is used to simulate the extraction column. RKA requires polar parameters which must be regressed from experimental data using the Aspen Data Regression System. The RK-Aspen property method is based on the Redlich-Kwong-Soave EOS [52]:

$$P = \frac{RT}{V_m - b} - \frac{a}{V_m(V_m + b)} \tag{49}$$

RK-Aspen property method differs of Redlich-Kwong-Soave EOS in the location of the binary interaction parameters in the mixing rule, the type of temperature-dependency on this interaction parameters and the introduction of a polar factor in the alpha function to account for polar compounds.

The method uses the quadrating mixing rule:

$$a = \sum_i \sum_j x_i x_j \left(a_i a_j\right)^{0.5} (1 - k_{a,ij}) \tag{50}$$

$$b = \sum_i \sum_j x_i x_j \frac{(b_i + b_j)}{2} (1 - k_{b,ij}) \tag{51}$$

The method assumes linear dependence for temperature of the interaction parameters:

$$k_{a,ij} = k_{a,ij}^0 + k_{a,ij}^1 \frac{T}{1000} \tag{52}$$

$$k_{b,ij} = k_{b,ij}^0 + k_{b,ij}^1 \frac{T}{1000} \tag{53}$$

This binary interaction parameters can be determined by applying regression to experimental phase equilibrium data.

To extend the application to highly polar components, a modification to the Redlich-Kwong-Soave EOS was done by Mathias so the energy parameter include the alpha function as follows:

$$a_i = \alpha_i 0.42747 \frac{R^2 T_{ci}^2}{P_{ci}} \tag{54}$$

The pure component co-volume parameter is the same as in the original Redlich-Kwong-Soave EOS.

$$b_i = 0.08664 \frac{R T_{ci}}{P_{ci}} \tag{55}$$

Mathias alpha-function is used to calculate the pure component energy parameter of the subcritical components.

$$\alpha_i(T) = [1 + m_i(1 - \sqrt{T_{ri}}) - \eta_i(1 - T_{ri})(0.7 - T_{ri})]^2 \tag{56}$$

$$m_i = 0.48508 + 1.55171w_i - 0.15613w_i^2 \tag{57}$$

On the other hand, Boston Mathias extrapolation of the alpha function is used to calculate energy parameters of supercritical components.

$$\alpha_i = [exp(c_i(1 - T_{ri}^{di}))]^2 \tag{58}$$

$$c_i = 1 - \frac{1}{d_i} \tag{59}$$

$$d_i = 1 + \frac{m_i}{2} + 0.3\eta_i \tag{60}$$

$$m_i = 0.48508 + 1.55171w_i - 0.15613w_i^2 \tag{61}$$

EOS methods represent better the phase equilibrium behavior at high pressure than activity coefficients so an EOS method is needed.

Table 3-2 lists flexible and predictive equation-of-state property methods. These methods are suitable for mixture of polar and non-polar components and light gases. In addition they can deal with high pressures and temperatures, mixtures close to the critical point, and liquid-liquid separation at high pressures. Applications examples of this equations of states are gas drying with glycols, gas sweetening with methanol, and supercritical extraction [43]. They use the Peng-Robinson or Redlich-Kwong-Soave equations of state for modelling the pure component thermodynamic behavior extended with flexible alpha-functions using up to three parameters for very accurate fitting of vapor pressures. That fact improves the predictions for systems of very close boiling points and polar compounds. In some cases a volume translation term is included for accurate fitting of liquid densities.

Table 3-2. Flexible and predictive Equation-of-State property methods available in Aspen Plus software.

Property method name	Equation-of-state	Volume shift	Mixing Rule	Predictive?
HYSGLYCO	Twu-SIM-Tassone	-	-	X
PC-SAFT	Copolymer PC-SAFT	-	-	-
PRMHV2	Peng-Robinson	-	MHV2	X
PRWS	Peng-Robinson	-	Wong-Sandler	X
PSRK	Redlich-Kwong-Soave	-	Holderlbaum-Gmehling	X
RK-ASPEN	Redlich-Kwong-Soave	-	Mathias	-
RKSMHV2	Redlich-Kwong-Soave	-	MHV2	X
RKSWS	Redlich-Kwong-Soave	-	Wong-Sandler	X
SR-POLAR	Redlich-Kwong-Soave	X	Schwarzentruber-Renon	-

An X in the Volume shift column indicates that the property method include volume shift and in the predictive column indicates that the property method is predictive.

Some advantages of RKA are:

- RKA can represent polar components due to the inclusion of the polar factor.
- The method give good results for non-polar and slightly polar components with light gases such as CO_2 at medium to high pressure.
- The method distinguishes between the supercritical and subcritical components.
- You can expect reliable results at any condition, but results are less accurate close to the critical point.

3.5 Methods for estimation pure critical parameters

Critical properties are very important in the simulation because they are explicitly in the equation of states. However, the experimental determination of some components is impossible due to decomposition (chemical degradation) before the critical point is reached.

The property Constant Estimation System (PCES) use several estimation methods to estimate the pure critical properties.

The most widely used methods for estimating critical properties in Aspen Plus are:

- Joback method
- Lydersen method
- Ambrose method
- Gani method
- Definition method
- Lee-Kesler method

In almost every estimation method, a group contribution approach is employed. The group contribution method is based on assumed that the property of a substance, Q is a function of the structure of the molecule.

There are many ways to estimate critical properties such as T_c and P_c. The estimated property is denoted as Q̧̄. Group contribution method can be expressed as:

$$\bar{Q} = a + \sum_{j=1}^{M} n_j \Delta_j + b \left[\sum_{j=1}^{M} n_j \Delta_j \right]^2 \tag{62}$$

The contribution of group j is Δ_j, n_j is the number of that groups and M the total number of different types of groups presents. Table 3-3 shows Q̧̄, a and b values for several methods [53].

Table 3-3. $\bar{Q}$ function of different group contribution estimation methods.

Author	$\bar{Q}$ Function	a	b
	Critical temperature		
Lydersen	$\frac{T_b}{T_C}$	0.5667	-1
Ambrose	$\frac{T_b}{(T_C - T_b)}$	1.242	0
	Critical pressure		
Lydersen	$(\frac{M_w}{P_c})^{0.5}$	0.33	0
Ambrose	$(\frac{M_w}{P_c})^{0.5}$	0.339	0

- Joback method

Can be used to estimate: critical temperature T_C and critical pressure P_C. This method requires the molecular structure and normal boiling point information for estimating T_C .Joback method is a modification of the Lydersen method and is also the best method to use. It tested about 400 organic compounds. The errors are listed in Table 3-4.

Table 3-4. Errors obtained using Joback estimation method [43].

Parameter	No. of components	Average Relative Error (%)	Average Error
TC	400	0.8	4.8 (K)
PC	390	5.2	0.21 (MPa)

- Lydersen method

The method can estimate T_C and P_C. Normal boiling point and molecular structure are needed to estimate T_C. Molecular structure and molecular weight are required to estimate P_C. The estimated error for T_C is usually less than 2 %. For high molecular weight nonpolar compounds the errors are 5 % of higher. For P_C the errors were approximately 4 % [43].

- Ambrose method

To estimate T_C molecular structure and boiling point are required. Molecular structure and molecular weight for estimating P_C. The errors are smaller than the Joback and Lydersen methods as we can see in Table 3-5.

Table 3-5. Errors using Ambrose estimation method [43].

Parameter	No. of components	Average Relative Error (%)	Average Error
TC	400	0.7	4.3 (K)
PC	390	4.6	180 (KPa)

- Gani method

It uses first-order and second-order contribution groups. The second-order contribution groups account for the effect of neighboring atoms so the accuracy is higher [54]. The errors are tabulated below Table 3-6.

Table 3-6. Errors obtained using Gani estimation method [43].

Parameter	No. of components	Average Relative Error (%)	Average Error
TC	400	0.85	4.8 (K)
PC	390	2.89	113 (KPa)

Definition method

The definition method can estimate the acentric factor. For doing that estimation, vapor pressure is required. The acentric factor is calculated with that equation:

$$w_i = -\log_{10}\left(\frac{P_i^*}{P_{ci}}\right) - 1 \qquad (63)$$

Where P^*_i is the vapor pressure calculated at reduced temperature (T/T_c) of 0.7.

- Lee-Kesler method.

For the estimation of the acentric factor, the normal boiling point, the critical temperature and the critical pressure are required. This method is recommended for hydrocarbons.

3.6 Supercritical in Aspen

When a component of the mixture is above the critical point, Aspen considers it as supercritical. Aspen Plus does not have a designation of supercritical, therefore the phase can be assigned as either liquid or vapor.

The rough convention for phase designation is:

If the temperature is greater that the critical temperature (T_c), the phase should be vapor. If the temperature is less than the critical temperature (T_c), but the pressure is greater than the critical pressure (P_c), the phase should be liquid.

T_c and P_c of the mixture are not calculated a priori; therefore, the designation is only approximate. Creating a PT envelope for a stream using properties environment, Stream/Analysis is probably the easiest way to tell if a mixture is supercritical.

Since an equation of state (EOS) should be used to calculate both liquid and vapor properties, it does not matter what phase the stream has assigned to it. Activity coefficient models should not be used for supercritical mixture since the vapor and liquid calculations are inconsistent in the critical range. Not all of the EOS property methods use the EOS to calculate every the property. For example, a number of EOS property methods such as PENG-ROB and RK-Soave use Rackett to calculate liquid molar volume. PR-BM and PSRK use the EOS.

3.7 The data regression system

Aspen Plus has a tool that can be used to fit several kinds of pure component physical property data such as vapor pressure data, but it’s mainly use is to represent thermodynamic models fitting vapor-liquid equilibrium (VLE) and liquid-liquid equilibrium (LLE) [55].

The first pass proposed to fit a set of data is using a linear equation.

$$y = ax + b \tag{64}$$

Using the method of least squares the following objective function is defined:

$$\psi = \sum_{i}^{n\,data} (y_{calc} - ax_{data} - b)^2 \tag{65}$$

The method is defined as the sum of squares of errors between the y data points observed and the values of y_{calc} rom the model. Setting $\partial\psi/\partial a$ and $\partial\psi/\partial b$ equal to zero the minimum of the function is found. A set of linear equations are generated. This equations can be solved for the values of a and b that best fit the data. In Aspen Plus, several objective function can be selected Table 3-7.

Table 3-7. Objective function using in Aspen for regressing data.

Objective Function	All measured variables
Maximum likelihood	All measured variables
Ordinary least squares	Pressure and vapor compositions for isothermal VLE data Temperature and vapor compositions for isobaric VLE data
Barker's method	Pressure only
Modified Barker's method	Pressure and vapor compositions
Activity coefficients	Activity coefficients
Equilibrium constants	Equilibrium constants (K values)
Relative volatility	Relative volatility relative to first component

Maximum objective likelihood objective function is minimized with the condition of keep the constraints imposed by the applicable thermodynamic relationship through nonlinear programming methods [56]. The remaining objective functions are minimized by setting the partial derivatives of the objective function equal to zero and solving the nonlinear equations obtained.

Partial derivatives of the objective function calculation is done by perturbing each of the parameters by a small value Δa keeping the remain parameters constant.

$$\frac{\partial\psi}{\partial a} = \frac{\psi_{a+\Delta a} - \psi_a}{\Delta a} \tag{66}$$

The default regression method chosen by Aspen is maximum likelihood. The objective function of that method is:

$$\psi = \sum_{i}^{n\,data} \left[\frac{(T_i^e - T_i^m)^2}{\sigma_{T,i}^2} + \frac{(P_i^e - P_i^m)^2}{\sigma_{P,i}^2} + \frac{(x_i^e - x_i^m)^2}{\sigma_{x,i}^2} + \frac{(y_i^e - y_i^m)^2}{\sigma_{y,i}^2} \right] \tag{67}$$

The superscripts e and m means estimated and measured values.

For each point the next constraints are applied, Poynting correction is neglected:

$$y_i \phi_i^v P - \gamma_i x_i f_i^{\circ} = 0 \tag{68}$$

$$\gamma_i = \gamma(T, x) \tag{69}$$

$$\phi_i^v = \phi^v(T, P, y) \tag{70}$$

$$\sum_{i}^{ncomp} x_i - 1 = 0 \tag{71}$$

$$\sum_{i}^{ncomp} y_i - 1 = 0 \tag{72}$$

Aspen plus help does not provide documentation on the implementation of the minimization procedure. However, possibilities are described in [57, 58].

3.8 Equilibrium separator units

3.8.1 Basic equations

Distillation and extraction blocks involves the solution of mass, equilibrium and energy balance equations [55]. All models are based on the analysis of a single stage such as Figure 3-1.

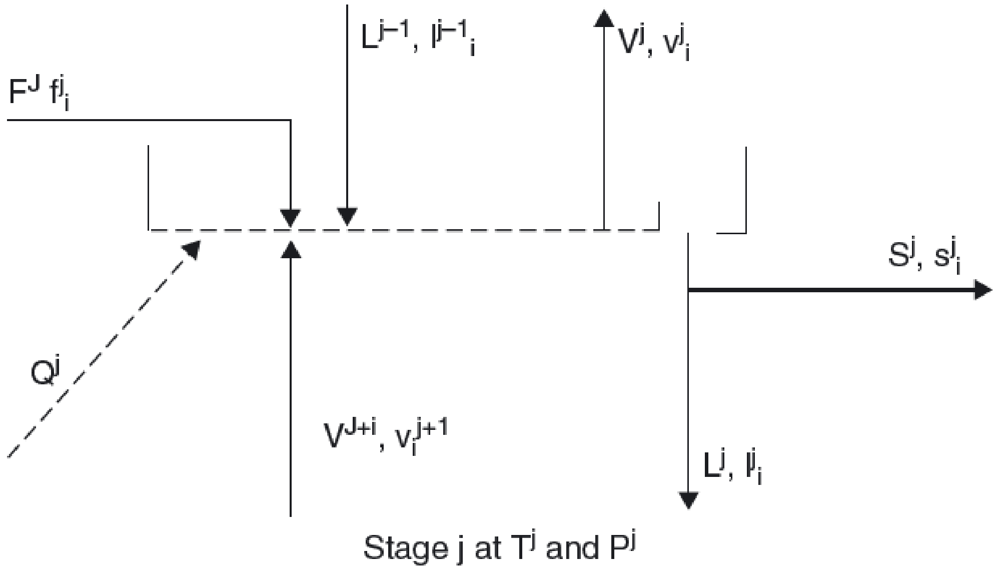

Figure 3-1. Theoretical stage.

v_i^j and l_i^j represent the component i vapor and liquid leaving stage j; f_i^j the amount of component feeding the stage j; s_i^j amount of component i leaving the stage j, T^j and P^j, the temperature and pressure of stage j. Q^j, the total energy entering or leaving stage j. The equilibrium constant K^j depends on the stage temperature, pressure, liquid and vapor mole fractions, x_i^j and y_i^j.

Liquid mole fraction can be calculated by:

$$x_i^j = \frac{l_i^j}{\sum_{k=1,m} l_k^j} \tag{73}$$

m is the number of compounds, V^j and L^J are the total molar vapor and liquid leaving stage j and are calculated by adding the componential flows in the vapor and liquid:

$$V_J = \sum_{k=1,m} v_k^j \tag{74}$$

$$L_J = \sum_{k=1,m} l_k^j \tag{75}$$

The mass balance for component i on stage j is :

$$f_i^j + v_i^{j-1} + l_i^{j+1} - v_i^j - l_i^j - s_i^j = 0 \tag{76}$$

There are n times m material balances, being n the number of theoretical stages. The basic equilibrium equations for component i, on stage j , are:

$$y_i^j = K_i^j x_i^j \tag{77}$$

Substituting Eqs. (73), (74) and (75) into Eq. (77) the following expression is obtained:

$$v_i^j = K_i^j (v_i^j, l_i^j, T^j, P^j) \frac{l_i^j \sum_{k=i,m} v_k^j}{\sum_{k=i,m} l_k^j} \tag{78}$$

There are n times m equilibrium equations.

The enthalpy per mole of liquid and vapor flows H^j and h^j refer to vapor and liquid leaving stage j. The energy balance obtained is:

$$H_F^j \sum_{k=1,m} f_k^j + H^{j-1} \sum_{k=1,m} v_m^{j-1} + h^{j+1} \sum_{k=1,m} l_k^{j+1} - H^j \sum_{k=1,m} v_k^j - h^j \sum_{k=1,m} l_m^j - h^j \sum_{k=1,m} S^j + Q^j = 0 \tag{79}$$

There are n energy balance equations.

3.8.2 Extract block

Is a simulation block available in Aspen to simulate a rigorous extraction column. For extraction columns, the vapor terminology refers to the lighter of the two phases. Extraction column usually operate virtually isothermally due to there are no phase changes.

4 CASE STUDY: TERNARY MIXTURE OF FAME-TOCOPHEROLS-CO_2

4.1 Selection of the ternary mixture

Due to the poor solubility of FFA in supercritical carbon dioxide, the esterification process is needed. The most important step for isolating natural tocopherols from the stream obtained after the esterification (EE-ODD, Ethyl Esters of Oil Deodorizer Distillates) is the removal of FAMEs and FAEEs. fatty esters are the majority components in ODD after the esterification process, this fact is shown in Table 5-9. To analyze the tocopherol isolation process, the complex system of EE-ODD + CO_2 is regarded as a pseudo-ternary system (FAME/Tocopherols/CO_2). The reasons for choosing these three components are:

- FAME is the main component in our feedstock after the esterification process, doing the assumption that FAEE are similar to FAME in physicochemical properties.
- Tocopherol is selected because is one of the minor components in which we are interested.
- CO_2 is the solvent of the extraction process. Therefore, for understanding the behaviour of EE-ODD with scCO_2 the study of this pseudo-ternary system is done.

In this chapter, two binary systems of FAME/CO_2 and Tocopherols/CO_2 are analyzed and in Chapter 5 the real system (EEODD+CO_2) is investigated.

4.2 Binary phase equilibria

Experimental binary phase equilibrium data for FAME/CO_2 and α-tocopherol/CO_2 in the pressure ranges of 8 to 23 MPa for FAME and 8.6 to 30 MPa for α-tocopherol were investigated. This experimental data is extracted from Fang et al. [59].

Vapor-liquid equilibrium data of FAME/CO_2 are represented at 313.15 K, 333.15 K and 353.15 K in Figure 4-1. For the system Tocopherol/CO_2 the equilibrium data is represented at 313.15 K, 333.15 K and at 353.15 K in Figure 4-2.

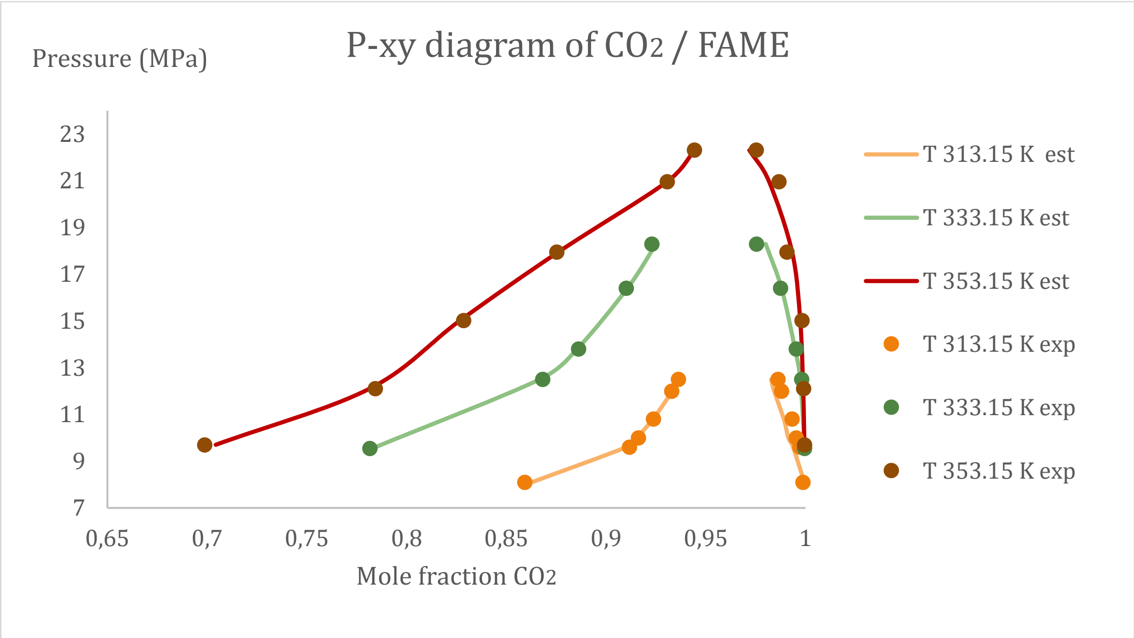

Figure 4-1. Px-diagram for the vapor-liquid equilibria for the system CO_2/FAME. Experimental data is represented by dots at 313.15 K (orange), 333.15 K (green) and 353.15 K (red). Simulation data with RK-Aspen is represented by lines at 313.15 K (orange), 333.15 K (green) and 353.15 K (red).

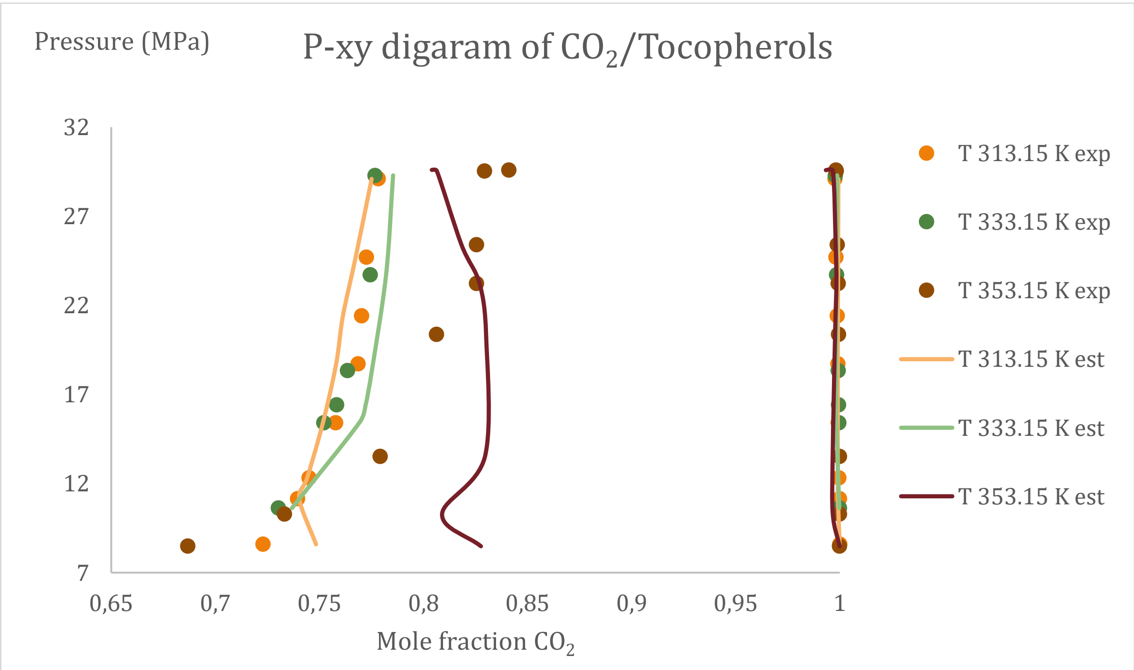

Figure 4-2. Px-diagram for the vapor-liquid CO_2/Tocopherol system. Experimental data is represented by dots at 313.15 K (orange), 333.15 K (green) and 353.15 K (red). Simulation data with RK-Aspen is represented by lines at 313.15 K (orange), 333.15 K (green) and 353.15 K (red).

Experimental vapor-liquid equilibrium data illustrate that at constant temperature the FAME and tocopherol content in gas phase increases, as pressure increase (gas CO_2 composition decrease when pressure is increased). Looking at the liquid phase, CO_2 content rises when pressure is increased. Analyzing the effect of temperature on gas composition, the FAME and tocopherol content decreases with increasing temperature (gas CO_2 composition increase when pressure is increased). In addition, the influence of the temperature on FAME/CO_2 is also shown Figure 4-1**¡Error! No se encuentra el origen de la referencia.** and on Tocopherols/CO_2 in Figure 4-2.

RK-Aspen model was used to predict the vapor liquid equilibrium data for this binary systems. Polar factor (η) and binary interaction parameters k_a and k_b were obtained applying the Deming algorithm to perform a maximum likelihood estimation. The resulting polar factor and binary interaction parameters are shown in Table 4-1.

Table 4-1. Parameters of the Redlich-Kwong-Aspen (RKA) model of the binary systems: FAME/CO_2 and Tocopherols/CO_2.

	CO2		
	$k_{a,\,ij}$	$k_{b,\,ij}$	η
FAME	0.1086	0.2034	2.4979
TOCOS	0.1140	0.0177	0.8733

The phase equilibrium of the ternary system predicted using RK-Aspen EOS agrees well with the experimental data used (see Figure 4-1 and Figure 4-2). On the one hand, P-xy diagram of CO_2/FAME fits correctly in the study range. On the other hand, P-xy diagram of the system CO_2 /tocopherol fit liquid phase really well at low temperatures and also vapor phase in the range of study. As a remark, liquid phase at high temperatures shows big differences with the experimental data. This fact could be due to thermal decomposition of tocopherols at high temperatures.

The distribution coefficient is defined by:

$$K_i = \frac{y_i}{x_i} \tag{80}$$

With increasing pressure, at constant temperature, the distribution coefficient of FAME and tocopherols increases significantly, shown respectively in Figure 4-3 and Figure 4-4.

Distribution coefficient of FAME is one or two orders of magnitude higher than distribution coefficient of tocopherol. That difference between both compounds indicates that the isolation of tocopherols from EE-ODD is possible. However, it needs to be verify by further study of the ternary system and the real system.

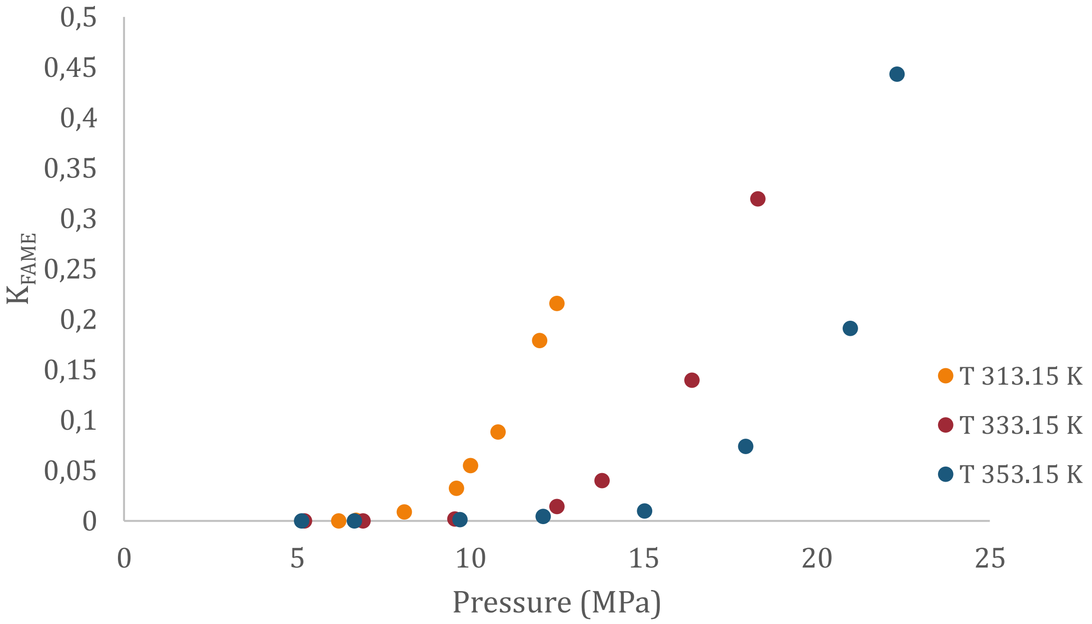

Figure 4-3. Influence on temperature and pressure in the FAME distribution coefficient.

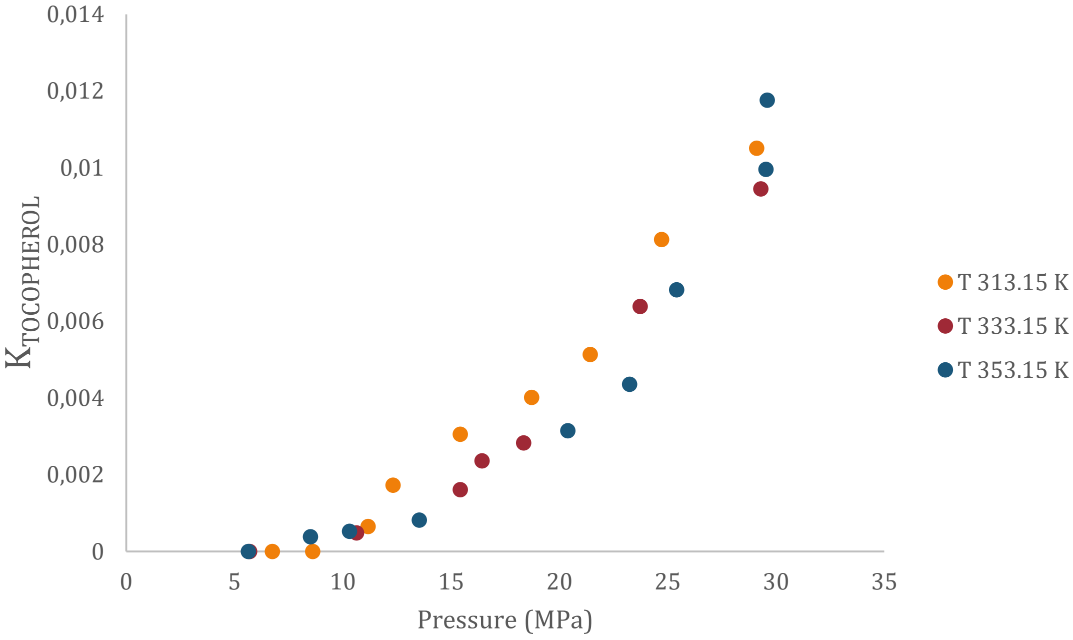

Figure 4-4. Influence on temperature and pressure in the Tocopherols distribution coefficient.

4.3 Ternary phase equilibria

Phase equilibrium information of EE-ODD in supercritical CO_2 is not available. However, the ternary phase equilibrium of the system FAME/Tocopherol/CO_2 is published by Fang et al. [40]. Analyzing the phase behaviors for the ternary and real system will provide fundamental information for modelling the separation process.

In this paragraph, influence on two factors on phase behavior will be investigated: pressure from 10 to 29 MPa and temperature from 313.15 K to 353.15 K.

Increasing pressure, the two-phase region of the ternary diagram shrinks. Therefore, the mutual solubility of the components in scCO_2 increased. Table 4-2 shows that the composition of CO_2 in the liquid phase rises with higher pressures while the CO_2 composition in gas is reduced, which means that the solubility others components in the gas phase increases.

Table 4-2. Influence of increasing pressure on the ternary diagram of the system FAME/tocopherols/CO_2 with a mass tocopherol content in the feed of 10, 19 % at 313.15.

Pressure (MPa)	X_{FAME}	X_{CO2}	$X_{tocopherols}$	Y_{FAME}	Y_{CO2}	$Y_{tocopherols}$
10	0.4137	0.5201	0.0662	0.00165	0.9831	0.0004
15	0.3396	0.5829	0.0775	0.0911	0.905	0.0039
20	0.2611	0.6752	0.0637	0.1261	0.863	0.0109
29	0.2105	0.7301	0.0594	0.1605	0.8226	0.0169

On the other hand, increasing temperature the two-phase region is expanded, Tocopherol composition in the gas phase decrease and FAME composition increase. This effect is shown in Table 4-3. Influence of temperature on the gas compositions seems to be less important than on the liquid composition at this pressure.

Table 4-3. Influence of temperature on ternary diagram of the system FAME/tocopherols/CO_2 with a mass tocopherol content in the feed of 10, 19 % at 10 MPa.

Temperature (K)	X_{FAME}	X_{CO2}	$X_{tocopherols}$	Y_{FAME}	Y_{CO2}	$Y_{tocopherols}$
313.15	0.4137	0.5201	0.0662	0.00165	0.9831	0.0004
333.15	0.5882	0.3286	0.0832	0.0029	0.997	0.0001
353.15	0.6905	0.2285	0.081	0.0027	0.9972	0.0001

We are interested in analyze the separation of tocopherol and FAME. The separation factor (S) between tocopherol (compound 2) and FAME (compound 1) is calculated by:

$$S = \frac{\frac{y_2}{x_2}}{\frac{y_1}{x_1}} \tag{81}$$

Where y_i and x_i are the mass fractions of component i in gas and liquid, respectively. The separation factor represents the selectivity for separating tocopherols from FAME. Therefore, a low value indicates high selectivity and a high value represent that the separation of this two components under this conditions is difficult. In addition a separation factor equals unity means that gas and liquid composition is similar and the supercritical extraction process cannot separate FAME from tocopherols.

The effect of pressure at constant temperature (313.15 K) on separation factor is analyze in Figure 4-5. At higher pressure, the separation factor increase as well, more tocopherol is going to the vapor phase and this is not desired.

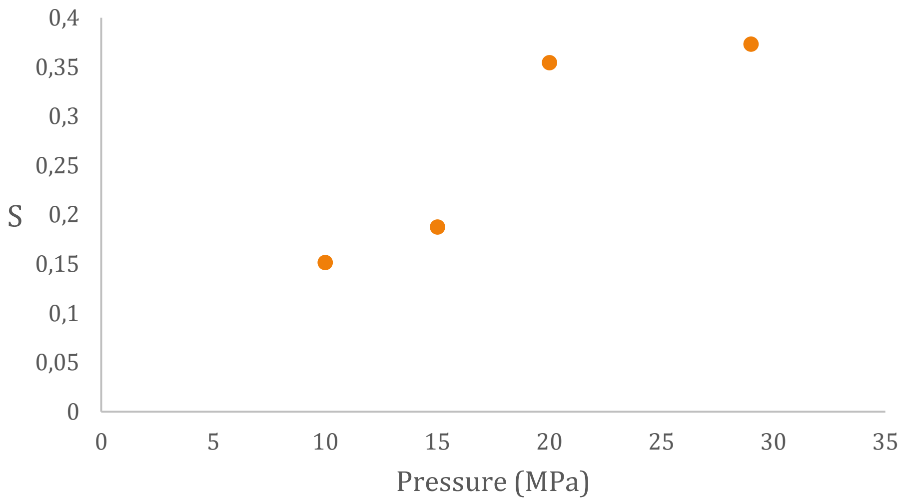

Figure 4-5. Influence of pressure on separation factor at 313.15 K for the system FAME/Tocopherols/CO_2.

Temperature influence at 10 MPa on the separation factor is shown in Figure 4-6. Higher temperatures leads to higher values of the separation factor so less tocopherol content in liquid phase.

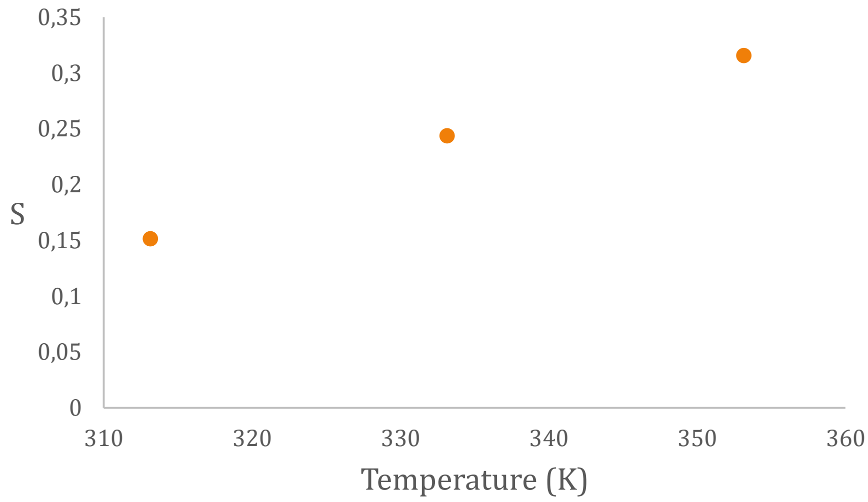

Figure 4-6. Effect of Temperature on separation factor at 313.15 K for the system FAME/Tocopherols/CO_2.

In conclusion, it is possible to establish a preliminary separation strategy. Low pressures and temperatures are interesting to minimize tocopherol content in vapor phase during the first extraction process. Therefore the simulation will be performed 10 MPa and 313.15 K in the first extraction column.

4.3.1 Regression to experimental data

RK-Aspen model was used to correlate the vapor liquid equilibrium data for this ternary system. Correlation procedure was completed with Aspen Plus. The temperature-dependent parameter polar factor (η) and binary interaction parameters k_a and k_b were obtained using the Deming algorithm to perform a maximum likelihood estimation. The resulting polar factor and binary interaction parameters are shown in Table 4-4 Figure 4-7-Figure 4-12 provide a comparison between experimental and estimated mass fraction of the components of the system.

Table 4-4. Regression results of binary interaction parameters and polar factor using Deming algorithm to perform a maximum likelihood estimation.

	CO2		
	$k_{a,\,ij}$	$k_{b,\,ij}$	η
FAME	0.037	0.3774	2
TOCOS	0.6583	-0.2344	2

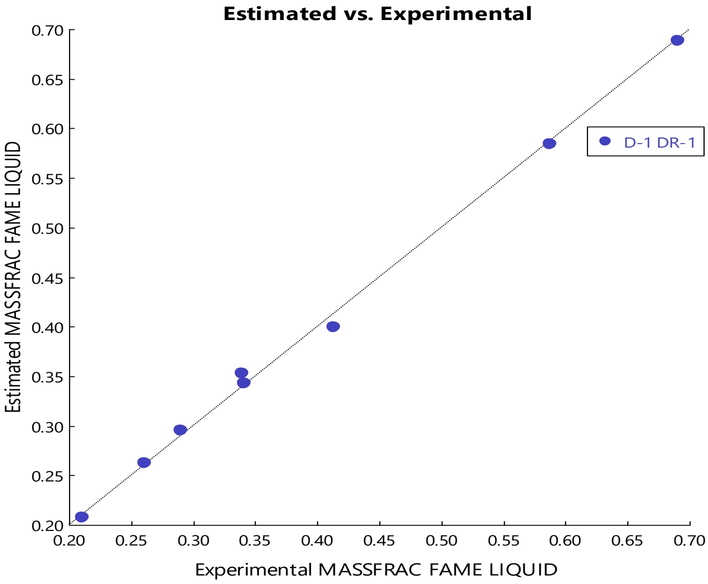

Figure 4-7. Estimated vs Experimental mass fraction of FAME in the liquid phase.

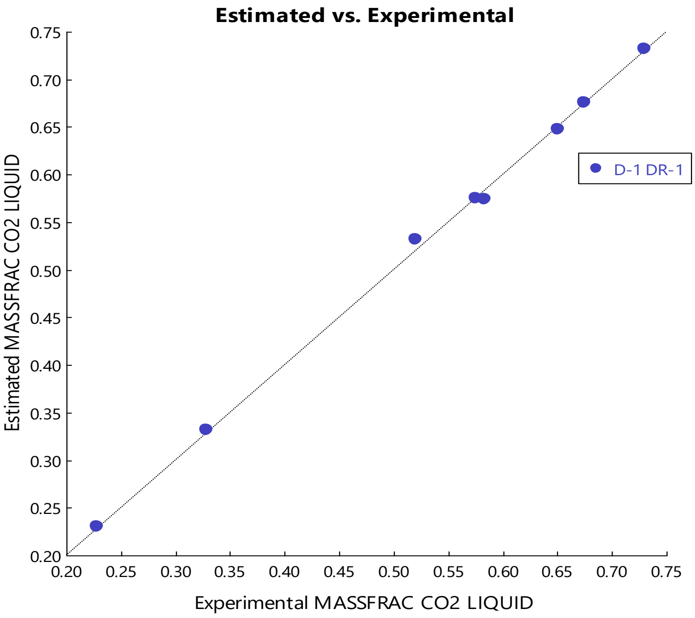

Figure 4-8. Estimated vs Experimental mass fraction of CO_2 in the liquid phase.

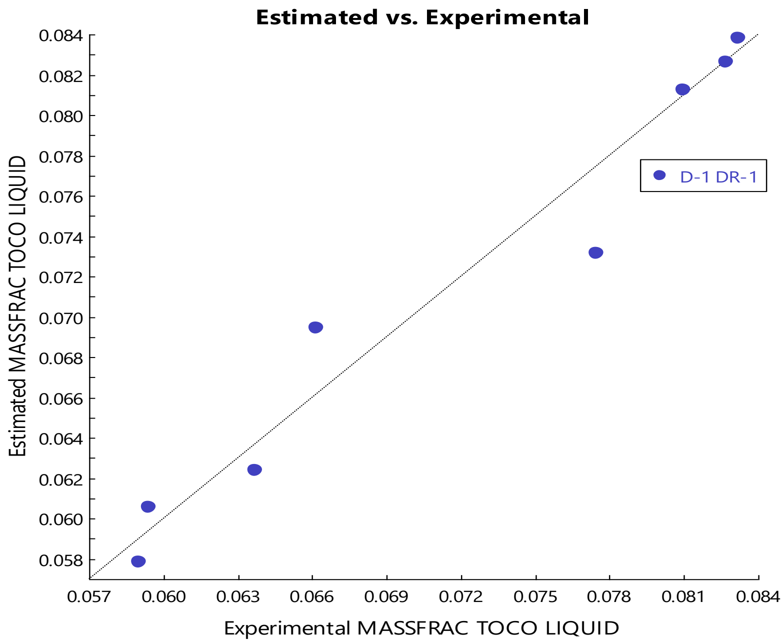

Figure 4-9. Estimated vs Experimental mass fraction of Tocopherols in the liquid phase.

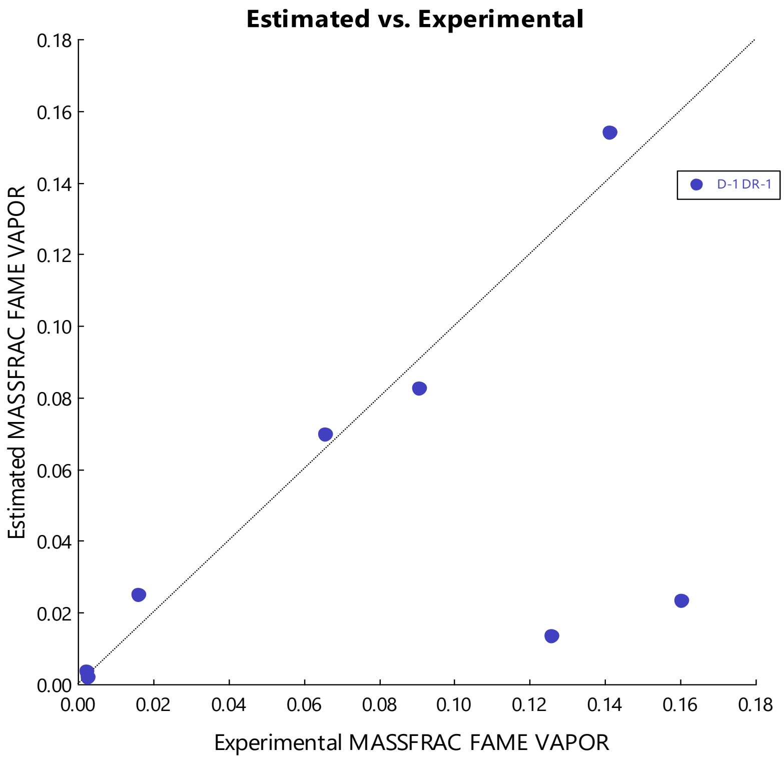

Figure 4-10. Estimated vs Experimental mass fraction of FAME in the vapor phase.

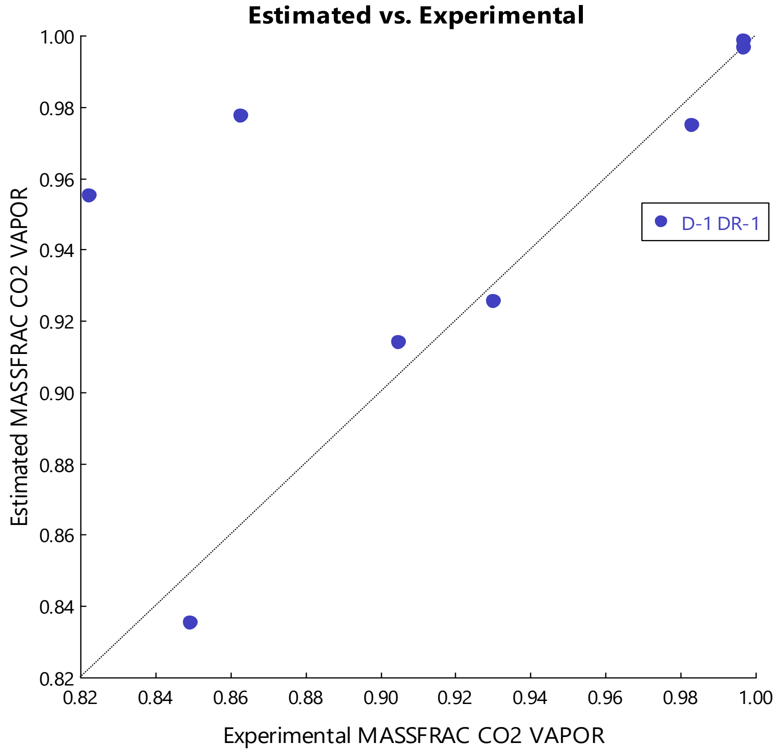

Figure 4-11. Estimated vs Experimental mass fraction of CO_2 in the vapor phase

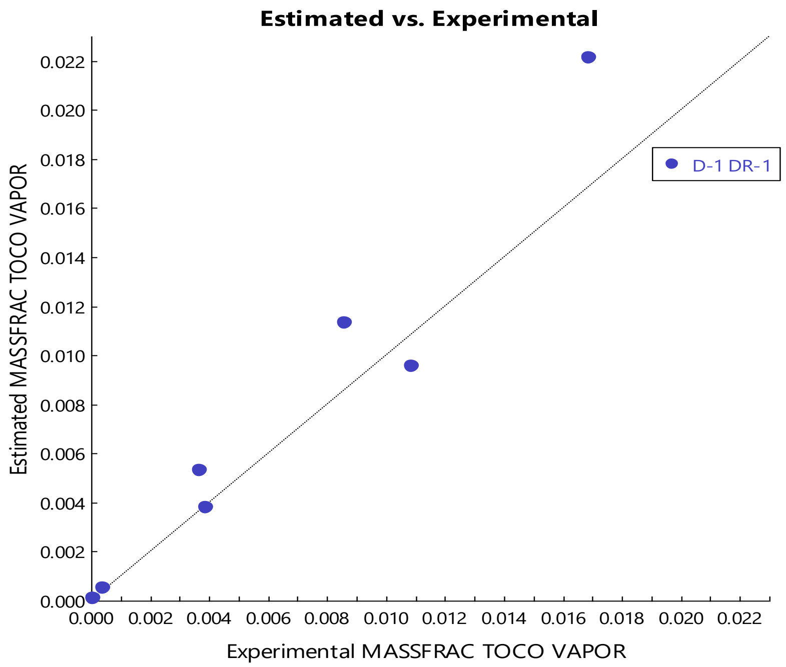

Figure 4-12. Estimated vs Experimental mass fraction of tocopherols in the vapor phase

4.3.2 Importance of binary interaction parameters

A simulation of the extraction was run in Aspen Plus software at 313.15 K and 10 MPa using a two stages extractor column. Supercritical CO_2 is introduced by bottom and a feedstock with a mass composition of 96 % in FAME and 4 % of tocopherols flows from top to bottom. That column is fed with a solvent, feed mass ratio of 10 Figure 4-13.

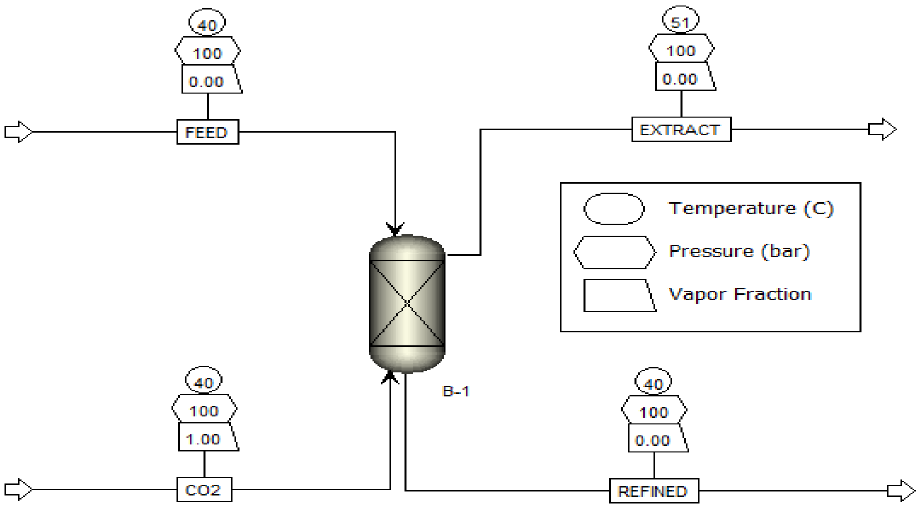

Figure 4-13. Simulation of the extraction column at 313.15 K and 10 MPa .

Running the simulation just with the data retrieved by Aspen the results obtained are shown in Table 4-5.

Table 4-5. Simulation results of the extraction process at 313.15 K and 10 MPa without including the binary interaction parameters for the pair of components.

	CO_2 (kg h^{-1})	Feed (kg h^{-1})	Extract (kg h^{-1})	Refined (kg h^{-1})
FAME	-	0.96	0.0544	0.9056
Tocopherols	-	0.04	0.0023	0.0377
CO_2	10	-	9.1471	0.8529
Total	10	1	9.2038	1.7962

Table 4-6 shows the simulation results from Aspen Plus when binary interaction parameters (as listed in Table 4-4) are include in the properties environment through Aspen's data regression system of vapor liquid equilibrium data from the ternary system FAME/Tocopherols/CO2.

Table 4-6. Simulation results of the extraction process at 313.15 K and 10 MPa including the binary interaction parameters for the pair of components.

	CO_2 (kg h^{-1})	Feed (kg h^{-1})	Extract (kg h^{-1})	Refined (kg h^{-1})
FAME	-	0.96	0.96	-
Tocopherols	-	0.04	0.0003	0.0397
CO_2	10	-	10	-
Total	10	1	10.9603	0.0397

As is shown, doing the simulation including the binary interaction parameters, the solubility of FAME in $scCO_2$ is higher because mass flow of FAME in extract stream is much higher. However tocopherol solubility is lower due to the mass flow of Tocopherols in extract stream. Totally different behaviors are obtained without the inclusion of these parameters so one can conclude that binary interaction parameter is fundamental for achieving reliable results.

5 MODELLING OF SUPERCRITICAL EXTRACTION

5.1 Properties environment

To predict suitable phase equilibria, several steps are carried out working in the Aspen Plus properties environment: Model component choice, Estimation of critical properties and finally regressing parameters.

5.1.1 Model component choice

The first step in modelling the phase equilibrium of the multicomponent ODD system is the selection of the components that will be used in Aspen to represent the complex stream.

Table 5-1 show chemical structure of common fatty acids presents in vegetable edible oils such as sunflower and soybean vegetable oils. Chemical composition of these oils is shown in Table 5-2. As it is shown, oleic and linoleic acid are the main fatty acids present in normal sunflower and soybean oils [60]. In this thesis, high oleic sunflower oil and high oleic soybean oil are studied, therefore oleic acid was chosen to represent FFA. Mono-, di- and triglycerides are represented by mono-, di- and triolein. α-tocopherol was selected to represent tocopherols because it represents 93 % of the total tocopherol content. On the other hand, several sterols are present in ODD mixture, but the all the sterols are represented by β-sitosterol since it has the highest composition, as shown in

Table 5-3.

Table 5-1. Chemical structure of fatty acids present in sunflower and soybean vegetable oils.

Fatty acid	Systematic name	Structure [a]	Formula
Palmitic	Hexadecanoic	16:0	$C_{16}H_{32}O_2$
Stearic	Octadecanoic	18:0	$C_{18}H_{36}O_2$
Oleic	Cis-9-Octadecaenoic	18:1	$C_{18}H_{34}O_2$
Linoleic	Cis-9, cis-12-Octadecadienoic	18:2	$C_{18}H_{32}O_2$
Linolenic	Cis-9, cis-12, cis-15-Octadecatienoic	18:3	$C_{18}H_{30}O_2$

[a] XX:Y indicates XX carbons in the fatty acid chain bounded with Y double bonds.

Table 5-2. Chemical composition of vegetable oils.

Vegetable oil	Fatty acid composition				
	16:0	18:0	18:1	18:2	18:3
Soya bean	12	3	23	55	6
Sunflower	6	3	17	74	0

Table 5-3. Component selection to represent ODD mixture.

ODD composition		
Glycerides	% in sun oil-ODD	Aspen model component
monoglycerides	2.07	monoolein
Diglycerides	1.98	diolein
Triglycerides	14.51	triolein
Fatty acids	% in sun oil-ODD	Aspen model component
FFA	43.03	oleic acid
FAME	1.16	methyl oleate
Tocopherol	% in sun oil-ODD	Aspen model component
α-tocopherol	2.85	α-tocopherol
β-tocopherol	0.12	-
γ-tocopherol	0.03	-
δ-tocopherol	0.05	-
Total tocopherol	3.05	-
Sterol	% in sun oil-ODD	Aspen model component
brassicasterol	0.04	-
β-sitosterol	4.19	β-sitosterol
campesterol	0.65	-
Cholesterol	0.07	β-cholesterol
δ-5-avensterol	0	-
minor sterol	1.71	-
stigmasterol	0.93	stigmasterol
steryl esters	1.12	-
Totaal sterol	8.71	
Others	% in sun oil-ODD	Aspen model component
Squalene	2.27	squalene

5.1.2 Estimation of critical properties

The next step is the estimation of critical properties. This is necessary because the critical properties are included in the thermodynamic model calculations (as discuss in section 3.4). Often, no experimental data is available for some components, due to thermal decomposition of these components at high temperature. Therefore it is necessary to estimate the critical properties of these components, using the group contribution method explained in section 3.5.

5.1.2.1 Properties extracted from Aspen Databanks

Aspen has the access to several databanks which include parameters for several components. That content is continually updated, expanded and improved. Using the "Retrieve Parameters Aspen Tool" the interaction parameters obtained are shown in Table 5-4. The two databanks used in this thesis are PURE 35 and NIST-TRC.

- PURE 35 Databank

Pure35 Databank is the main source of pure component parameters for the Aspen Physical property system. It is based on de data developed by the AICHE DIPPR® data compilation, AspenTech, ASPENPCD databank, and other sources. This databank store parameters for 2161 (mostly organic) compound.

- NIST-TRC Databank

NIST-TRC Databank store pure component data for 24037 compounds (mostly organic). The database is developed under an agreement with the National Institute of Standards and Technology's (NIST) Standard Reference Data Program (SRDP). Thermodynamics Research Center (TRC) have collected and evaluated the property parameters and experimental data using the NIST Thermo Data Engine (TDE) and the NIST/TRC source Data Archival System for experimental and thermochemical property data. This databank was add to Aspen in the last updates of the software.

Table 5-4. Critical properties obtained from Aspen Databanks.

Retrieved by Aspen				
Component	Tc (K)	Pc (Pa)	Ω (-)	Aspen Databank
FFA	781	1390000	1.1681	PURE35
MG	856.9	1201000	1.0985	PURE35
DG	916	425970	1.8439	PURE35
TG	935.3	200200	2.0883	PURE35
FAME	764	1280000	1.0494	PURE35
TOCO	964.3	1080000	1.0314	PURE35
STEROL	953	1120000	1.0543	PURE35
SQUALENE	832	708841	0.6340	NIST-TRC
FAEE	772.1	1098000	0.9426	PURE35

5.1.2.2 Properties estimated by Property Estimation Tool in Aspen Plus

Another possibility, is the estimation of the critical properties based on some group contribution methods. Table 5-5 show the estimated values using the “Property Estimation Tool” available in Aspen Plus ®.

Table 5-5. Critical properties generated by Aspen Plus estimation tool using group contribution method.

Estimated by Aspen					
Component	Tc (K)	Pc (Pa)	Method	Ω	Method
FFA	786.79	1354840	Ambrose	1.1681	Lee-Ksl
MG	863.279	1289640	Ambrose	1.1097	Lee-Ksl
DG	954.798	687349	Ambrose	1.87219	Lee-Ksl
TG	991.29	468201	Ambrose	2.1331	Lee-Ksl
FAME	738.208	1089300	Gani	1.0541	Lee-Ksl
TOCO	955.882	1081740	Ambrose	1.0408	Lee-Ksl
STEROL	970.051	1060290	Ambrose	1.065	Lee-Ksl
SQUALENE	828.602	581175	Gani	0.6380	Lee-zsl
FAEE	748.643	1030160	Gani	0.9686	Lee-Ksl

5.1.2.3 Properties found in literature

As last option, on can relate on literature for values of the critical parameters. Table 5-6 shows critical properties found in several articles. X Data not founded in literature.

Table 5-6. Critical properties collected from several articles.

Literature					
Component	Tc (K)	Pc (kPa)	Method	Ω	Method
FFA [61]	813.6	1250	Dohr and Brunner	0.81	Pilzer
MG [62]	955.1	1689	Ambrose	X	X
DG [62]	1077.8	779	Ambrose	X	X
TG [62]	1068.3	2536	Klincewicz	1.8 [61]	Pilzer
FAME [59]	770.9	1150	Gani	0.68	Lee-Ksl
TOCO [59]	1020	1370	Gani	1.195[61]	Lee-Ksl
STEROL	X	X	X	X	X
SQUALENE [63]	782.1	1112.1	Fitting the EOS to reported vapor pressure data	1.9083	
FAEE[64]	782	1210	Lydersen	0.992	X

As it is shown, there are big differences between the properties obtained from databanks, the Aspen estimation tool and the literature. The most distinguished difference is for the component squalene. A sensitivity analysis could be carried out to analyze the influence of the critical parameters in the simulation. In this thesis we will work with the parameters obtained from Aspen's databanks.

5.1.3 Regressing parameters

In order to get a good model, binary interaction parameters should be regressed using vapor liquid experimental data. In our case, own experimental data was not available. Therefore vapor liquid equilibrium was found in literature. Multicomponent equilibrium data for the system EEODD/CO_2 is not reported in literature, but based on several assumptions from literature on can neglect solute-solute interactions. The solute concentration is very low and satisfactory results have been reported in the literature on the prediction of the phase equilibrium of complex oil mixtures while neglecting the solute-solute interactions [61, 65-67].

Table 5-7 shows all phase equilibrium solute/CO_2 systems used in the simulation process and their range of measurements. The VLE used in this work are shown in 8 (Appendix B).

Table 5-7. Vapor liquid equilibrium data for several systems solute/CO_2.

System EEODD compound/CO_2	No. of experimental points	Ref.	Temperature (K)	Pressure (MPa)
FAEE	37	[64]	313.15, 323.15, 333.15	1.14-18.62
FFA	12	[68]	313.15, 333.15 , 353.15	10-30
TG	8	[68]	313.15, 333.15	15-31
FAME	8	[69]	313.15, 333.15	2.91-13.69
Tocopherols	48	[70]	292-333	9-26
Ethanol+Water	20	[71]	283-305	4.5-8.8
FAME+ Squalene	23	[63]	313-343	11-21
Sterol+TG	7	[72]	323- 383	20-35

Table 5-8 summarizes the interaction parameters obtained from the regression of the experimental data. The polar factor regressed value was fixed between the lower bound -2 ant the upper bound 2.

The average absolute deviation (AAD) between the experimental and calculated data was used to show the quality of the regressed data.

$$AAD\ (\%) = \frac{1}{N}\sum_{I=1}^{N}|d_i|x100 \qquad (82)$$

Where

d_i = error between experimental and calculated data

N = The number of data points.

The AAD obtained during the regression are summarizes in 8 (Appendix C).

Table 5-8. Binary interaction parameters for the RK-ASPEN model.

	CO2		
	$k_{a,\,ij}$	$k_{b,\,ij}$	η
FAEE	-1.0051	-4.7929	2
FFA	0.0637	0.1814	-0.918
TG	-0.0015	-0.0946	-2
FAME	0.1047	0.0757	2
TOCOS	0.2151	-0.0326	2
ETHANOL	-0.6979	-1.6887	2
WATER	-0.3819	-0.088	-0.2168
SQUALENE	0.0783	-0.0321	-2
STEROLS	1.06	1.0257	2

FAEE and sterols have the highest value of the binary interaction parameters. They are one order of magnitude bigger than the others pairs.

In some cases, negative $k_{a\,i,j}$ is needed. This fact is explained due to the geometric rule employed in RKA for the energy parameter (a) is derived from the London theory of dispersion forces and cannot be expected to be valid for mixtures with strong interactions. In the case of strongly systems, we expect that energy term (a) is larger than the value provided by the geometric mean rule so a negative $k_{a,\,i\,j}$ is needed. As an example, negative $k_{a,\,ij}$ for the system chloroform-acetone using SRK model provides good VLE correlation [73].

5.2 Simulation environment

The next step after selecting a suitable model to represent the behavior of our system, is the simulation of the extraction process. In this thesis, the goal is to optimize the squalene isolation process using sunflower EE-ODD as a feedstock. In addition, several feedstocks has been used to analyze the influence of the difference in initial composition on the feasibility of the process. Sunflower, low content of tocopherol in soya ODD and high content of tocopherol in soya ODD had been used as feedstock for the extraction process. Moreover, the block unit selection for the simulation is also discussed in this section. A group of bachelor students were working on the esterification process to transform the FFA into FAEE shown in Figure 5-1. This process is carried out at 553 K and 15 MPa. F1-L is the stream which will be used as feedstock in the extraction process of this thesis. The simulation results of the esterification process were obtained using UNIQ-RK model in Aspen.

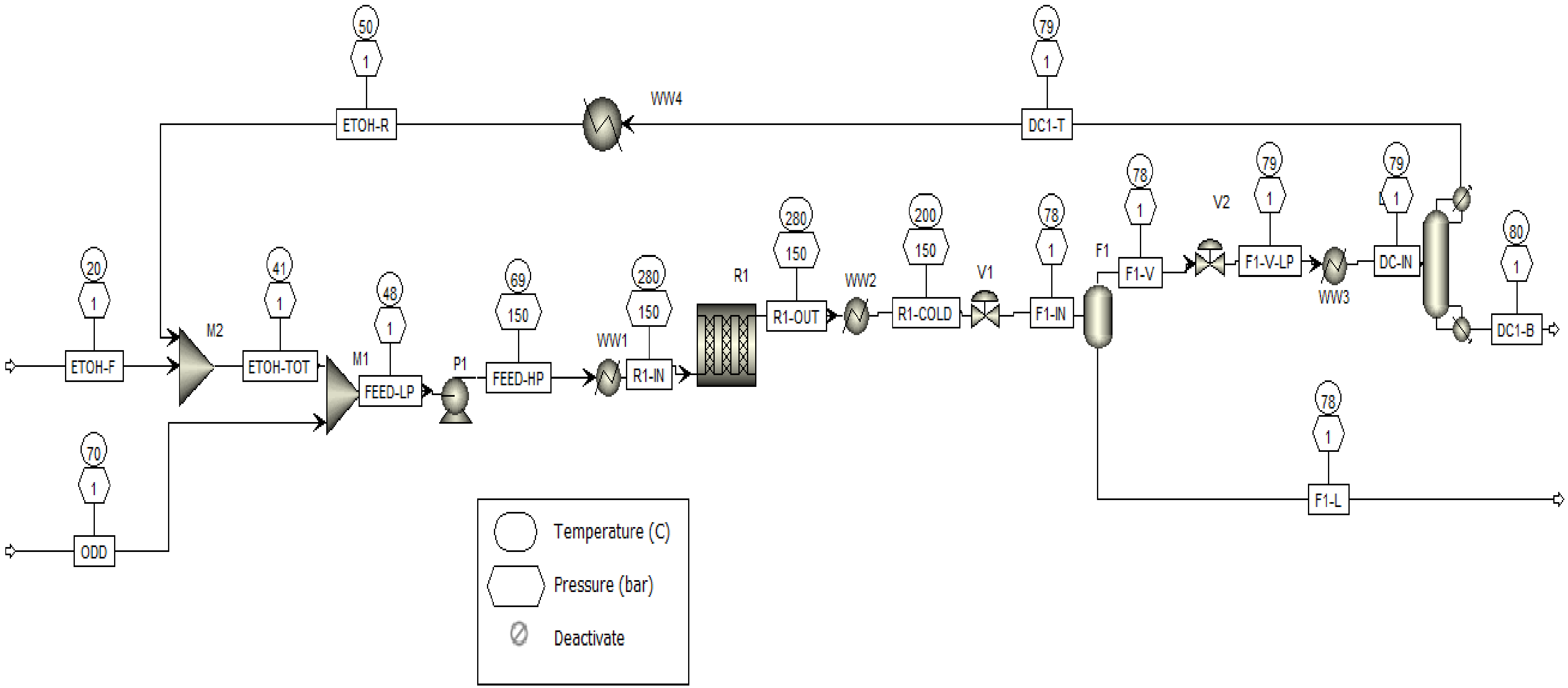

Figure 5-1. Transesterification process of ODD using supercritical ethanol azeotropic at 553 K and 15 MPa.

The extraction process simulated in this thesis is shown in Figure 5-2. The process consists of two extraction columns, the first one (E-1) is operated at 313.15 K and 10 MPa and a second one (E-2) at 313.15 K and 16 MPa. A separation section after each column is needed, to achieve the recovery of the solvent, otherwise the process would not be feasible. The aim of the first column is to achieve separation of the fatty acids esters, since they have the highest solubility with $scCO_2$. Further, one will look for the conditions that minimize the minor component content in the extracted stream (EXTRACT) because of that stream will be a side stream. Since this stream will not be treated, and thus, the minor components present in that stream will not be recovered. On the other hand, squalene separation is the target of the second column, so it will be collected from (EXTRACT 3). As it is explained before, it is not interesting to have tocopherols and sterols in EXTRACT 3. Therefore, the optimal conditions are those that separate squalene in EXTRACT 3 with the minimum tocopherols and sterols content. The extraction process is simulated at the same conditions for the different ODD sources.

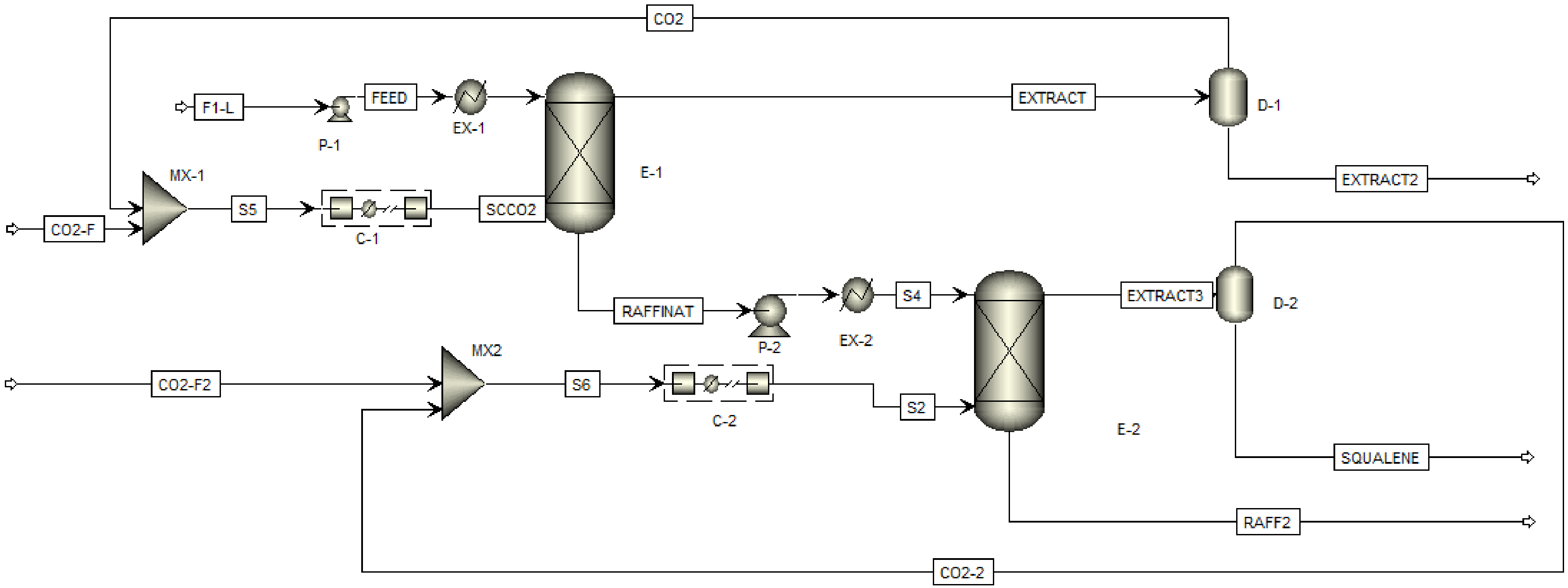

Figure 5-2. Extraction process of minor components using scCO$_2$.

5.2.1 Simulation of the supercritical extraction process

As it said before, F1-L is the stream simulated using UNIQ-RK in Aspen for a group of bachelor students during their bachelor thesis project. Sunflower ODD (of which the mass composition is shown in Table 5-9) is used as feedstock for the simulation.

Table 5-9. Sunflower EE-ODD composition.

Component	%wt
Ethanol	9.99
FFA	2.16
TG	15.91
Tocopherols	3.34
FAEE	49.5
Water	1.29
MG	2.27
DG	2.17
FAME	1.31
Sterols	9.55
Squalene	2.49
Total minor components	15.38

5.2.1.1 First extraction column (E-1)

The supercritical extraction is carried out in a extraction column (E-1) with a S/F (solvent/feed) mass ratio of 10, 14 stages and at 313 K and 10 MPa as it is shown in Figure 5-3.

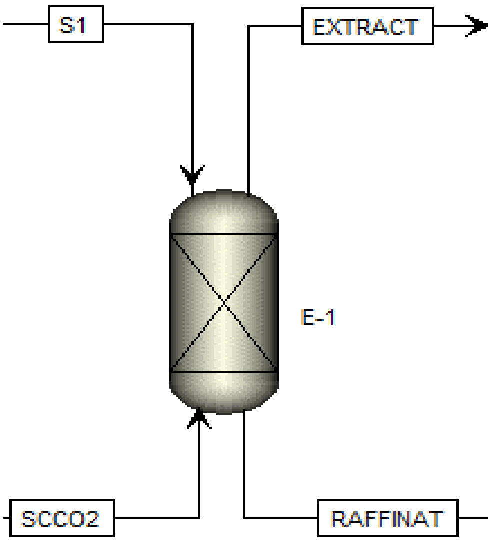

Figure 5-3. Extraction column (E-1) at 313 K and 10 MPa, S/F ratio of 10.

The results of this extraction are shown in Table 5-10.

Table 5-10. Simulation results using RK-Aspen for the block E-1.

Component	S1 (kg h^{-1})	ScCO_2 (kg h^{-1})	Extract (kg h^{-1})	Raffinat (kg h^{-1})
Ethanol	0.0999	0.0427	0.1424	0.0002
FFA	0.0216	-	0.0216	-
TG	0.1591	-	0.1591	-
Tocopherols	0.0334	-	0.0067	0.0268
FAEE	0.4950	-	-	0.4950
Water	0.0129	0.0055	0.0183	0.0001
MG	0.0227	-	0.0227	-
DG	0.0217	-	0.0217	-
FAME	0.0131	-	0.0131	-
CO_2	-	9.9958	9.9958	-
Sterols	0.0955	-	-	0.0955
Squalene	0.0249	-	0.0061	0.0188
Total (kg h^{-1})	1	10.0440	10.4075	0.6365

As it is shown in Table 5-10, ethanol, FFA, TG, water, MG, DG, FAME, CO_2 and a small amount of tocopherols and squalene are collected at the top. All the sterols are in the refined stream, FAEE as well and a high amount of tocopherols and squalene. The recovery yield for tocopherols in the refined phase is 80.11 % and for squalene is 75.46 %. After this extraction column, one obtained a first separation of the most soluble compounds in extract stream and collected a high amount of the minor components in the refined phase. This stream is sent to a second extraction column (E-2) to achieve the squalene isolation.

The evolution of the mass profile composition on E-1 is analyzed and shown for the extract and the refined phase, respectively in Figure 5-4 and Figure 5-5. The extract phase is the stream that flows from bottom (stage 14) to top (stage 1), as it is shown, the mass fraction of FAME and FFA is increasing after every stage due to the transference of these components to the extract phase.

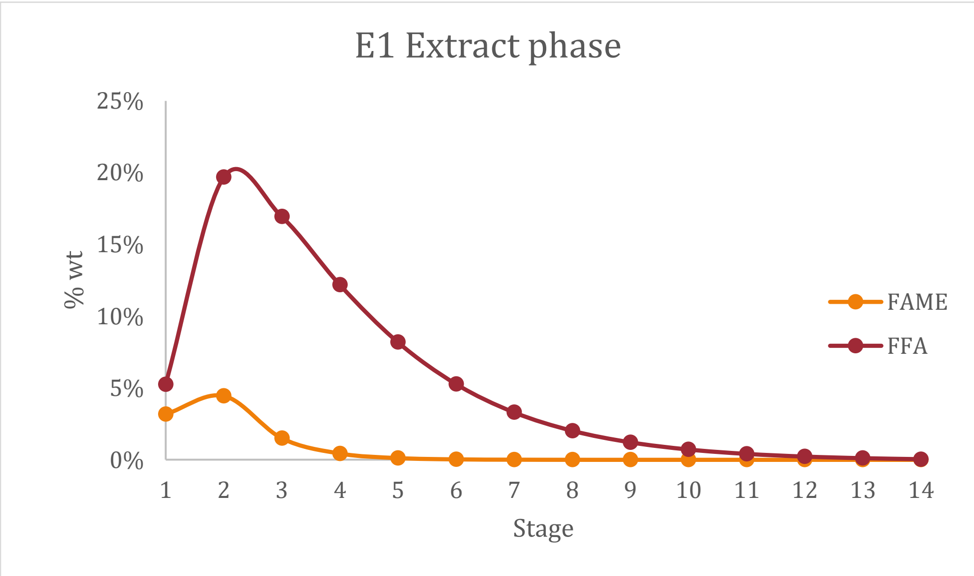

Figure 5-4. Evolution of the extract phase mass composition (CO_2-free basis) inside the extraction column, with stage 1 corresponding to the top of the column.

On the other hand, in the phase that flows from top (stage 1) to bottom (stage 14), both the squalene and the tocopherol compositions are investigated. As it is shown, squalene and tocopherol are transferred to the extract phase due to at first stage, squalene and tocopherol composition are higher than in the last one.

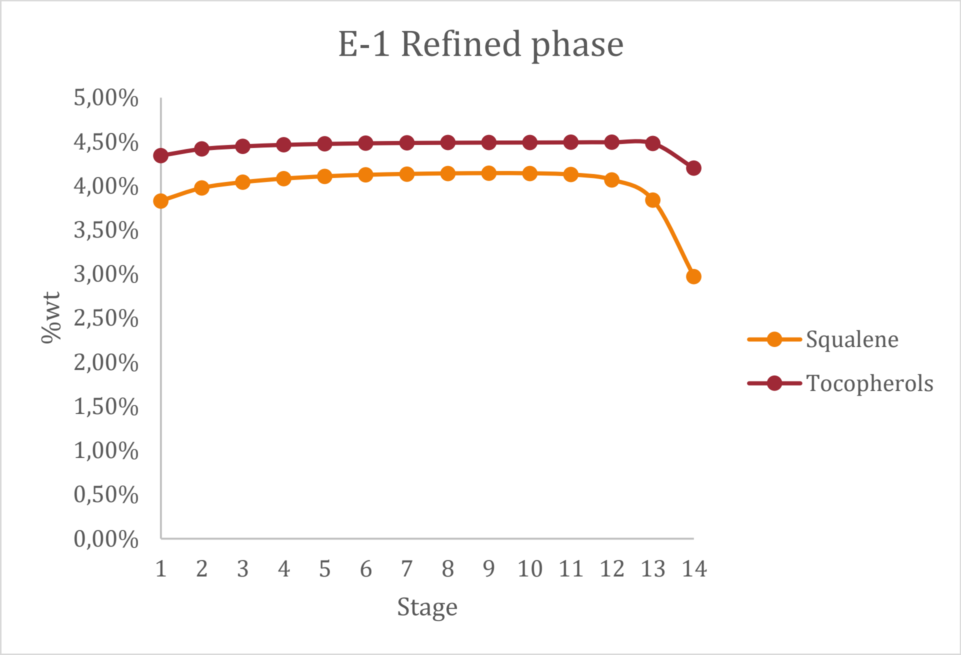

Figure 5-5. Evolution of the refined phase mass composition (CO_2-free basis) inside the extraction column, with stage 1 corresponding to the top of the column.

The model predict that the FAEE are collected at bottom. This fact could be due to the different order of magnitude observed in FAME/CO_2 binary interaction parameters shown in Table 5-8.

5.2.1.2 Second extraction column (E2)

The next step is to achieve squalene isolation, therefore, one will work at higher pressures. The extraction column (E-2) is shown in Figure 5-6 and this column works at 313.15 K and 16 MPa with a S/F ratio of 7.88 and 10 stages.

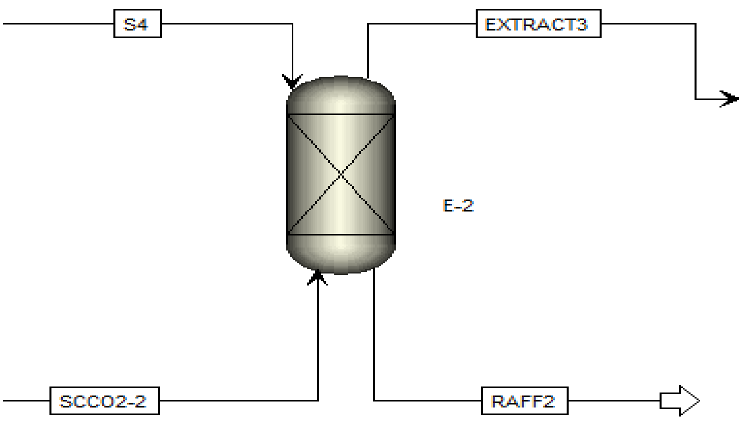

Figure 5-6. Extraction column (E-2) at 313 K and 16 MPa, S/F ratio of 7.88.

Table 5-11. Simulation results using RK-Aspen for the block E-2.

Component	S4 (kg h^{-1})	ScCO_2 (kg h^{-1})	Extract3 (kg h^{-1})	Raff2 (kg h^{-1})
Ethanol	0.0002	0.0001	0.0003	-
FFA	-	-	-	-
TG	-	-	-	-
Tocopherols	0.0267	-	0.0002	0.0266
FAEE	0.4950	-	-	0.4950
Water	0.0001	-	0.0001	-
MG	-	-	-	-
DG	-	-	-	-
FAME	-	-	-	-
CO_2	-	5	5	-
Sterols	0.0955	-	-	0.0955
Squalene	0.0189	-	0.0170	0.0019
Total (kg h^{-1})	0.6365	5.0001	5.0176	0.6190

Table 5-11 summarizes the simulation results. Extract 3 is mainly the solvent (CO_2), together with squalene and a small amount of tocopherols, water and ethanol. Almost all the tocopherols remains in the refined phase of this extraction column together with sterols. The yield recovery of squalene in extract phase for that stage is 89.95 %.

Mass composition of squalene inside E-2 is investigated in Figure 5-7. As in it shown, the stream flowing from bottom (stage 10) to top (stage 1) is enriched in squalene content along the column.

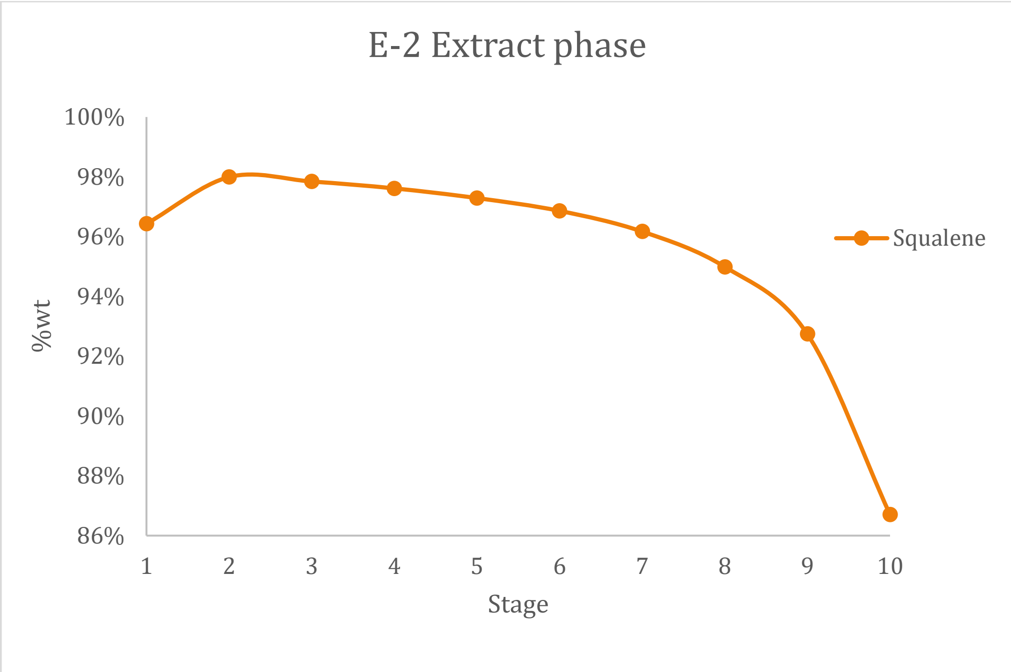

Figure 5-7. Evolution of the extract phase mass composition (CO_2-free basis) inside the extraction column E-2, with stage 1 corresponding to the top of the column..

5.2.1.3 Squalene isolation

After this unit, a flash separation is needed to recovery the solvent by depressurization and squalene is finally collected in the stream called SQUALENE (Figure 5-2) with a squalene mass flow of 0.017 kg h^{-1} quality of 98.43 wt% and with a global squalene recovery of 68.27 %. High purity squalene isolation is possible according to this simulation results.

5.2.2 Optimization of E-1

In this section we will discuss the influence of conditions on the first extraction process using sunflower EE-ODD as a feedstock.

5.2.2.1 Effect of pressure in E-1

Squalene, tocopherols, FAME and FFA content in the refined phase will be analysed by changing the pressure in the first column in the range of 9.25 to 10 MPa. Figure 5-8 shows how the mass fraction of squalene, tocopherols, FAME and FFA in the refined phase varies when pressure is increased. With increasing pressure, less squalene recovery could be achieved, the FAME and FFA content in the refined phase decrease very quickly. This effect is interesting because of a high content of FAME or FFA in the refined phase after E-1, this means that those components will be collected in the extract phase after E-2 together with squalene. This fact leads to a lower squalene quality values so therefore one will work at the highest pressure possible in which the content of FFA and FAME in refined phase after E-1 is low enough. Thus, the first extraction column will operate at 10 MPa. In addition, tocopherol content in refined phase increases a bit when pressure increases leading to lower tocopherol waste.

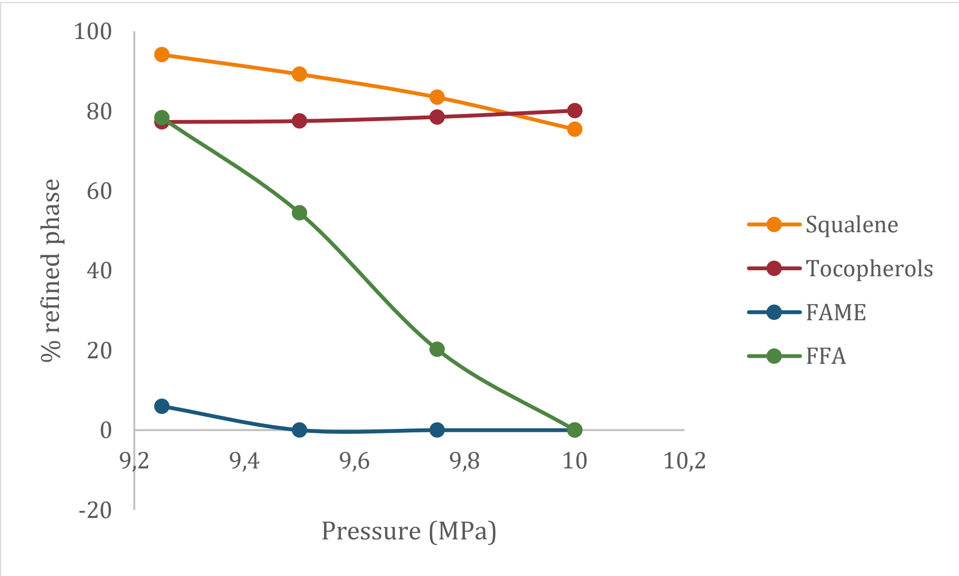

Figure 5-8. Influence of pressure on the first extraction column.

5.2.2.2 Effect of Temperature in E-1

The squalene, tocopherols, FAME and FFA content in the refined phase will be analysed by changing the temperature in the first column in the range of 308 to 318 K. Figure 5-9 show how by increasing temperature, the FAME and FFA content in refined phase increases a lot. Since one is interested in collecting those components in the extract phase, low temperatures are more suitable. However, with increasing temperature, the squalene content in the refined phase increases. So a temperature in which not too much of the FAME and FFA are present in the refined phase and squalene content in refined phase is high enough is the target. 313 K is selected as extraction temperature. In addition, higher temperatures leads to lower tocopherol content in the refined phase.

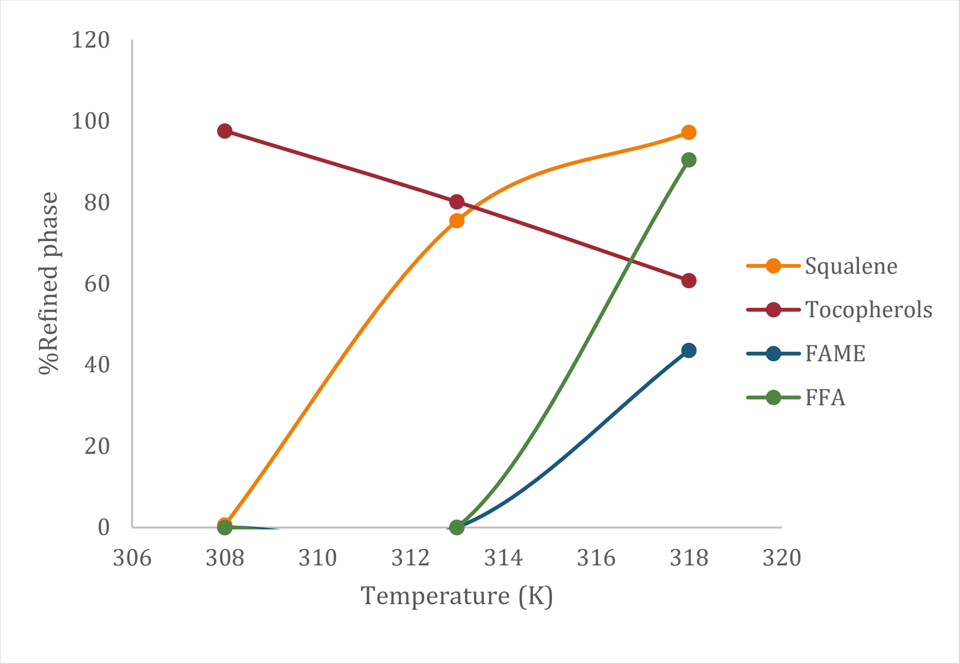

Figure 5-9. Influence of temperature on the first extraction column.

5.2.3 Optimization of E-2

In this section the influence of pressure on the second extraction process is discussed using sunflower EE-ODD as a feedstock.

The squalene and tocopherol content in the refined phase were analysed. With increasing pressure, the squalene content in refined phase decreases until a pressure value of 16 MPa. Afterwards the squalene content in refined phase start to increase again (Figure 5-10). The target of this column is collecting squalene in the extract phase with a so low content as possible of squalene in refined phase. Therefore, high pressures are suitable. A pressure of 16 MPa is selected for the extraction process. On the other hand, the tocopherol content in the extract phase seems to be independent of pressure in the range of study.

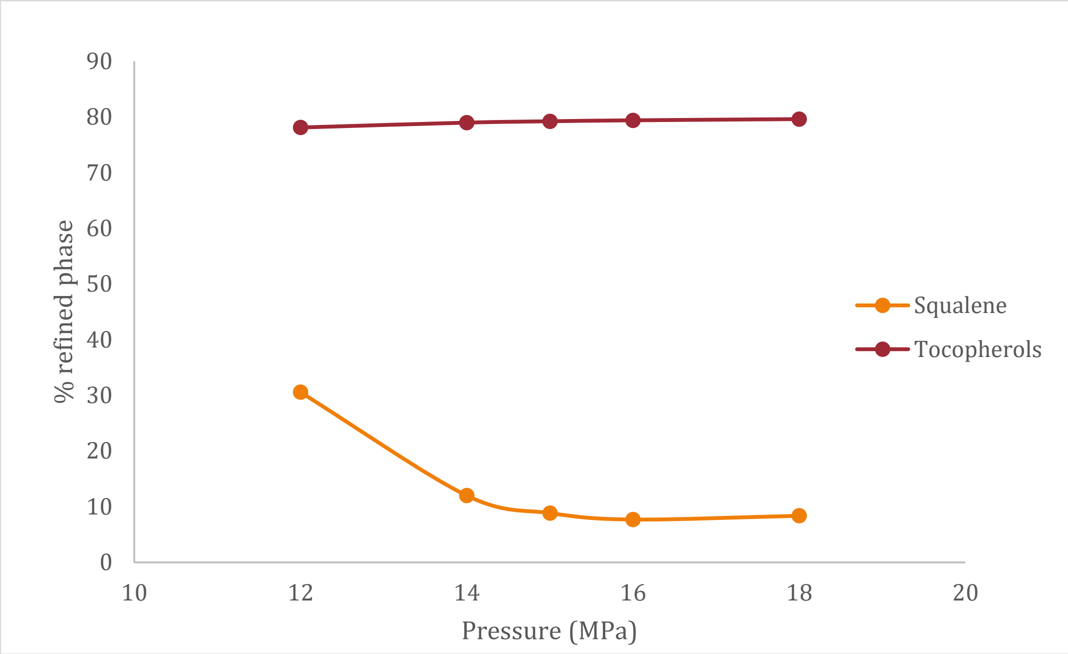

Figure 5-10. Influence of pressure on E-2.

5.2.4 Effect of feedstock composition

5.2.4.1 High tocopherol soybean EE-ODD feedstock

The same process (Figure 5-2) is simulated using soybean EE-ODD feedstock with high tocopherol content, with the composition shown in Table 5-12. This raw materials has a much higher minor components content (57.92 wt%). The tocopherols and sterols composition is much higher than with sunflower EE-ODD.

Table 5-12. Composition of soybean EE-ODD with high tocopherol content.

Component	%wt
Ethanol	6.9137
FFA	0.3926
TG	1.9483
Tocopherols	24.1818
FAEE	19.9323
Water	0.6435
MG	3.856
DG	6.526
FAME	1.8669
Sterols	30.7675
Squalene	2.972
Total minor components	57.9213

5.2.4.1.1 First extraction column

The supercritical extraction is carried out in a extraction column (E-1) with a S/F (solvent/feed) mass ratio of 10 , 14 stages and at 313 K and 10 MPa as it is shown in Figure 5-3.

The simulation results of E-1 are shown in Table 5-13.

Table 5-13. Extraction results predicted with RK-Aspen for E-1.

Component	S1 (kg h^{-1})	ScCO_2 (kg h^{-1})	Extract (kg h^{-1})	Raffinat (kg h^{-1})
Ethanol	0.0691	0.0295	0.0985	0.0002
FFA	0.0039	-	0.0039	-
TG	0.0195	-	0.0195	-
Tocopherols	0.2418	-	0.0337	0.2082
FAEE	0.1993	-	-	0.1993
Water	0.0064	0.0027	0.0091	-
MG	0.0386	-	0.0386	-
DG	0.0653	-	0.0653	-
FAME	0.0187	-	0.0187	-
CO_2	-	9.9998	9.9998	-
Sterols	0.3077	-	-	0.3076
Squalene	0.0297	-	0.0065	0.0232
Total (kg h^{-1})	1	10.0320	10.2934	0.7386

In this case , 13.94 % of tocopherols and 21.89 % of squalene are sent to the extract phase. Moreover, all the sterols are collected from bottom. However, FAEE and FFA separation from minor components is achieved and these are collected in the extract phase. Therefore, with this results, the minor components separation in E-1 shows higher yields than using sunflower as a feedstock.

5.2.4.1.2 Second extraction column

The refined stream is sent to a second extraction column to achieve squalene isolation. Again higher pressures will be used. The extraction column (E-2) is shown in Figure 5-6 and this column works at 313.15 K and 16 MPa with a S/F ratio of 7.88 and 10 stages.

Table 5-14. Extraction results predicted with RK-Aspen for E-2.

Component	S4 (kg h^{-1})	ScCO2 (kg h^{-1})	Extract3 (kg h^{-1})	Raff2 (kg h^{-1})
Ethanol	0.0002	0.0001	0.0002	-
FFA	-	-	-	-
TG	-	-	-	-
Tocopherols	0.2082	-	0.0014	0.2068
FAEE	0.1993	-	-	0.1993
Water	-	-	0.0001	-
MG	-	-	-	-
DG	-	-	-	-
FAME	-	-	-	-
CO_2	-	5.0000	5.0000	-
Sterols	0.3076	-	-	0.3076
Squalene	0.0232	-	0.0191	0.0042
Total (kg h^{-1})	0.7386	5.0001	5.0208	0.7179

Table 5-14 shows the results during this extraction. Squalene is transferred to the extract with a yield of 82.33 % and only 0.6 % of tocopherol content is lost in extract phase.

5.2.4.1.3 Squalene isolation

After this unit, a flash separation is needed to recover the solvent by depressurization and squalene is finally collected in the stream called SQUALENE (Figure 5-2) with a squalene mass flow of 0.0191 kg h^{-1}, a quality of 92.66 wt% and with a global squalene recovery of 64.17 %. So high purity squalene isolation is possible according to this simulation results, but with lower yields of squalene recovery.

5.2.4.2 Low tocopherol soybean EE-ODD feedstock

The same process (Figure 5-2) is simulated using soybean EE-ODD feedstock with low tocopherol content, of which the composition shown in Table 5-15. The minor components content is much lower, especially for the sterols and tocopherols amount.

Table 5-15. Composition of soybean EE-ODD with low tocopherol content.

Component	%wt
Ethanol	13.4874
FFA	2.3911
TG	0.8024
Tocopherols	0.4518
FAEE	74.5836
Water	1.8720
MG	0.2336
DG	0.2806
FAME	4.7599
Sterols	0.4908
Squalene	0.6466
Total minor components	1.5892

5.2.4.2.1 First extraction column

The supercritical extraction is carried out in a extraction column (E-1) with a S/F (solvent/feed) ratio of 10 , 14 stages and at 313 K and 10 MPa as it is shown in Figure 5-3.

The results predicted using RK-Aspen are shown in Table 5-16.

Table 5-16. Results predicted using RK-Aspen for the block E-1.

Component	S1 (kg h^{-1})	ScCO_2 (kg h^{-1})	Extract (kg h^{-1})	Raffinat (kg h^{-1})
Ethanol	0.1349	0.0575	0.1920	0.0004
FFA	0.0239	-	0.0239	-
TG	0.0080	-	0.0080	-
Tocopherols	0.0045	-	0.0005	0.0040
FAEE	0.7458	-	-	0.7458
Water	0.0187	0.0080	0.0266	0.0001
MG	0.0023	-	0.0023	-
DG	0.0028	-	0.0028	-
FAME	0.0476	-	0.0476	-
CO_2	-	9.9996	9.9996	-
Sterols	0.0049	-	-	0.0049
Squalene	0.0065	-	0.0008	0.0057
Total (kg h^{-1})	1.0000	10.0651	10.3042	0.7609

All the sterols are in the refined phase, 11.11 % of tocopherol content is transferred to extract phase. About 12% of the squalene is lost to the extract phase in this step. FAME and FFA transference to the extract phase is achieved. So this column work with higher yields, than when one work with the other raw materials.

5.2.4.2.2 Second extraction column

The extraction column (E-2) is shown in Figure 5-6 and this column works at 313.15 K and 16 MPa with a S/F ratio of 7.88 and 10 stages.

Table 5-17 shows the simulation results of the column E-2. In this step all the tocopherols are collected in the refined phase and also all the sterols. Squalene recovery in the extract phase in this step is 80.7 %. In this case, tocopherols missing are minimum during the extraction but squalene present the lowest transfer to extract phase.

Table 5-17. Simulation results of the extraction column E-2 using RK-Aspen model.

Component	S4 (kg h^{-1})	ScCO_2 (kg h^{-1})	Extract3 (kg h^{-1})	Raff2 (kg h^{-1})
Ethanol	0.0004	0.0002	0.0005	-
FFA	-	-	-	-
TG	-	-	-	-
Tocopherols	0.0040	-	-	0.0040
FAEE	0.7458	-	-	0.7458
Water	0.0001	-	0.0002	-
MG	-	-	-	-
DG	-	-	-	-
FAME	-	-	-	-
CO_2	-	5.0000	5.0000	-
Sterols	0.0049	-	-	0.0049
Squalene	0.0057	-	0.0046	0.0011
Total (kg h^{-1})	0.7609	5.0002	5.0053	0.7558

5.2.4.2.3 Squalene isolation

After the solvent recovery (Figure 5-2), a stream with a purity of 98.81 wt% of squalene with a flow of 0.0046 kg h^{-1} is obtained. Resulting in, a global squalene recovery of 70.46 %. So this feedstock results in higher quality and yield of squalene, but a lower amount of squalene.

5.2.5 Block unit for extraction process

In this section, the selection of the block unit to simulate the extraction process in the software Aspen Plus ® will be discussed. Two possibilities have been analysed, the column unit EXTRACT, and the separator unit FLASH2. Both use equilibrium calculations, as it was described in 3.8.1. The main difference is that EXTRACT uses liquid-liquid equilibrium calculations and FLASH2 vapor-liquid equilibrium. The phase of a supercritical fluid is not vapor or liquid . The rough convention in Aspen for phase allocation is explained in 3.6.

A comparison of the EXTRACT and FLASH2 block is performed by simulating the extraction of minor components from a sunflower EE-ODD using the same conditions S/F mass ratio of 10, 313 K and 9.5 MPa and two equilibrium stages.

5.2.5.1 EXTRACT block

The results using the EXTRACT block to simulate a two stages extraction column at 313 K and 9.5 MPa using a S/F mass ratio of 10 are shown in Table 5-18.

Table 5-18. Simulation results of two stages extractor unit at 313 K and 9.5 MPa with a S/F ratio of 10 using RK-Aspen method.

Component	S1 (kg h^{-1})	ScCO_2 (kg h^{-1})	Extract (kg h^{-1})	Raffinat (kg h^{-1})
Ethanol	0.0999	-	0.0999	-
FFA	0.0216	-	0.00568	0.01594
TG	0.1591	-	0.1591	-
Tocopherols	0.0334	-	0.008	0.0255
FAEE	0.495	-	-	0.495
Water	0.0129	-	0.0129	-
MG	0.0227	-	0.0181	0.0459
DG	0.0217	-	0.0162	0.0056
FAME	0.0131	-	0.0097	0.0033
CO_2	-	10	10	-
Sterols	0.0955	-	-	0.0955
Squalene	0.0249	-	0.0018	0.0231
Total (kg h^{-1})	1	10	10.3314	0.6686

5.2.5.2 FLASH2 block

The column simulated by two equilibrium stages is shown in Figure 5-11. The simulation results are shown in Table 5-19.

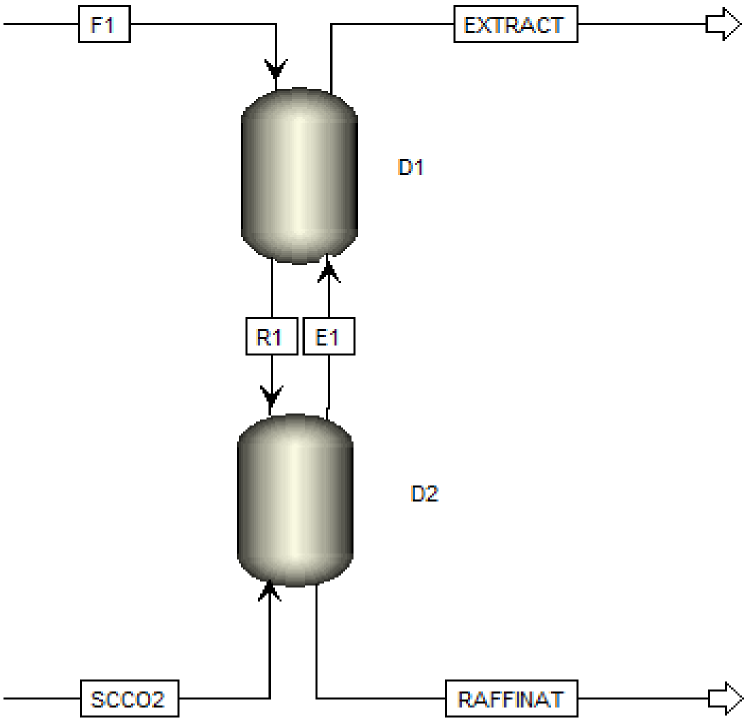

Figure 5-11. Extractor simulation using Flash2 units in Aspen Plus ®.

Table 5-19. Simulation results of two stages flash2 unit at 313 K and 9.5 MPa with a S/F ratio of 10 using RK-Aspen method.

Component	S1 (kg h^{-1})	$ScCO_2$ (kg h^{-1})	Extract (kg h^{-1})	Raffinat (kg h^{-1})
Ethanol	0.0999	-	0.0999	-
FFA	0.0216	-	0.0175	0.0041
TG	0.1591	-	0.1591	-
Tocopherols	0.0334	-	0.0031	0.0303
FAEE	0.495	-	-	0.4950
Water	0.0129	-	0.0129	-
MG	0.0227	-	0.0222	0.0004
DG	0.0217	-	0.0211	0.0006
FAME	0.0131	-	0.0123	0.0008
CO_2	-	10	10	-
Sterols	0.0955	-	-	0.0955
Squalene	0.0249	-	0.0086	0.0163
Total (kg h^{-1})	1	10	10.3568	0.6432

In conclusion, using the flash unit, FAME separation is better. The extract phase is richer in FAME and more tocopherols remain in the refined phase However, the squalene content in the extract phase is higher.

Due to this, one will work at pressure much higher than critical pressure of CO_2 and therefore Aspen will consider it as a liquid phase. At this conditions, above the critical pressure, one can simulate the process using the extractor block unit. However, the option of simulating the process using FLASH could be considered as well. The two options should be verified again, by comparing the simulations with experimental results obtained from a pilot plant and verify which one represent better data.

6 CONCLUSIONS

Over the last decade the production rates for the major oils has varied a lot, generally with a growing trend due to increases in consumption mainly because of the additional use as biodiesel feedstock. These crude oils are subjected to a refining process where these oils are made suitable for human consumption (edible oils). One of the most important by-products of this process are, the oil deodorizer distillates (ODD). ODD is a complex mixture of free fatty acids (FFA), tri- di and mono glycerides, and minor components such as tocopherols, sterols and squalene. These minor components are considered valuable compounds from cosmetic and pharmaceutical industries. The classical methods to isolate these minor components have some drawbacks, and therefore, supercritical extraction technology has been investigated. Flexible and predictive thermodynamics methods available in Aspen Plus are recommended to simulate supercritical extraction process. Equilibrium data were correlated using RK-Aspen model. That method is based on the Redlich-Kwong-Aspen equation of state using quadratic mixing rules. A fairly good representation of the data was obtained and therefore the process was simulated using this equation of state. In this work, the importance of binary interaction parameters were analyzed in respect to represent the mixture more close to the real behavior.

Critical properties delivered by Aspen, estimated using Aspen and values from literature were compared. This comparison show big differences and a sensitivity analysis should be carried out to observed how the simulation is affected by the pure critical properties.

The extraction process is investigated for three kinds of raw materials, such as sunflower, high tocopherol and low tocopherol content in soybean oil ODDs. The supercritical extraction process is simulated using two different extraction columns. The optimal conditions for the first extraction column are a pressure of 10 MPa and 313 K. This results in a selected separation of FAME and FFA, while squalene and tocopherols losses to the extract phase are low. In the second extraction column , squalene isolation is achieved with a maximum content in extract phase at 16 MPa and 313 K. In addition, tocopherol content in E-2 is independent of pressure changes so at this conditions tocopherol losses are low.

Using sunflower ODD as feedstock a good squalene purity is achieved with a global squalene recovery of 68 %. Treating high tocopherol content in soybean oil ODDs, results in a lower purity of squalene. Finally, low tocopherol soybean ODDs produce a stream with a high squalene quality and a global squalene recovery of 70.46 %, but with a too small mass flow to be feasibility produced at industrial level.

The last aspect which was studied, was the Aspen block unit used to simulate the extraction process. Calculations taking account vapor-liquid equilibrium (FLASH2) and liquid-liquid equilibrium (EXTRACTOR) were compared at the same conditions. Using the FLASH2 unit, the esters are better separated. However, the process needs pressures far above the critical pressure so are so Aspen will consider stream phases as a liquid. Therefore, it is more favorable to use the EXTRACTOR unit.

To improve the insights in the extraction process, vapor liquid experimental data for ODD mixtures with supercritical carbon dioxide should be measured. In this way one can conclude whether the solute-solute interaction can be neglected or not. That fact could produce significant deviation of model prediction from experimental data especially in the mixture critical and working with high solutes concentrations.

Generally, the solubility of the components in $scCO_2$ in the simulations will be higher than under the process conditions. Since thermodynamic equilibrium cannot be reached in an industrial extractor (solvent and solute have not an infinite contact time). Therefore, an empirical extraction efficiency η_e must be used to correct these solubility deviations under operation conditions. This extraction efficiency could be calculated for the company in a pilot plant.

7 REFERENCES

1. REA Holding, *World production of oils & fats*.

2. Gunstone, F., *Vegetable oils in food technology: composition, properties and uses*. 2011: John Wiley & Sons.

3. Gavin, A.M., *Edible oil deodorization.* Journal of the American Oil Chemists' Society, 1978. **55**(11): p. 783-791.

4. Torres, C.F., G. Reglero, and G. Torrelo, *Extraction and Enzymatic Modification of Functional Lipids from Soybean Oil Deodorizer Distillate*. 2011: INTECH Open Access Publisher.

5. Ramamurthi, S. and A.R. McCurdy, *Enzymatic pretreatment of deodorizer distillate for concentration of sterols and tocopherols.* Journal of the American Oil Chemists' Society, 1993. **70**(3): p. 287-295.

6. Fernandes, P. and J. Cabral, *Phytosterols: applications and recovery methods.* Bioresource technology, 2007. **98**(12): p. 2335-2350.

7. De Lucas, A.d., et al., *Supercritical fluid extraction of tocopherol concentrates from olive tree leaves.* The Journal of Supercritical Fluids, 2002. **22**(3): p. 221-228.

8. SHISHIKURA, A., et al., *Concentration of tocopherols from soybean sludge by supercritical fluid extraction.* Journal of Japan Oil Chemists' Society, 1988. **37**(1): p. 8-12.

9. KOVARI, K., et al., *15e Conference internationale du tournesol (Toulouse, 13-15 juin 2000)-Physical refining of sunflower oil Physical refining of sunflower oil.*

10. KÖVARI, K. *Silica refining of vegetable oils*. in *Poster presented at AOCS World Conference, Budapest*. 1992.

11. Hénon, G., et al., *Deodorization of vegetable oils. Part I: Modelling the geometrical isomerization of polyunsaturated fatty acids.* Journal of the American Oil Chemists' Society, 1999. **76**(1): p. 73-81.

12. Müller-Mulot, W., *Rapid method for the quantitative determination of individual tocopherols in oils and fats.* Journal of the American Oil Chemists Society, 1976. **53**(12): p. 732-736.

13. Popov, A., T. Milkova, and N. Marekov, *Free and bound sterol content of sunflower, soy bean and maize oils.* Die Nahrung, 1974. **19**(7): p. 547-549.

14. Sam De Schepper (Indinox), K.S.E.T., Patrick Gonry, et al., *Title: FISCH-ICON Supercritical Solutions for Side-stream valorisation*.

15. Mendes, M., F. Pessoa, and A. Uller, *An economic evaluation based on an experimental study of the vitamin E concentration present in deodorizer distillate*

of soybean oil using supercritical CO 2. The Journal of supercritical fluids, 2002. **23**(3): p. 257-265.

16. Mendes, M., et al., *Recovery of the high aggregated compounds present in the deodorizer distillate of the vegetable oils using supercritical fluids.* The Journal of supercritical fluids, 2005. **34**(2): p. 157-162.

17. Vázquez, L., et al., *Supercritical fluid extraction of minor lipids from pretreated sunflower oil deodorizer distillates.* European Journal of Lipid Science and Technology, 2006. **108**(8): p. 659-665.

18. Wagner, K.-H., A. Kamal-Eldin, and I. Elmadfa, *Gamma-tocopherol–an underestimated vitamin?* Annals of nutrition and metabolism, 2004. **48**(3): p. 169-188.

19. Jiang, Q., et al., *γ-Tocopherol, the major form of vitamin E in the US diet, deserves more attention.* The American journal of clinical nutrition, 2001. **74**(6): p. 714-722.

20. Ito, V.M., et al. *Natural compounds obtained through centrifugal molecular distillation*. in *Twenty-Seventh Symposium on Biotechnology for Fuels and Chemicals*. 2006. Springer.

21. Martins, P.F., et al., *Comparison of two different strategies for tocopherols enrichment using a molecular distillation process.* Industrial & engineering chemistry research, 2006. **45**(2): p. 753-758.

22. Sumner Jr, C.E., S.D. Barnicki, and M.D. Dolfi, *Process for the production of sterol and tocopherol concentrates*. 1995, Google Patents.

23. Mau, J. and H. Tsen, *Investigation on the Conditions for the Preparation of High-Purity Vitamin E Concentrate from Soybean Oil Deodorizer Distillate.* JOURNAL-CHINESE AGRICULTURAL CHEMICAL SOCIETY, 1995. **33**: p. 686-697.

24. Martinez, J.L., *Supercritical fluid extraction of nutraceuticals and bioactive compounds*. 2007: CRC Press.

25. https://en.wikipedia.org/wiki/Sterol. 10/03/2016].

26. Ostlund, R.E., S.B. Racette, and W.F. Stenson, *Inhibition of cholesterol absorption by phytosterol-replete wheat germ compared with phytosterol-depleted wheat germ.* The American journal of clinical nutrition, 2003. **77**(6): p. 1385-1389.

27. Ibáñez, E., et al., *Concentration of sterols and tocopherols from olive oil with supercritical carbon dioxide.* Journal of the American Oil Chemists' Society, 2002. **79**(12): p. 1255-1260.

28. Stavroulias, S. and C. Panayiotou, *Determination of optimum conditions for the extraction of squalene from olive pomace with supercritical CO2.* Chemical and biochemical engineering quarterly, 2005. **19**(4): p. 373-381.

29. Akgün, N.A., *Separation of squalene from olive oil deodorizer distillate using supercritical fluids.* European Journal of Lipid Science and Technology, 2011. **113**(12): p. 1558-1565.

30. Kraujalis, P. and P.R. Venskutonis, *Supercritical carbon dioxide extraction of squalene and tocopherols from amaranth and assessment of extracts antioxidant activity.* The Journal of Supercritical Fluids, 2013. **80**: p. 78-85.

31. Wejnerowska, G., P. Heinrich, and J. Gaca, *Separation of squalene and oil from Amaranthus seeds by supercritical carbon dioxide.* Separation and Purification Technology, 2013. **110**: p. 39-43.

32. Demirbaş, A., *Biodiesel fuels from vegetable oils via catalytic and non-catalytic supercritical alcohol transesterifications and other methods: a survey.* Energy conversion and Management, 2003. **44**(13): p. 2093-2109.

33. Ghosh, S. and D. Bhattacharyya, *Isolation of tocopherol and sterol concentrate from sunflower oil deodorizer distillate.* Journal of the American Oil Chemists' Society, 1996. **73**(10): p. 1271-1274.

34. Lin, K., *National Chung Hsing University.* MS, Texas A & M University, 2002.

35. Chu, B., B. Baharin, and S. Quek, *Factors affecting pre-concentration of tocopherols and tocotrienols from palm fatty acid distillate by lipase-catalysed hydrolysis.* Food chemistry, 2002. **79**(1): p. 55-59.

36. Rohr, R., R. Rohr, and J.A. Trujillo-Quijano, *Process for separating unsaponifiable valuable products from raw materials*. 2005, Google Patents.

37. Meng, K.H. and B. Winton, *Process for recovery of tocopherols and sterols*. 1963, Google Patents.

38. Ramamurthi, S., P.R. Bhirud, and A.R. McCurdy, *Enzymatic methylation of canola oil deodorizer distillate.* Journal of the American Oil Chemists Society, 1991. **68**(12): p. 970-975.

39. Shimada, Y., et al., *Facile purification of tocopherols from soybean oil deodorizer distillate in high yield using lipase.* Journal of the American Oil Chemists' Society, 2000. **77**(10): p. 1009-1013.

40. Fang, T., et al., *Phase equilibria for the ternary system methyl oleate+ tocopherol+ supercritical CO2.* Journal of Chemical & Engineering Data, 2005. **50**(2): p. 390-397.

41. Torres, C.F., et al., *Production of phytosterol esters from soybean oil deodorizer distillates.* European journal of lipid science and technology, 2009. **111**(5): p. 459-463.

42. Lutišan, J., J. Cvengroš, and M. Micov, *Heat and mass transfer in the evaporating film of a molecular evaporator.* Chemical Engineering Journal, 2002. **85**(2): p. 225-234.

43. AspenTech, *Aspen Physical Property System*, ed. I. Aspen technollogy. 2001.

44. Haar, L., J.S. Gallagher, and G.S. Kell, *NBS/NRC steam tables: Thermodynamic and transport properties and computer programs for vapor and liquid states of water in SI units, 320 p.* Hemisphere, Washington, DC, 1984.

45. Soave, G., *Equilibrium constants from a modified Redlich-Kwong equation of state.* Chemical Engineering Science, 1972. **27**(6): p. 1197-1203.

46. Peng, D.-Y. and D.B. Robinson, *A new two-constant equation of state.* Industrial & Engineering Chemistry Fundamentals, 1976. **15**(1): p. 59-64.

47. Mathlas, P., *A versatile phase equilibrium equation of state.* Ind. Eng. Chem. Process Des. Dev.;(United States), 1983. **22**(3).

48. Schwartzentruber, J. and H. Renon, *Extension of UNIFAC to High Pressures and Temperatures by the Use of a Cubic Equation of State.* Industrial & engineering chemistry research, 1989. **28**(7): p. 1049-1055.

49. Lermite, C. and J. Vidal, *Les règles de mélange appliquées aux équations d'état.* Revue de l'Institut français du pétrole, 1988. **43**(1): p. 73-94.

50. Huron, M.-J. and J. Vidal, *New mixing rules in simple equations of state for representing vapour-liquid equilibria of strongly non-ideal mixtures.* Fluid Phase Equilibria, 1979. **3**(4): p. 255-271.

51. Brule, M., et al., *Multiparameter corresponding‐states correlation of coal‐fluid thermodynamic properties.* AIChE Journal, 1982. **28**(4): p. 616-625.

52. Zamudio, M., C. Schwarz, and J. Knoetze, *Experimental measurement and modelling with Aspen Plus® of the phase behaviour of supercritical CO 2+(n-dodecane+ 1-decanol+ 3, 7-dimethyl-1-octanol).* The Journal of Supercritical Fluids, 2013. **84**: p. 132-145.

53. K. M. Klincewicz and R.C. Reid, *Estimation of Critical Properties with Group Contribution Methods.* AIChe Journal, 1984. **30**: p. 137-142.

54. Constantinou, L. and R. Gani, *New group contribution method for estimating properties of pure compounds.* AIChE Journal, 1994. **40**(10): p. 1697-1710.

55. Schefflan, R., *Teach yourself the basics of Aspen Plus*, ed. I. John Wiley & Sons. 2011, New Jersey and Canada.

56. Biegler, L.T., *Nonlinear programming: concepts, algorithms, and applications to chemical processes*. 2010: SIAM.

57. Anderson, T.F., Abrams, D. D., and Hrens. E. A., Aiche. J. **24**(1): p. 20-39.

58. Fabries, J.F.a.R., H.,, AIChe Journal, 1976. **21**(4): p. 735-742.

59. Fang, T., et al., *Phase equilibria for binary systems of methyl oleate–supercritical CO 2 and α-tocopherol–supercritical CO 2.* The Journal of supercritical fluids, 2004. **30**(1): p. 1-16.

60. Srivastava, A. and R. Prasad, *Triglycerides-based diesel fuels.* Renewable and sustainable energy reviews, 2000. **4**(2): p. 111-133.

61. Lim, C.S., Z.A. Manan, and M.R. Sarmidi, *Simulation modeling of the phase behavior of palm oil-supercritical carbon dioxide.* Journal of the American Oil Chemists' Society, 2003. **80**(11): p. 1147-1156.

62. Pilar Olivares-Carrillo, J.Q.-M., Antonia Perez de los Rios, Francisco J. Hernandez-Fernandez, *Estimation of critical properties of reaction mixtures obtained in different reaction conditions during the synthesis of biodiesel with supercritical methanol from soybean oil.* Chemical Engineering Journal, 2014. **241**: p. 418-432.

63. Rui ruivo, A.P., Pedro Simoes, *Phase equilibria of the ternary system methyl oleate/squalene/carbon dioxide at high pressure conditions.* The Journal of supercritical fluids, 2004. **29**: p. 77-85.

64. Ragunath Bharath, H.I.a.K.A., *Vapor-Liquid Equilibria for binary mixtures of Carbon Dioxide and Fatty Acid Ethyl Esters.* Fluid Phase Equilibria, 1989. **50**: p. 315-327.

65. Araujo, M.E., N.T. Machado, and M.A.A. Meireles, *Modeling the Phase Equilibrium of Soybean Oil Deodorizer Distillates+ Supercritical Carbon Dioxide Using the Peng− Robinson EOS.* Industrial & engineering chemistry research, 2001. **40**(4): p. 1239-1243.

66. CARDOZO-FILHO, L., F. WOLFF, and M.A.A. MEIRELES, *High pressure phase equilibrium: prediction of essential oil solubility.* Food Science and Technology (Campinas), 1997. **17**(4): p. 485-488.

67. Sovová, H., R.P. Stateva, and A.A. Galushko, *Essential oils from seeds: solubility of limonene in supercritical CO 2 and how it is affected by fatty oil.* The Journal of Supercritical Fluids, 2001. **20**(2): p. 113-129.

68. Ragunath Bharath, H.I., Tadafumi Adschiri and Kunio Arai, *Phase equilibrium study for the separation and fractionation of fatty oil components using supercritical carbon dioxide.* Fluid Phase Equilibria, 1992. **81**: p. 307-320.

69. Yu, Z.-R., S.S. Rizvi, and J.A. Zollweg, *Phase equilibria of oleic acid, methyl oleate, and anhydrous milk fat in supercritical carbon dioxide.* The Journal of Supercritical Fluids, 1992. **5**(2): p. 114-122.

70. Paulo J. Pereira, M.G., Baudilio Coto, Edmundo Gomes de Azevedo, Manuel Nunes da Ponte, *Phase equilibria of CO2 + Dl-alpha-Tocopherol at Temperatures from 292 K to 333K and Pressures up to 26 MPa.* Fluid Phase Equilibria, 1993. **91**: p. 133-143.

71. H. Inomata, K.A., S. Saito, S. Ohba and K. Takeuchi, *Measurement and prediction of phase equilibria for the CO2-Ethanol-Water system.* Fluid Phase Equilibria, 1989. **53**: p. 23-30.

72. J. Stoldt, G.B., *Phase equilibrium measurements in complex systems of fats, fat compounds and supercritical carbon dioxide.* Fluid Phase Equilibria, 1998. **146**: p. 269-295.

73. Kontogeorgis, G.M. and G.K. Folas, *Thermodynamic models for industrial applications: from classical and advanced mixing rules to association theories*. 2009: John Wiley & Sons.

8 APPENDICES

APPENDIX A. NEWTON- RAPHSON METHOD TO SOLVE NONLINEAR EQUATIONS

Newton-Raphson method can solve a set of n equation in the format:

$$f_1(x_{1,}x_2, \dots x_n) = 0 \tag{83}$$

$$f_2(x_{1,}x_2, \dots x_n) = 0 \tag{84}$$

$$f_n(x_{1,}x_2, \dots x_n) = 0 \tag{85}$$

Each of the function is expressed as a first-order Taylor's serie about a point X^k :

$$f_1(X^{k+1}) = f_1(X^k) + \left.\frac{\partial f_1}{\partial x_1}\right\rangle_{X^k} \left(x_1^{k+1} - x_1^k\right) + \left.\frac{\partial f_1}{\partial x_2}\right\rangle_{X^k} \left(x_2^{k+1} - x_2^k\right) + \cdots + \left.\frac{\partial f_1}{\partial x_n}\right\rangle_{X^k} (x_n^{k+1} - x_n^k) \tag{86}$$

$$f_2(X^{k+1}) = f_2(X^k) + \left.\frac{\partial f_2}{\partial x_1}\right\rangle_{X^k} \left(x_1^{k+1} - x_1^k\right) + \left.\frac{\partial f_2}{\partial x_2}\right\rangle_{X^k} \left(x_2^{k+1} - x_2^k\right) + \cdots + \left.\frac{\partial f_2}{\partial x_n}\right\rangle_{X^k} (x_n^{k+1} - x_n^k) \tag{87}$$

$$f_\mathrm{n}(X^{k+1}) = f_\mathrm{n}(X^k) + \left.\frac{\partial f_\mathrm{n}}{\partial x_1}\right\rangle_{X^k} \left(x_1^{k+1} - x_1^k\right) + \left.\frac{\partial f_\mathrm{n}}{\partial x_2}\right\rangle_{X^k} \left(x_2^{k+1} - x_2^k\right) + \cdots + \left.\frac{\partial f_\mathrm{n}}{\partial x_n}\right\rangle_{X^k} (x_n^{k+1} - x_n^k) \tag{88}$$

Doing the assumption of the value of all functions in the X^{k+1} are zero, evaluating all derivatives at the point X^k and with Δx definition:

$$\Delta x_i = x_i^{k+1} - x_i^k \tag{89}$$

The set of equations obtained are:

$$f_1(X^{k+1}) = 0 = f_1(X^k) + \left.\frac{\partial f_1}{\partial x_1}\right\rangle_{X^k} \left(\Delta x_1^k\right) + \left.\frac{\partial f_1}{\partial x_2}\right\rangle_{X^k} \left(\Delta x_2^k\right) + \cdots + \left.\frac{\partial f_1}{\partial x_n}\right\rangle_{X^k} (\Delta x_n^k) \tag{90}$$

$$_2(X^{k+1}) = 0$$

$$= f_2(X^k) + \left.\frac{\partial f_2}{\partial x_1}\right\rangle_{X^k} \left(\Delta x_2^k\right) + \left.\frac{\partial f_2}{\partial x_2}\right\rangle_{X^k} \left(x_2^{k+1} - x_2^k\right) + \cdots \tag{91}$$

$$+ \left.\frac{\partial f_2}{\partial x_n}\right\rangle_{X^k} (\Delta x_n^k)$$

$$f_{\mathrm{n}}(X^{k+1}) = 0 = f_{\mathrm{n}}(X^k) + \left.\frac{\partial f_{\mathrm{n}}}{\partial x_1}\right\rangle_{X^k} \left(\Delta x_1^k\right) + \left.\frac{\partial f_{\mathrm{n}}}{\partial x_2}\right\rangle_{X^k} \left(\Delta x_2^k\right) + \cdots \tag{92}$$

$$+ \left.\frac{\partial f_{\mathrm{n}}}{\partial x_n}\right\rangle_{X^k} (\Delta x_n^k)$$

The algorithm for solving that equations is:

1. Guess X^k
2. Evaluate all functions in the point X^k
3. Check if all $|f_i(X^k)| <\in$ because in that case the problem is solved
4. Calculate all partial derivatives at X^k
5. Solve the matrix-vector equations

$$P\Delta X = -F \; for \; \Delta X \quad \Delta X = P^{-1}(-F) \tag{93}$$

P is the matrix of partial derivatives, ΔX the vector of x and F the vector of function values

6. For all xi calculate:

$$x_i^{k+1} = x_i^k + \Delta x_i \tag{94}$$

7. Return to step 2, The new X^k is now the X^{k+1} of before.

If the equations are not analytical , derivatives are calculated numerically.

APPENDIX B. EQUILIBRIUM

Table 8-1. Vapor liquid equilibria for CO_2/FAME system.

TEMPERATURE	PRESSURE	Liquid phase		Vapor phase	
(K)	(MPa)	xCO2	xFAME	yCO2	yFAME
313.15	8.09	0.8592	0.1408	0.9987	0.0013
313.15	9.6	0.9118	0.0882	0.9971	0.0029
313.15	10	0.9163	0.0837	0.9954	0.0046
313.15	10.8	0.9238	0.0762	0.9933	0.0067
313.15	12	0.9330	0.0670	0.9880	0.0120
313.15	12.5	0.9363	0.0638	0.9863	0.0138
333.15	9.55	0.7816	0.2184	0.9996	0.0004
333.15	12.5	0.8683	0.1317	0.9981	0.0019
333.15	13.8	0.8862	0.1138	0.9954	0.0046
333.15	16.4	0.9102	0.0898	0.9875	0.0125
333.15	18.3	0.9231	0.0769	0.9754	0.0246
353.15	9.7	0.6988	0.3012	0.9996	0.0004
353.15	12.1	0.7844	0.2156	0.9990	0.0010
353.15	15.03	0.8286	0.1714	0.9983	0.0017
353.15	17.95	0.8753	0.1247	0.9908	0.0092
353.15	20.97	0.9306	0.0694	0.9868	0.0132
353.15	22.32	0.9444	0.0556	0.9754	0.0246

Table 8-2. Vapor liquid equilibria for CO_2/Tocopherols system.

TEMPERATURE	PRESSURE	Liquid phase		Vapor phase	
(K)	(Mpa)	xCO2	xTocopherols	yCO2	yTocopherols
313.15	8.6	0.7229	0.2771	1	0
313.15	11.16	0.7395	0.2605	0.9998	0.0002
313.15	12.32	0.7450	0.2550	0.9996	0.0004
313.15	15.42	0.7578	0.2422	0.9993	0.0007
313.15	18.72	0.7686	0.2314	0.9991	0.0009
313.15	21.42	0.7703	0.2297	0.9988	0.0012
313.15	24.71	0.7726	0.2274	0.9982	0.0019
313.15	29.11	0.7783	0.2217	0.9977	0.0023
333.15	10.63	0.7303	0.2697	0.9999	0.0001
333.15	15.42	0.7521	0.2479	0.9996	0.0004
333.15	16.43	0.7583	0.2417	0.9994	0.0006
333.15	18.35	0.7635	0.2365	0.9993	0.0007
333.15	23.73	0.7745	0.2255	0.9986	0.0014
333.15	29.3	0.7767	0.2233	0.9979	0.0021
353.15	8.5	0.6867	0.3133	0.9999	0.0001
353.15	10.3	0.7331	0.2669	0.9999	0.0001
353.15	13.53	0.7791	0.2209	0.9998	0.0002
353.15	20.38	0.8063	0.1937	0.9994	0.0006
353.15	23.24	0.8255	0.1745	0.9992	0.0008
353.15	25.41	0.8255	0.1745	0.9988	0.0012
353.15	29.54	0.8293	0.1707	0.9983	0.0017
353.15	29.6	0.8410	0.1590	0.9981	0.0019

Table 8-3. Vapor liquid equilibria for CO_2/FAME/Tocopherols system.

TEMPERATURE	PRESSURE	Liquid phase			Vapor phae		
(K)	(MPa)	FAME	CO2	Tocopherols	FAME	CO2	Tocopherols
313.15	10	0.4137	0.5201	0.0662	0.0165	0.9831	0.0004
313.15	15	0.3396	0.5829	0.0775	0.0911	0.905	0.0039
313.15	20	0.2611	0.6752	0.0637	0.1261	0.863	0.0109
313.15	29	0.2105	0.7301	0.0594	0.1605	0.8226	0.0169
333.15	10	0.5882	0.3286	0.0832	0.0029	0.997	0.0001
333.15	20	0.2904	0.6506	0.059	0.1417	0.8497	0.0086
353.15	10	0.6905	0.2285	0.081	0.0027	0.9972	0.0001
353.15	20	0.3416	0.5757	0.0827	0.066	0.9303	0.0037

Table 8-4. Vapor liquid equilibria for CO_2/ethyl oleate system.

TEMPERATURE	PRESSURE	Liquid phase		Vapor phase	
(K)	(MPa)	xCO2	x FAEE	y CO2	y FAEE
313.15	2.98	0.52	0.48	1	0
313.15	5.01	0.627	0.373	1	0
313.15	7.07	0.756	0.244	1	0
313.15	8.13	0.809	0.191	0.999	0.001
313.15	9.1	0.851	0.149	0.999	0.001
313.15	9.95	0.871	0.129	0.995	0.005
313.15	12.25	0.905	0.095	0.985	0.015
313.15	12.5	0.919	0.081	0.985	0.015
323.15	2.08	0.367	0.633	1	0
323.15	4.01	0.518	0.482	1	0
323.15	5.77	0.622	0.378	1	0
323.15	7.22	0.697	0.303	1	0
323.15	8.23	0.753	0.247	1	0
323.15	9	0.776	0.224	0.999	0.001
323.15	10.05	0.813	0.187	0.999	0.001
323.15	11.04	0.84	0.16	0.999	0.001
323.15	12.05	0.859	0.141	0.997	0.003
323.15	13.01	0.873	0.127	0.994	0.006
323.15	14.05	0.888	0.112	0.991	0.009
323.15	15.43	0.912	0.088	0.982	0.018
323.15	15.95	0.926	0.074	0.979	0.021
333.15	1.14	0.195	0.805	1	0
333.15	3.14	0.399	0.601	1	0
333.15	5.1	0.537	0.463	1	0
333.15	6.48	0.611	0.389	1	0
333.15	8.07	0.686	0.314	1	0
333.15	9	0.723	0.277	1	0
333.15	10.08	0.759	0.241	1	0
333.15	11.1	0.79	0.21	0.999	0.001
333.15	12.11	0.818	0.182	0.999	0.001
333.15	13.03	0.834	0.166	0.998	0.002
333.15	14.08	0.849	0.151	0.997	0.003
333.15	15.1	0.869	0.131	0.995	0.005
333.15	15.9	0.877	0.123	0.993	0.007
333.15	17.12	0.898	0.102	0.988	0.012
333.15	18.1	0.917	0.083	0.983	0.017
333.15	18.62	0.961	0.039	0.977	0.023

Table 8-5. Vapor liquid equilibria for CO_2/FFA system.

TEMPERATURE	PRESSURE	Liquid phase		Vapor phase	
(K)	(MPa)	xCO2	xFFA	yCO2	yFFA
313.15	15.39	0.4238	0.5762	0.9915	0.0085
313.15	20.02	0.4352	0.5648	0.9852	0.0148
313.15	24.99	0.4335	0.5665	0.9782	0.0218
313.15	30	0.4336	0.5664	0.967	0.033
333.15	15.15	0.2886	0.7114	0.9927	0.0073
333.15	20.4	0.3353	0.6647	0.9896	0.0104
333.15	24.92	0.3664	0.6336	0.9818	0.0182
333.15	30.02	0.4002	0.5998	0.9716	0.0284
353.15	16.34	0.2634	0.7366	0.9937	0.0063
353.15	20.95	0.3155	0.6845	0.9932	0.0068
353.15	25.7	0.3537	0.6463	0.9855	0.0145
353.15	29.34	0.3826	0.6174	0.9744	0.0256

Table 8-6. Vapor liquid equilibria for CO_2/TG system.

TEMPERATURE	PRESSURE	Liquid phase		Vapor phase	
(K)	(Mpa)	xCO2	xTG	yCO2	yTG
313.15	15.34	0.3063	0.6937	0.9964	0.0036
313.15	20.1	0.3227	0.6773	0.9936	0.0064
313.15	24.82	0.3519	0.6481	0.991	0.009
313.15	29.08	0.3453	0.6547	0.9901	0.0099
333.15	15.4	0.2679	0.7321	0.9963	0.0037
333.15	22.5	0.3146	0.6854	0.9959	0.0041
333.15	24.9	0.3398	0.6602	0.9945	0.0055
333.15	31	0.3569	0.6431	0.987	0.013

Table 8-7. Vapor liquid equilibria for CO_2/FAME system.

TEMPERATURE	PRESSURE	Liquid phase		Vapor phase	
(K)	(MPa)	xCO2	xFAME	yCO2	yFAME
313.15	2.91	0.425	0.575	0.9998	0.0002
313.15	5.12	0.627	0.373	0.9998	0.0002
313.15	7.99	0.806	0.194	0.9991	0.0009
313.15	10.77	0.887	0.113	0.9927	0.0073
333.15	7.36	0.648	0.352	0.9999	0.0001
333.15	9.15	0.725	0.275	0.9999	0.0001
333.15	11.55	0.801	0.199	0.9995	0.0005
333.15	13.69	0.842	0.158	0.9983	0.0017

Table 8-8. Vapor liquid equilibria for CO_2/Tocopherols system.

TEMPERATURE	PRESSURE	Liquid phase		Vapor phase	
K	MPa	xCO2	xTocopherols	yCO2	ytocopherols
298.1	26.25	0.7331	0.2669	0.9987	0.0013
298.1	24.85	0.7444	0.2556	0.9986	0.0014
298.1	23.95	0.7432	0.2568	0.9988	0.0012
298.1	20.2	0.7267	0.2733	0.9988	0.0012
298.1	17.35	0.6937	0.3063	0.9992	0.0008
298.1	14.3	0.6905	0.3095	0.9993	0.0007
298.1	11.65	0.708	0.292	0.9994	0.0006
298.1	9.2	0.6852	0.3148	0.9995	0.0005
306.1	26.2	0.73	0.27	0.9986	0.0014
306.1	25.75	0.7618	0.2382	0.9989	0.0011
306.1	25.1	0.7422	0.2578	0.9987	0.0013
306.1	23.1	0.7403	0.2597	0.9987	0.0013
306.1	20.4	0.7289	0.2711	0.9986	0.0014
306.1	17.55	0.7368	0.2632	0.9987	0.0013
306.1	15.1	0.7357	0.2643	0.9992	0.0008
306.1	11.95	0.7063	0.2937	0.9994	0.0006
306.1	9.35	0.7132	0.2868	0.9997	0.0003
313.1	25.85	0.7335	0.2665	0.9983	0.0017
313.1	24.5	0.7477	0.2523	0.9983	0.0017
313.1	24.15	0.7294	0.2706	0.9986	0.0014
313.1	24.1	0.7419	0.2581	0.9987	0.0013
313.1	21.35	0.7279	0.2721	0.9988	0.0012
313.1	20.35	0.7244	0.2756	0.9990	0.0010
313.1	18.6	0.7119	0.2881	0.9990	0.0010
313.1	15.65	0.7252	0.2748	0.9991	0.0009
313.1	13.75	0.7115	0.2885	0.9993	0.0007
313.1	11.5	0.7007	0.2993	0.9995	0.0005
313.1	11.05	0.6927	0.3073	0.9997	0.0003
313.1	9.5	0.6858	0.3142	1.0000	5.00E-05
323.1	26.1	0.7619	0.2381	0.9986	0.0014
323.1	25.25	0.7416	0.2584	0.9987	0.0014
323.1	24.15	0.7434	0.2566	0.9986	0.0014
323.1	22.3	0.7316	0.2684	0.9987	0.0013
323.1	20.15	0.721	0.279	0.9992	0.0009
323.1	18.3	0.726	0.274	0.9992	0.0008
323.1	15.25	0.7087	0.2913	0.9996	0.0004
323.1	12.05	0.7025	0.2975	0.9999	0.0001
323.1	9.1	0.6946	0.3054	0.9999	7.00E-05
333.1	25.85	0.7575	0.2425	0.9985	0.0015
333.1	25.3	0.758	0.242	0.9986	0.0014
333.1	25.2	0.7704	0.2296	0.9987	0.0013
333.1	23.55	0.7576	0.2424	0.9989	0.0011

333.1	23.5	0.7703	0.2297	0.9992	0.0008
333.1	21.1	0.7646	0.2354	0.9992	0.0008
333.1	18.05	0.7457	0.2543	0.9991	0.0009
333.1	14.9	0.7317	0.2683	0.9996	0.0004
333.1	12	0.7134	0.2866	0.9998	0.0002
333.1	9.05	0.6488	0.3512	0.99995	5.00E-05

Table 8-9. Vapor liquid equilibria for CO_2/Ethanol/Water system.

TEMPERATURE	PRESSURE	Liquid phase			Vapor phase		
(K)	(Mpa)	xCO2	xETHANOL	xWATER	yCO2	yETHANOL	yWATER
282.75	4.56	0.0275	0.0173	0.9552	0.9993	0.0002	0.0005
282.75	59.3	0.0271	0.0178	0.9551	0.9964	0.0019	0.0017
282.75	7.36	0.0283	0.0176	0.9541	0.9964	0.0018	0.0018
282.75	8.76	0.0287	0.0174	0.9539	0.9961	0.0019	0.002
290.35	4.51	0.0226	0.0156	0.9618	0.9992	0.0003	0.0005
290.35	6	0.025	0.0186	0.9564	0.9957	0.0031	0.0012
290.35	7.36	0.0288	0.0181	0.9531	0.9952	0.0024	0.0024
290.35	8.81	0.027	0.018	0.955	0.9955	0.0022	0.0023
292.75	4.59	0.0226	0.0148	0.9626	0.999	0.0003	0.0007
292.75	5.97	0.0255	0.0172	0.9573	0.9961	0.0024	0.0015
292.75	7.4	0.0248	0.0173	0.9579	0.9952	0.0025	0.0023
292.75	8.76	0.0272	0.0168	0.956	0.995	0.0026	0.0024
298.15	4.52	0.0206	0.0149	0.9645	0.9987	0.0004	0.0009
298.15	5.95	0.0243	0.013	0.9627	0.9984	0.0006	0.001
298.15	7.37	0.0252	0.0158	0.959	0.9953	0.0021	0.0026
298.15	8.71	0.0258	0.0157	0.9585	0.9946	0.0026	0.0028
305.15	4.54	0.0186	0.0121	0.9693	0.9985	0.0005	0.001
305.15	5.93	0.0203	0.0116	0.9681	0.9983	0.0006	0.0011
305.15	7.45	0.0239	0.0166	0.9595	0.9957	0.002	0.0023
305.15	8.86	0.025	0.0151	0.9599	0.9949	0.0022	0.0029

Table 8-10. Vapor liquid equilibria for FAME/Squalene/CO_2 system.

TEMPERATURE (K)	PRESSURE (Mpa)	Liquid phase FAME	SQUALENE	CO2	Vapor phase FAME	SQUALENE	CO2
313.2	11.15	0.1253	0.02	0.8547	0.0043	0.0002	0.9955
313.2	13.09	0.1057	0.0223	0.872	0.0095	0.0008	0.9897
323.2	13.14	0.1302	0.0221	0.8477	0.0036	0.0001	0.9963
323.2	15.13	0.1039	0.0256	0.8705	0.0074	0.0006	0.992
313.2	11.12	0.1072	0.0769	0.8159	0.0022	0.0002	0.9976
313.2	13.07	0.0949	0.0807	0.8244	0.0036	0.0006	0.9958
313.2	14.98	0.0899	0.0826	0.8275	0.0046	0.0012	0.9942
313.2	16.91	0.0713	0.0815	0.8472	0.0057	0.0019	0.9924
323.2	13.09	0.1083	0.0791	0.8126	0.0024	0.0003	0.9973
323.2	16.86	0.0788	0.0812	0.84	0.0046	0.0013	0.9941
313.2	11.16	0.0597	0.1444	0.7959	0.0013	0.0005	0.9982
313.2	13.06	0.0512	0.141	0.8078	0.0013	0.0006	0.9981
313.2	14.96	0.0427	0.1423	0.815	0.0017	0.0012	0.9971
313.2	20.52	0.0328	0.1254	0.8418	0.0027	0.0028	0.9945
323.2	13.16	0.0637	0.1397	0.7966	0.0011	0.0004	0.9985
323.2	15	0.0516	0.1363	0.8121	0.0013	0.0006	0.9981
323.2	18	0.0443	0.1306	0.8251	0.0019	0.0013	0.9968
323.2	20.83	0.037	0.1229	0.8401	0.0024	0.0023	0.9953
343.2	15	0.0685	0.1383	0.7932	0.0002	0.0001	0.9997
343.2	18.03	0.0604	0.1323	0.8073	0.0007	0.0003	0.999
343.2	20.96	0.0499	0.1263	0.8238	0.0012	0.0008	0.998
313.2	15.23	0.0198	0.1791	0.8011	0.001	0.0017	0.9973
323.2	15.18	0.0232	0.1912	0.7856	0.0005	0.0009	0.9986

Table 8-11. Vapor liquid equilibria for CO_2 /Sterols/TG system.

TEMPERATURE	PRESSURE	Liquid phase			Vapor phase		
(K)	(MPa)	CO2	STEROLS	TG	CO2	STEROLS	TG
343.15	20	0.2051	0.0892	0.7057	0.9984	0.0006	0.001
343.15	26	0.237	0.084	0.679	0.9953	0.0014	0.0033
343.15	29	0.2567	0.0835	0.6598	0.9932	0.0017	0.0051
343.15	35	0.2895	0.0742	0.6363	0.9892	0.0024	0.0084
323.15	26	0.2567	0.0832	0.6601	0.9935	0.0018	0.0047
363.15	26	0.2181	0.0841	0.6978	0.9969	0.0011	0.002
383.15	26	0.1973	0.0854	0.7173	0.9978	0.0007	0.0015

APPENDIX C. REGRESSION RESULTS

Table 8-12. Average absolute deviation and maximum deviation obtained during the regression.

	Liquid phase		Vapor phase	
	AAD (%)	Maximum deviation	AAD (%)	Maximum deviation
FAEE	5.9803	-0.099	37.6954	-0.0067
FFA	1.5656	0.0235	49.6856	0.0114
TG	0.9154	0.0143	65.69	0.0085
FAME	1.7885	-0.0222	47.0828	0.0035
Tocopherols	6.3577	0.059	277.82	0.013
Ethanol	2.4905	0.0016	19.8713	-0.0013
Water	0.0918	2.60E-03	17.9462	0.001
Squalene	1.4889	-0.0093	15.7549	-0.0006
Sterols	1.5531	0.003	9.07683	0.0002

AAD is the average absolute deviation between experimental and predicted data.